BNL-52351-98/12-REV

Laboratory Directed Research & Development Program

Annual Report to the Department of Energy
December 1998

Gregory J. Ogeka
Interim Assistant Laboratory Director for Finance & Administration

Kevin J. Fox
Special Assistant to the
Interim Assistant Laboratory Director for Finance & Administration

BROOKHAVEN NATIONAL LABORATORY
BROOKHAVEN SCIENCE ASSOCIATES
UPTON, NEW YORK 11973-5000
UNDER CONTRACT NO. DE-AC02-98CH10886
UNITED STATES DEPARTMENT OF ENERGY

DISCLAIMER

Acknowledgments

*T*he Laboratory Directed Research and Development (LDRD) Program is directed by Peter Paul, Deputy Director for Science & Technology, and is administered by Gregory J. Ogeka, Interim Assistant Laboratory Director for Finance & Administration (ALDFA). Preparation of the FY 1998 report was coordinated and edited by Gregory Ogeka and Kevin Fox, Special Assistant to the ALDFA, who wish to thank Regina Paquette, Susan Cuevas, and D.J. Greco for their assistance in organizing, typing, and proofing the document. A special thank you is also extended to the Photography and Graphic Arts Group for their help in publishing. Of course, a very special acknowledgement is extended to all of the authors of the project annual reports and to their secretaries.

Table of Contents

Introduction 1

Management Process 7

Summary of FY 1998 LDRD Program 13

Project Program Summaries

Positron Emission Magnetic Resonance Imaging (PEMRI) 17

Research into New Database Methodology Based on the Object Protocol Model 25

Tailored Pulse UV/XUV Photon Source Development 29

BNCT for Leukemia Through *Ex Vivo* Purging of Bone Marrow 33

Autecology of the Peconic Bay Brown Tide Organism, *Aureococcus anophagefferens* 39

The Development and Demonstration of Accelerator Based BNCT Capability 43

Physics Goals for a New Intense Muon Facility 47

A Novel Curved Proportional Counter for X-ray Powder Diffraction Studies at NSLS 51

Plasma Window for Transmission of Synchrotron Radiation 57

Development of New Techniques in Picosecond Pulse Radiolysis 61

X-ray Circular Dichroism of Biological Macromolecules 65

X-ray Schlieren Computed Tomography 71

Biodistribution, Toxicity & Boron Neutron-Capture Therapy in Animals Using Metallotetracarboranylporphyrins 79

Development of Pump-&-Probe LIDAR for the *In-situ* Study of Fast Atmospheric Chemical Reactions 85

Center for Imaging in Drug Abuse Research 95

Table of Contents

Molecular Biological markers as Potential Prognostic Indicators for BNCT 99

Beam Enhancement in a High Brightness Electron Linac 103

Novel Mechanisms of Hydroxy Fatty Acid Biosynthesis 107

Target Design for an AGS-based Spallation Neutron Source 109

Sensitive Detection and Rapid Identification of Biological Agents by Single Molecule Detection 111

LDRD - 1999 Proposed Program 115

Introduction

Background: Brookhaven National Laboratory (BNL) was established in 1947 on the site of the former Army Camp Upton. Brookhaven is a multidisciplinary laboratory that carries out basic and applied research in the physical, biomedical and environmental sciences, and in selected energy technologies. As of March 1, 1998, the Laboratory came under new management. It is managed by Brookhaven Science Associates, LLC, under contract with the U. S. Department of Energy. BNL's total annual budget has averaged about $380 million, and its facilities are valued at over $2.2 billion. There are about 3,050 employees, and another 4,600 guest scientists and students who come each year to use the Laboratory's facilities and work with the staff. BNL's Relativistic Heavy Ion Collider (RHIC), due to open in June 1999, will be the world's foremost facility for nuclear physics research. RHIC will create the hot, dense plasma of quarks and gluons from which particles condensed after the "Big Bang" of the early universe.

Mission and Core Competencies: Brookhaven National Laboratory's mission is to produce excellent science in a safe, environmentally benign manner with the cooperation, support, and appropriate involvement of our many communities. Brookhaven was founded as a laboratory which would provide specialized research facilities that could not be designed, built and operated at a university or industrial complex, and provides a scientific core effort for these facilities. This still remains a basic mission of the Laboratory.

Brookhaven National Laboratory has four core competencies: Research Facilities, Scientific Research, Technology Development, and Knowledge Transfer are not independent isolated competencies. They are interrelated in a complex manner.

MAJOR CORE COMPETENCIES
RESEARCH FACILITIES Conceive, design, construct, and operate complex, leading-edge, user-oriented facilities in a safe and environmentally benign manner that is responsive to the DOE, and the needs of the users.
SCIENTIFIC RESEARCH Carry out basic and applied research in long-term programs at the frontier of science that supports DOE missions and the needs of the Laboratory's users community.
TECHNOLOGY DEVELOPMENT Develop advanced technologies that address national needs and initiate their transfer to other organizations and to the commercial sector.
KNOWLEDGE TRANSFER Disseminate technical knowledge to educate new generations of scientists and engineers, to maintain technical currency in the nation's workforce, and to encourage scientific awareness in the general public.

Research Facilities and Scientific Research have a synergistic relationship. To maintain and constantly improve a research facility, and to keep it at the cutting edge, it is essential that the Laboratory have a significant research staff of excellent stature. The staff drives the performance of the facility. Having the several complementary facilities at one location, such as the National Synchrotron Light Source and the Alternating Gradient Synchrotron, allows unique research capabilities. The other two core competencies: Technology Development and Knowledge Transfer, bridge all of the research facilities and research programs.

Brookhaven's core competencies support and cut across the four central activities of the Department of Energy as defined in its Strategic Plan.

DOE Strategic Plan Activities	
SCI	**Science and Technology**
ENV	**Environmental Quality**
ENER	**Energy Resources**
SEC	**National Security**

BNL plays a major role in the Science and Technology, the Environmental Quality, the Industrial Competitiveness and the Energy Resources sectors, with a smaller, but special role in the National Security arena. In order to better see the connection between the various Brookhaven activities that form the core competencies and the Department of Energy Strategic Plan activities, each BNL activity/competency is followed with the letter code describing the match in the Table 1, "Major Activity Clusters."

Summary of the LDRD Program: As one of the premier scientific laboratories of the DOE, Brookhaven must continuously foster the development of new ideas and technologies, promote the early exploration and exploitation of creative and innovative concepts, and develop new "fundable" R&D projects and programs. At Brookhaven National Laboratory one such method is through its Laboratory Directed Research and Development Program. This discretionary research and development tool is critical in maintaining the scientific excellence and long-term vitality of the Laboratory. Additionally, it is a means to stimulate the scientific community, fostering new science and technology ideas, which is a major factor in achieving and maintaining staff excellence and a means to address national needs within the overall mission of the DOE and BNL.

The Project Summaries with their accomplishments described in this report reflect the above. Aside from leading to new fundable or promising programs and producing especially noteworthy research, they have resulted in numerous publications in various professional and scientific journals and presentations at meetings and forums.

TABLE 1:
MAJOR ACTIVITY CLUSTERS

LARGE RESEARCH FACILITIES

ALTERNATING GRADIENT SYNCHROTRON
(SCI)
- Research in Particle and Nuclear Physics
- High-Intensity Frontier of Particle Physics
- World's Only High Energy Polarized Proton Source
- At Present, Nation's Only High Energy, Heavy Ion Synchrotron
- Research in Radiobiology
- Over 900 Users

RELATIVISTIC HEAVY ION COLLIDER
(under construction)
(SCI)
- Dedicated Colliding Beams Facility for Ultra Relativistic Collisions of Heavy Nuclei
- Highest Priority Construction Project for U.S. Nuclear Physics
- New Phases of Nuclear Matter High-Temperature Frontier
- Large and Unique High Energy Physics Potential (e.g. spin physics)
- International Community of Over 800 Scientists

HIGH FLUX BEAM REACTOR
(SCI, ENER, ENV)
- 16 Instruments for Research in Condensed-Matter Physics, Biology, Chemistry, Applied Sciences and Industrial Applications
- Facilities for Radio Isotope Production and Radiation Damage Studies
- 270 Users

NATIONAL SYNCHROTRON LIGHT SOURCE
(SCI, ENV, ENER)
- Two Storage Rings Providing Intense UV and X-ray Photon Sources
- 83 Beamlines for Research in Materials Science, Biology, Chemistry, Medical and Industrial Applications
- R&D on Free Electron Lasers and on Production and Utilization of Synchrotron Radiation
- Over 2300 Users. Including 400 Industrial Users

BIOMEDICAL FACILITIES

BROOKHAVEN CENTER FOR IMAGING AND NEUROSCIENCE
(SCI)
- Positron Emission Tomography (PET)
- Single Photon Emission Computed Tomography (SPECT)
- High-Field (4 Tesla) Magnetic Resonance Imaging (MRI)
- Used for Research in the Basic and Clinical Neuroscience (Substance Abuse; Aging; Brain Cancer; Drug Research) and the Development of New Forms of Imaging

BROOKHAVEN LINEAR ISOTOPE PRODUCTION FACILITY
(SCI)
- Production of Isotopes for Medical Purposes
- Approximately 20 Isotopes Produced for Commercial and/or Research Use

MEDICAL RADIATION FACILITY
(SCI)
- Cancer Patient Treatment: 250 patients annually

BROOKHAVEN MEDICAL RESEARCH REACTOR
(SCI)
- Neutron Capture Cancer Therapy Research

SCANNING TRANSMISSION ELECTRON MICROSCOPE
(SCI)
- Structural Biology, Molecular Masses
- Over 75 Users

PROTEIN DATA BANK
(SCI)
- World-Wide Repository for Three-Dimensional Structures of Biological Macromolecules
- 6,380 Structures on File, 350,000 Accesses/Year

GENOME SEQUENCING CENTER
(under development)
(SCI)
- Large-Scale DNA Sequencing

OTHER FACILITIES

TANDEM VAN DE GRAAFF FACILITY
(SCI, SEC, ENV, ENER)
- Injector (source) for Heavy Ions for AGS/RHIC
- Microchip Radiation Testing Facility
- Film Irradiation Plant for Track Etching Filter Membranes
- 250 Users from 45 Institutions

ACCELERATOR TEST FACILITY
(SCI, SEC)
- Advanced Acceleration Concepts and Generation of Coherent Radiation
- Short Wavelength Free-Electron Laser Research

CENTER FOR RADIATION CHEMISTRY RESEARCH
(SCI, ENER, ENV)
- Study of Rapid Chemical Reactions: Catalysis, Energy Conversion and Storage, Waste Management

NATIONAL NUCLEAR DATA CENTER
(SCI, SEC, ENV)
- Nuclear Cross-Section and Structure Data
- 1,100 Users

BOOSTER APPLICATIONS FACILITY
(under development)
(SCI, SEC)
- Proton and Heavy Ion Radiobiology
- Microelectronics Radiation Effects

SCIENTIFIC RESEARCH

HIGH ENERGY PARTICLE AND NUCLEAR PHYSICS
(SCI)
- Beyond the Standard Model
  - Rare Kaon Decays
  - Muon Anomalous Magnetic Moment
  - Exotics and Glueball Spectroscopy
  - Strange Matter
  - Solar Neutrinos
- Relativistic Heavy Ions
  - Nuclear Matter In Extreme States of Temperature and Density
  - QCP Phase Transitions: Hadrons to Quark-Gluon Plasma
  - Recreate Conditions of the Early Universe, Microseconds after the Big Bang

ADVANCED ACCELERATOR CONCEPTS
(SCI, SEC)
- Short Wavelength Accelerating Structures
- Production of Coherent Radiation Free Electron Laser
- Muon Collider
- Neutron Sources
- Interlaboratory Cooperation to Design and Build SNS

MATERIALS SCIENCES
(SCI, ENER)
- Magnetism and Superconductivity
- Surface Studies – Catalysis, Corrosion, and Adhesion
- Condensed Matter Theory: Metallic Alloys and Cooperative Phenomena
- Materials Synthesis and Characterization with Neutron and X-Ray Scattering:
- Structure and Dynamics
- Defect Structure with Positrons

CHEMICAL SCIENCES
(SCI, ENER, ENV)
- Dynamics and Energetics and Reaction Kinetics
- Thermal, Photo- and Radiation-Induced Reactions
- Catalysis and Interfacial Chemistry
- Homogeneous Catalysis with Metal Hybride Complexes
- Porphyrin Chemistry
- Electrochemistry

ENVIRONMENTAL SCIENCES
(SCI, ENV)
- Global Change
- Atmospheric Chemistry
- Marine Science
- Soil Chemistry
- Cycling of Pollutants
- Environmental Remediation

MEDICAL SCIENCE
- (SCI)
- Medical Imaging: PET, SPECT, MRI, Coronary Angiography
- Nuclear Medicine
- Radionuclides, Radiopharmaceuticals, Synthesis and Applications
- Advanced Cancer Therapies: Neutron Capture, Microbeam Radiation, Proton Radiation, Photon Activation Therapy (PAT)
- Mechanisms of Oncogenesis

MOLECULAR BIOLOGY AND BIOTECHNOLOGY
- (SCI)
- Genome Structure, Gene Expression, Molecular Genetics
- DNA Replication, Damage and Repair
- Structure and Function of Enzymes, Protein Engineering
- Plant Genomics, Biochemistry and Energetics
- Solution Structure, Kinetics and Interaction of Biomolecules
- Bio-Structure Determination by X-ray and Neutron Scattering
- Bio-Structure Determination and Mass Measurements by Electron Microscopy

ADVANCED SCIENTIFIC COMPUTING AND SYSTEMS ANALYSIS
(SCI, ENV, ENER)

- Risk Assessment
- Energy Modeling
- Groundwater Modeling
- Traffic Congestion Simulation
- Atmospheric Transport Modeling

TECHNOLOGY DEVELOPMENT

PHYSICAL, CHEMICAL AND MATERIALS SCIENCE
(SCI, ENER, SEC)

- State-of-the-Art Instrumentation and Devices for Precision Electronics, Optics and Microelectronics
- Superconducting and Magnetic Materials
- X-ray Lithography
- Micromachining
- Battery Technology
- Permanent Magnets
- "Designer" Polymers
- Flat Planar Optic Displays

ACCELERATOR TECHNOLOGY
(SCI, SEC)

- High-Field, High-Quality Superconducting Magnets
- High-Power Radio Frequency Systems
- Ultrahigh Vacuum Systems
- Advanced Accelerator Designs
- High-Gradient Acceleration
- High-Beam Current Acceleration
- Novel Structures for Synchrotron Radiation Generation, FELs
- Novel Particle Beam Diagnostics
- Accelerator/Spallation Source Applications
- Insertion Device Development: Wigglers and Undulators
- High-Power, Short-Pulse Lasers

ENVIRONMENTAL AND CONSERVATION TECHNOLOGIES
(SCI, ENV, ENER, SEC)

- Environmental Remediation and Mitigation
- Energy-Efficiency Technologies
- Waste Treatment
- Disposal of Nuclear Materials
- Radiation Protection
- Infrastructure Modernization
- Transportation: Intelligent Transportation System, MAGLEV
- Ultra Sensitive Detection and Characterization

MEDICAL TECHNOLOGIES
(SCI)

- Biomedical Applications of Nuclear Technology
- Production of Radionuclides/ Radiopharmaceuticals
- Development of Particle Radiation Therapies for Cancer
- Medical Imaging
- X-ray Microbeam Therapy

BIOTECHNOLOGY
(SCI)

- Neutron and Synchrotron X-ray Scattering
- Large-Scale Genome Sequencing
- High-Resolution Scanning and Cryo Electron Microscopy
- Cloning, Expressing and Engineering Genes
- Metal Cluster Compounds for Electron Microscope Labels
- Phage Displays for Probing Specific Interactions

SAFETY, SAFEGUARDS, AND RISK ASSESSMENT
(SEC, SCI, ENV, ENER)

- Safeguards, Nonproliferation and Arms Control
- Safety Analysis of Complex Systems
- Probabilistic Risk Assessment and Management
- Human Reliability
- Material and Component Survivability Testing
- Remote Sensing of Chemical Signatures
- Technical Support for U.S. Policy
- Energy Systems Modeling and Assessment
- Biological and Chemical Weapons Detection and Mitigation

KNOWLEDGE TRANSFER

EDUCATING FUTURE GENERATIONS OF SCIENTISTS AND ENGINEERS
(SCI, ENV, ENER, SEC)

- Scientific Publishing, Lecturing, Conference Participation
- Visiting Scientist Program
- Accelerator Fellowship Program
- Postdoctoral Research Associates
- Engineering Intern Program
- Graduate Student Thesis Projects
- Adjunct Teaching Appointments at Local Colleges
- Office of Educational Program
- Precollege and College Programs for Students
- and Teachers

EDUCATING THE GENERAL PUBLIC
(SCI, ENV, ENER, SEC)

- Science Museum and Laboratory Tours (20,000 people/year)
- Speakers Bureau
- BNL Videos
- Laboratory Lectures for the Public
- Community Outreach Programs
- School Mentoring Program

TECHNOLOGY TRANSFER
(SCI, ENV, ENER, SEC)

- Scientific Publishing
- Industrial Users at the Research Facilities
- Consulting by Scientific Staff for Industry
- Technology Transfer Office
- Patenting and Licensing of BNL Inventions
- Technical Assistance for Industry
- CRADAs
- Personnel Exchange Program with Industry
- Research Partnerships with Industry
- Industry-Sponsored Proprietary Research and Development
- Long Island Research Institute
- (LIRI) (founding member)
- promotes Laboratory-Industry Interaction
- ARPA-Funded BNL/LIRI Defense Conversion Project
- NY State-Funded Biotechnology Initiative

INFORMATION TECHNOLOGY
(SCI, ENV, ENER, SEC)

- Electronic Library and Database Information Source
- Networking - "Information Superhighway"
- Technical and Scientific Publishing
- National Nuclear Data Center
- Protein Data Bank
- Data Visualization
- ALARA Center

TRAINING AND EDUCATION OF TECHNOLOGISTS
(ENER, SEC, ENV)

- Safety of Soviet-Designed Reactors
- Safeguards of Special Nuclear Materials in the former Soviet Union
- Mentoring within the DOE Complex
- Waste Management in the former Soviet/Arctic Regions

Management Process

PROGRAM DESCRIPTION:

Introduction: The Department of Energy's (DOE) Laboratory Directed Research & Development (LDRD) Program at Brookhaven National Laboratory (BNL) was originally established as the "Exploratory Research Program" under the guidelines set forth in DOE Order 5000.1 in May 1984. From inception through September 1999, a period spanning fifteen fiscal years, the Laboratory has authorized $38.8 million in Exploratory R&D, consisting of 201 separate projects.

BNL LDRD PROGRAM HISTORY 1985-1999

FISCAL YEAR	AUTH K$	COSTED K$	NO. REC'D	NEW STARTS
1985	1,842	1,819	39	13
1986	2,552	2,515	22	15
1987	1,451	1,443	29	8
1988	1,545	1,510	46	14
1989	2,676	2,666	42	21
1990	2,008	1,941	47	9
1991	1,353	1,321	23	14
1992	1,892	1,865	30	14
1993	2,073	2,006	35	14
1994	2,334	2,323	44	15
1995	2,486	2,478	46	13
1996	3,500	3,050	47	17
1997	4,500	3,459	71	10
1998	4,000	2,564	53	4
1999	4,612*	—	67	20
TOTALS	38,824	30,998	641	201

*Additional projects may be funded in FY 1999, pending the availability of funds.

Historical Perspective: Brookhaven National Laboratory was established in 1946. Throughout its history, certain projects of an exploratory nature, sometimes referred to in the past as "seed money projects," were supported with overhead funding. In 1979, as a result of a Review Audit in that year, the seed money accounting procedures were formalized, and oversight by the then DOE Brookhaven Group Manager was first established. This seed money program operated at a variable level of funding, which averaged about 0.1 percent of the Laboratory's operating budget over the period 1979 to 1984.

In May 1984, the program was expanded. The expanded program embraced the new Exploratory R&D guidelines of DOE Order 5000.1. The new program, called the Exploratory Research Program, was put into effect for FY 1985 funding. The current Laboratory Directed Research & Development Program reflects the operating styles and many of the procedures of the earlier programs, which have evolved somewhat informally over the years. It also encompasses the requirements of the current DOE Order 413.2.

Goals and Objectives: The goals and objectives of BNL's LDRD Program can be inferred from the Program's stated purposes. These are to (1) encourage and support the development of new ideas and technology, (2) promote the early exploration and exploitation of creative and innovative concepts, and (3) develop new "fundable" R&D projects and programs. The emphasis is clearly articulated by BNL to be on supporting exploratory research "which could lead to new programs, projects, and directions" for the Laboratory.

General Characteristics of the LDRD Program: Projects or studies that are appropriate candidates for the Laboratory's LDRD Program include, but are not limited to, (1) projects, normally relatively small, in the forefront areas of basic and applied science and technology for the primary purpose of enriching laboratory capabilities, (2) advanced study of new hypotheses, new concepts, or innovative approaches to scientific or technical problems, (3) experiments and analyses directed toward "proof of principle" or early determination of the utility of new scientific ideas, and (4) conception and preliminary technical analysis of experimental facilities or devices.

PROGRAM ADMINISTRATION:

Overall Coordination: Overall responsibility for coordination, oversight, and administration of BNL's LDRD Program resides with the Laboratory's Director. The Office of the Assistant Laboratory Director for Finance & Administration assists in the administration of the program. This includes administering the program budget, establishment of project accounts, maintaining summary reports, and reports of Program activities to the DOE through the Brookhaven Group Manager.

Responsibility for the allocation of resources and the orchestration, review, and selection of proposals lies with a management-level group called the Laboratory Directed Research & Development Program Committee.

The Program Committee is made up of nine members. For Fiscal Year 1998, the Laboratory's Deputy Director for Science & Technology is the chairperson of the Committee. The other members are the Associate Directors of the Laboratory, as well as members from several scientific departments and divisions, and the Assistant Director for Finance & Administration.

1998 LDRD PROGRAM COMMITTEE
(for Selection of 1999 Programs)

Peter Paul	**Chairperson**
Gregory J. Ogeka	**Administration**
Thomas Kirk	**High Energy & Nuclear Physics**
Denis B. McWhan	**Basic Energy Sciences**
Adrian Roberts	**Applied Science & Technology**
Richard B. Setlow	**Life Sciences**
Carl Anderson	**Biology**
Satoshi Ozaki	**RHIC**
Peter Takacs	**Instrumentation**

Allocating Funds: There are two types of decisions to be made each year concerning the allocation of funds for the LDRD Program. These are: (1) the amount of money that should be budgeted overall for the Program; and (2) of this, how much, if any, should go to each competing project or proposal. Both of these decisions are made by high-level management.

Concerning the overall budget, for each upcoming fiscal year the Laboratory Director, in consultation with the Assistant Laboratory Director for Finance & Administration, develops an overall level of funding for the LDRD Program. The budget amount is then incorporated into the Laboratory's LDRD Plan which formally requests authorization from the DOE to expend funds for the LDRD Program up to this ceiling amount.

The majority of projects are authorized for funding at the start of the fiscal year. However, projects can be authorized throughout the fiscal year, as long as funds are available and the approved ceiling for the LDRD Program is not exceeded.

The actual level, which may be less, is determined during the course of the year and is affected by several considerations including: the specific merits of the various project proposals, as determined by Laboratory management and the members of the LDRD Program Committee; the overall financial health of the Laboratory; and a number of budgetary tradeoffs between LDRD and other overhead expenses. At BNL the LDRD Program has historically amounted to a much smaller portion of the total budget area at comparable national labs.

LDRD COSTS VS. TOTAL LABORATORY COSTS
operating $ in millions

FISCAL YEAR	DOE FUNDS	WFO FUNDS	TOTAL FUNDS	LDRD FUNDS	% OF TOTAL
1985	153.0	40.4	193.1	1.82	0.9
1986	156.5	45.1	201.6	2.52	1.2
1987	161.7	45.6	207.3	1.44	0.7
1988	176.7	45.9	222.6	1.51	0.7
1989	193.6	46.7	240.3	2.67	1.1
1990	203.8	45.2	249.0	1.94	0.8
1991	220.9	50.3	271.2	1.32	0.5
1992	234.3	47.2	281.5	1.87	0.7
1993	231.4	47.3	278.7	2.01	0.7
1994	237.0	47.9	284.9	2.32	0.8
1995	243.0	53.7	296.7	2.48	0.8
1996	251.6	50.6	302.2	3.05	1.0
1997	257.2	52.5	309.7	3.46	1.1
1998	251.8	49.5	301.3	2.56	.8

Concerning the allocation of resources to specific topic areas or to individual project proposals, such issues are addressed on a case-by-case basis by the LDRD Program Committee, once specific proposals have been received. The Committee meets periodically to review and recommend project proposals and to determine the amount of funding to be made available to the LDRD Program. The requirements of DOE Order 413.2 are carefully considered during the selection process to ensure that proposals are consistent with DOE's criteria.

Request for Proposals: The availability of special funds for research under the LDRD Program is well publicized throughout the Laboratory. This is done using two methods --one occurring at yearly intervals, the other occurring irregularly. Each year in May a memo is sent by the Laboratory Director to all scientific staff issuing a "call for proposals." This memo is accompanied by a document entitled, "Guidelines and Procedures for Developing Proposals via the Laboratory Directed Research and Development (LDRD) Program." The other method is by announcement in the Brookhaven Bulletin, the Laboratory's weekly newspaper.

The "Guidelines and Procedures" document specifies the requirements necessary for participation in the program. It states the program's purpose, general characteristics, procedures for applying, and restrictions. An application for funding, that is, a project proposal, takes the form of a completed "Proposal Information Questionnaire." An application must be approved up the chain-of-command which includes the initiator's Department or Division Budget Administrator, the Department Chairperson or Division Head, and the cognizant Associate/Assistant Director. Plans to ensure the satisfactory continuation of the principal investigator's regularly funded programs must also be approved. The applications are then forwarded to the Chairperson of the LDRD Program Committee for further review and consideration for funding by the full Committee.

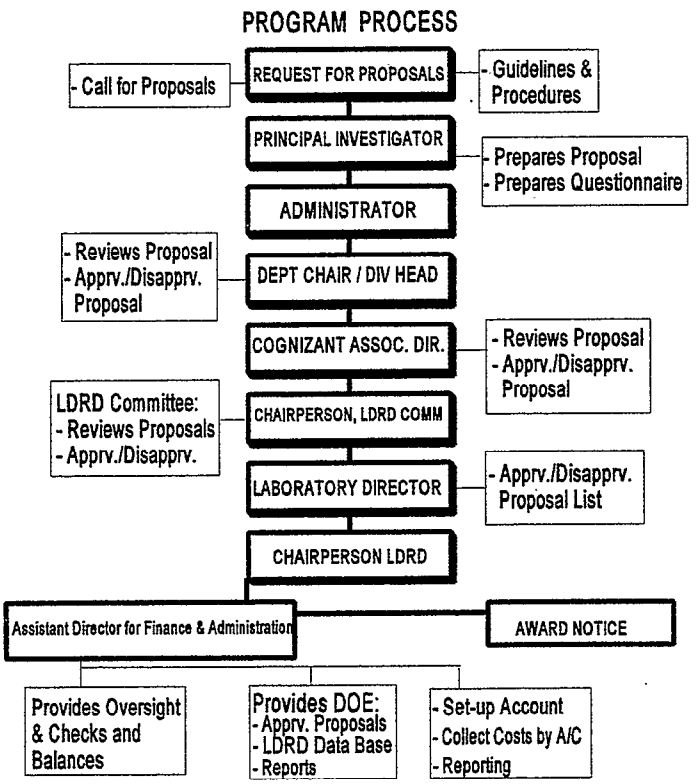

The process that solicits and encourages the development of proposals has evolved into two modes of operation. Specifically, the ideas for proposal development may originate among the scientific staff in response to the general call for proposals. Alternatively, they may be initiated by top-level Laboratory management. Eventually, both follow the standard procedure for proposal approval up the chain-of-command to the same decision makers. The fact that all proposals must be approved up the chain-of-command permits BNL managers to consider all ideas together when designing the mix of projects for the LDRD Program.

An initiative from management typically takes the form of a general topic area or item of special interest. It is not a directive, nor is it included in the call for proposals, but the idea is communicated to a group of scientific staff, which is known to be in a position capable of pursuing and developing the idea in the form of a more formal proposal.

Proposal Review: Once a proposal is approved by the cognizant line managers, all proposals are forwarded to the Chairperson of the Committee who transmits a copy of all proposals received to the Committee for review. The Committee considers all proposals that have met certain minimum requirements pertaining to the Department's and BNL's LDRD policies.

Lead responsibility for the review of a proposal is then assigned to that member of the Committee who last approved it in the chain-of-command, that is, the member who oversees and directs the technical area from which the proposal originated. All members have several weeks to review the proposals and prepare for the next Committee meeting. During this time, additional reviews, if desired, may be arranged.

Formal peer reviews, consisting of written comments by experts outside the normal lines of supervision, are not usually performed. The members of the Committee are considered to have sufficient technical knowledge so that peer reviews are seldom required.

At the next Committee meeting, the Committee member responsible for the review of the proposal presents the proposal to the other members of the Committee. This is done without the member necessarily becoming an advocate for the proposed project.

Selection Criteria: Before proposals can be considered by the Committee, they must be screened to ensure that they meet a set of minimum requirements concerning the Department's LDRD policies and the Laboratory's own guidelines.

Minimum requirements of each proposal are: (1) consistency with program purpose; (2) consistency with missions of BNL, DOE, and NRC; (3) approval by Department Chair-

person and/or Division Head, and cognizant Associate/Assistant Director; (4) assurance of satisfactory continuation of principal investigator's regularly funded programs; (5) modest size and limited to 3 years; (6) will not substitute for, supplement, or extend funding for tasks normally funded by DOE, NRC, or other users of the Laboratory; (7) will not require the acquisition of permanent staff; (8) will not create a commitment of future multi-year funding to reach a useful stage of completion; and (9) will not fund construction line-item projects, facility maintenance, or general purpose capital equipment.

The selection criteria used to evaluate and rank individual proposals are not formally stated or published. While the "Guidelines and Procedures" document clearly states that "awards will be made on a competitive basis," the factors or selection criteria to be considered in this competition are not listed. Nevertheless, selection is based on (1) scientific merit, (2) compliance with minimum requirements, (3) proposal cost as compared to the amount of available funding, (4) innovativeness, and (5) its potential for follow-on funding. The requirements of DOE Order 413.2 are also carefully considered during the selection process to ensure that proposals are consistent with DOE criteria.

Project Approval: After all presentations are heard, the Committee arrives at a consensus concerning the highest priority proposals. Differences, if any, are resolved by the Chairperson. Some funding may be held in reserve during the earlier meetings of the fiscal year so that funds remain available for proposals submitted at later dates. The funding amount requested in any one specific proposal may be changed or adjusted during the approval process. The Committee's recommendation is then submitted to the Director for his approval.

The Assistant Laboratory Director for Finance & Administration then sets up a separate Laboratory overhead account to budget and collect the costs for the project. Statistics on the number of projects approved, compared to those rejected, show an overall approval rate of about 31 percent for new starts. From inception of the program through September 1998 (for FY 1999), 641 project proposals were considered and 201 were approved. Eight scientific departments were represented in the FY 1998 LDRD Program.

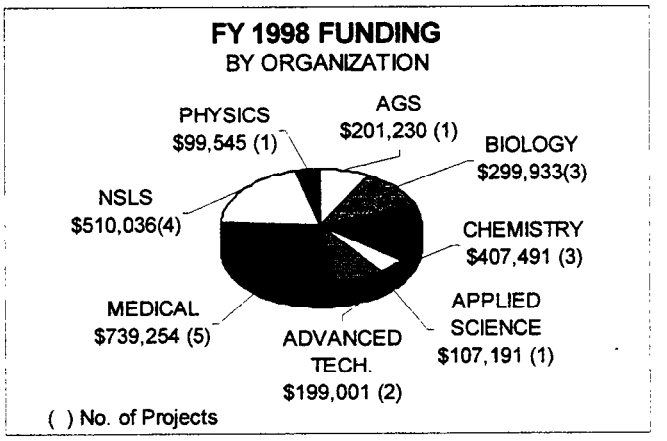

Project Supervision: Supervision over the actual performance of LDRD projects is carried out in the same way as other research projects at the Laboratory. Each principal investigator is assigned to an organizational unit (Department, Division), which is supervised by a manager.

Each manager is responsible for seeing that the obligations of the principal investigator are satisfactorily fulfilled and that the research itself is carried out according to standard expectations of professionalism and scientific method. The manager is kept informed of the project's status, schedule, and progress.

The manager ensures that the work is completed in a timely manner and that annual status reports are submitted to the Director.

In addition, LDRD Program activity is reported to the DOE Brookhaven Group Manager, including copies of all funded proposals, a LDRD Program data base, and a project funding and schedule summary report. *Project Reporting:* Routine documentation of each project funded under the LDRD Program consists of a file containing: (1) a copy of the written proposal; (2) all interim status reports; (3) notifications of changes in research direction, if any; and (4) reports on cost incurred. Also, a formal Annual Report on the LDRD Program is submitted to BNL management and the DOE, summarizing work progress, accomplishments, and project status on all projects.

Documentation for the overall Program consists of (1) various program history files, (2) a running list of all proposals with their acceptance/rejection status, (3) funding schedule and summary reports for all approved projects, (4) permanent records on cost accounting, and a data base containing information on each funded project (description, funding by fiscal year, status and accomplishments, follow-on funding, publications, etc.).

Some of the projects involve animals or humans. Those projects have received approval from the Laboratory's appropriate review committees. The projects which involve animals or humans are identified in this report as follows:

Note: This project involves animal vertebrates or human subjects.

This is noted on the summary sheet and also at the end of each report.

ALIGNMENT WITH DOE'S MISSION:

BNL is committed to exploiting the exceptional strength (including the LDRD Program) to mount programs of the highest quality that address DOE's Strategic Missions. Of the Four Businesses identified in the Secretary of Energy's Strategic Plan, Brookhaven National Laboratory contributes most strongly to Science and Technology.

While maintaining traditional strengths in science and technology, BNL intends to participate more effectively in the other three business areas defined by DOE: Energy Resources, National Security, and Environmental Quality.

Brookhaven National Laboratory's FY 1998 LDRD Program covered the following DOE mission areas.

Programs/Projects	Funding $000
Science & Technology	$2,258
Environmental Quality	207
Energy Resources	0
National Security	99
TOTAL	$2,564

SUCCESS INDICATORS:

Overall the BNL LDRD Program has been very successful. Some of the more common indicators/measures of success are: 1) amount of follow-on funding, 2) the number of patents applied for, and 3) the number of full-length pages published in other journals or publications.

An analysis of FY 98 projects shows that 1) Seven of the projects reported that proposals/grants had either been funded or submitted for funding, 2) Five projects have filed for a patent, 3) Thirteen formal journals were reported to be in publication or submitted for publication.

Summary of FY 1998 LDRD Program

In FY 1998, the BNL LDRD Program funded 20 projects, 4 of which were new starts, at a total cost of $2,563,681. The small number of new starts was a consequence of severe financial problems that developed between FY 1997 and 1998. Emphasis was given to complete funding for approved multi-year proposals. Following is a table which lists all of the FY 1998 funded projects and gives a history of funding for each by year.

Several of these projects have already experienced varying degrees of success as indicated in the individual Project Program Summaries which follow. A total of 17 informal publications (abstracts, presentations, BNL reports and workshop papers) were reported and an additional 13 formal (full length) papers were either published, are in press or being prepared for publication. The investigators on five projects have filed for a patent.

Seven of the projects reported that proposals/grants had either been funded or were submitted for funding. The complete summary of follow-on activities is as follows:

Follow-on Activity of LDRD Projects

	Number of Projects
Informal Publications	**17**
Formal Papers	**13**
Grants/Proposals/Follow-on Funding	**7**
Patents/Disclosures Applied For	
CRADA Application	**5**

In conclusion, a significant measure of success is already attributable to the FY 1998 LDRD Program in the short period of time involved. The Laboratory has experienced a significant scientific gain by these achievements.

LABORATORY DIRECTED RESEARCH AND DEVELOPMENT
FISCAL YEAR 1998 SUMMARY OF PROJECTS

Project		Principal		Actual Costs			Proposed	Total
Number	PROJECT TITLE	Investigator	Dept.	FY 1996	FY 1997	FY 1998	FY 1999	Funding
95-03	Ultraviolet FEL Research and Development *	Ben-Zvi	NSLS	99,491	299,099	980		399,570
96-06	Positron Emission Magnetic Resonance Imaging (PEMRI)	C. Springer	CHEM	100,208	169,224	174,052	20,000	463,484
96-26	Research into New Database Methodology Based on the Object Protocol Model	E. Abola	BIO	14,394	98,792	94,249		207,435
96-27	Tailored Pulse UV/XUV Photon Source Development	L. DiMauro	CHEM	71,570	114,097	119,319		304,986
96-38	BNCT for Leukemia Through Ex-Vivo Purging of Bone Marrow	J. Coderre	MED	82,116	86,342	93,575		262,033
96-49	Autecology of the Peconic Bay Brown Tide Organism, Aureococcus anophagefferens	J. La Roche	DAS	98,405	103,357	107,191		308,953
96-50	The Development and Demonstration of Accelerator-Based BNCT Capability	D. Raparia	AGS	188,449	412,137	201,230		801,816
97-02	Physics Goals for a New Intense Muon Facility	W. Marciano	PHYS		91,434	99,545		190,979
97-08	A Novel Curved Proportional Counter for X-ray Powder Diffraction Studies at NSLS	D.P. Siddons	NSLS		96,666	99,509		196,175
97-16	Plasma Window for Transmission of Synchrotron Radiation	A. Hershcovitch	NSLS		60,475	56,022		116,497
97-29	Development of New Techniques in Picosecond Pulse Radiolysis	J. F. Wishart	CHEM		104,103	114,120		218,223
97-39	X-ray Circular Dichroism of Biological Macromolecules	J.C. Sutherland	BIO		94,131	106,038		200,169
97-44	X-ray Schlieren Computed Tomography	A. Dilmanian	MED		59,792	94,212	44,000	198,004
97-45	Biodistribution Toxicity & Boron Neutron-Capture Therapy in Animals Using Metallotetracarboranylporphyrins	M. Miura	MED		86,157	108,857		195,014
97-50	Development of Pump-&-Probe LIDAR for the In Situ Study of Fast Atmospheric Chemical Reactions	A.J. Sedlacek, III	DAT		99,066	99,778	100,000	298,844
97-68	Center for Imaging in Drug Abuse Research	N.D. Volkow	MED		0	332,828	350,000	682,828
97-70	Molecular Biological Markers as Potential Prognostic Indicators for BNCT	J. Capala	MED		99,822	109,782		209,604
98-23	Beam Enhancement in a High Brightness Electron LINAC	E. Johnson	NSLS			252,738	450,000	702,738
98-27	Novel Mechanisms of Hydroxy Fatty Acid Biosynthesis	J. Shanklin	BIO			99,646	104,000	203,646
98-42	Target Design for an AGS-based Spallation Neutron Source	J. Hastings	NSLS			100,787		100,787
98-58	Sensitive Detection and Rapid Identification of Biological Agents by Single Molecule Detection	M. Wu	DAT			99,223	100,000	199,223
	*Completed in FY97, FY98 cost is a late shipping changes							
		Totals		654,633	2,074,694	2,563,681	1,168,000	6,461,008

LABORATORY DIRECTED RESEARCH AND DEVELOPMENT

1998 PROJECT PROGRAM SUMMARIES

Positron Emission Magnetic Resonance Imaging (PEMRI)

Charles S. Springer, Jr. *96-06*
Manoj K. Sammi
Jean Logan
Christoph A. Felder
Xin Li
Ildiko Palyka
William D. Rooney
Jing-Huei Lee
Nora D. Volkow and
Alejandro V. Levy

PROJECT DESCRIPTION:

Three of the most powerful medical imaging techniques in use today are positron emission tomography (PET), single photon emission computed tomography (SPECT), and magnetic resonance imaging (MRI). In a major new initiative, the Department of Energy and Brookhaven National Laboratory (BNL) have recently moved to incorporate SPECT and MRI Laboratories with the two-decade old, world-renowned, PET Laboratory at BNL. The entity encompassing these is called the *Brookhaven Center for Imaging and Neuroscience* (BCIN). Two years ago, a new SPECT Laboratory was set up in the Medical Building. A new High-Field MRI Laboratory Building has been completed by BNL (1.25 M$), housing an MRI instrument purchased by DOE (3.64 M$) with help from NIH, which features a magnet with a field strength of 4 Tesla. This is one of the largest field strengths used for humans, and there are only nine such instruments in the world. The MRI Lab achieved its first human images in June 1996 and had studied almost 200 subjects by October 1998. During this period, the complex Nuclear Magnetic Resonance (NMR) system has also undergone a number of significant upgrades. A next-generation PET instrument has been recently installed in the PET Lab. The PET Building is diagonally across an intersection from the MRI Building.

A charter mission of BCIN is to develop synergistic combinations of these imaging techniques. We are going about this in the most fundamental way possible, and this requires understanding exactly what information each kind of image contains. A significant fact is that the major strengths and weaknesses of PET and SPECT are rather complementary to those of MRI. We will illustrate this with PET, but similar comments can also be made with regard to SPECT.

The PET technique has the incomparable strength of being able to detect tiny (picomolar) concentrations of any of the vast array of bioactive compounds that clever chemists can label with the PET isotopes of nature. On the other hand, metabolic MRI is restricted to the detection of only a few of the handful of metabolic compounds that have concentrations greater than one millimolar. The spatial and temporal resolution of PET, however, is rather poor (no better than a few mm, and minutes, respectively). In sharp distinction, anatomical MR images made from the strong, ubiquitous ^1H_2O signal (the [^{1}H] in tissue water is *ca.* 100 molar) can have very favorable spatial and temporal resolution (sub-mm, and seconds). At a slight sacrifice of spatial resolution, ultra-fast MR images can even be obtained in less than 100 ms.

PREVIOUS TECHNICAL PROGRESS - Fiscal Year 1997:

During Fiscal Year 1997, the level of operation of the new *High-Field MRI Laboratory* was slowly increased. Although

the instrument had become operational in June, 1996, and the first human image was made then, the RF electronics system was already over eight years old. Even though some studies were initiated, the quality of the data was such that most meaningful work utilized phantom samples and some animal (laboratory rat) models, with only slow progress in human imaging. The first *relaxographic* MR image of a human subject was obtained in *October 1996*. The first *functional* MR image of a rat was obtained in *December 1996*. The first dog and baboon images were acquired in *February 1997*. In *June 1997*, Dr. William D. Rooney joined the MRI Lab as Assistant Chemist.

TECHNICAL PROGRESS AND RESULTS - Fiscal Year 1998:

The NMR system was finally brought to a tolerable level of operation with the completion of an upgrade of the entire RF electronics system in *January 1998*. The first *spectroscopic* MR images of a human subject were made that same month.

We began experimental work on this project by learning to make MR images that are as compatible as possible with PET images of the same subject. Multiple image slices from either PET or MRI acquisitions can be mathematically combined, and then interpolated into three-dimensional data sets. In principle, these can then be re-sliced in any orientation desired, and analogous PET and MRI slices can be computationally *co-registered*. That is, the axes of the image data sets are centered and aligned, and the data set sizes are proportionally scaled until they are equal. However, one of the advantages of the MRI technique is that an image can be actually acquired for any slice orientation desired - simply by the appropriate adjustments of the three orthogonal magnetic field gradients used to obtain the image. Thus, error generated in the co-registration process can be minimized if the MR image slice acquired is as similar to the PET image slice as possible. Drs. Felder, Lee, Rooney, and Levy have devoted effort to this goal.

We then proceeded to obtain both PET and MR images of several subjects. In some cases, PET images were obtained of the same subject using different tracers, on different occasions. This is important because different tracers are differently localized in the brain, and therefore produce different PET images.

It is just as important to understand the nature of the MR image to be utilized. As stated in the Project Description above, virtually all MR images are made from the relatively strong ^1H_2O MR signal. They thus, in some way, represent maps of water distribution in the body. However, simple quantitative maps of water distribution - called *spin density* images - are rarely exhibited. This is because, though they have the high resolution of MRI, they show little *contrast*. Water is rather uniformly distributed throughout most tissues.

Therefore, the exquisite contrast usually seen in MR images comes from a different source. To obtain this, appeal is made to different properties of the ^1H_2O MR signal - its relaxation times, T_1, T_2, or sometimes $T_{1\rho}$. These measure the rates at which the ^1H_2O magnetization returns to its equilibrium values (along different axes) after being perturbed by an RF pulse - or the rates at which the consequent MR signal disappears, when measured along different axes. It turns out that these properties differ for different tissues - mainly because of differential interactions of water molecules with macromolecules and macromolecular assemblies. By choosing a specific time

during magnetization recovery, great contrast can be achieved because the signals from different tissues are recovering at different rates and they have different strengths at this time. However, the contrast comes at the cost of discarding some ^1H_2O signal from each of the tissues (because they are all recovering) in different amounts. The images are no longer quantitative. Such images are called T_1-, or T_2-weighted MR images, and they comprise probably more than 90% of all MRIs used for clinical diagnosis.

Although there have been a number of reports of the combination of T_i-weighted MR images with PET images in the literature, these result in a contamination of the quantitative property of the PET (or SPECT) data with the non-quantitative MR image. We wish to avoid this problem.

In 1991, we introduced a fourth kind of fundamental MR image, the *relaxographic* image (RI).[1] This is an image made from a discrete portion of the distribution of T_1 values that completely describes the recovery of the MR signal - the *relaxogram*. The sum of all of the RIs that can be made from the relaxogram equals the spin density image.[2] Thus, the RI is an elemental component of the spin density image, edited to display the loci of the spins enjoying a particular range of T_1 values.[2] Since *all* of the MR signal is used to produce the relaxogram, all of the spins are represented. Given this, the RI is *quantitative*. It shows *all* of the spins -with those T_1 values. But, it also exhibits high resolution, and the high contrast lacking in the spin density image.

Investigators have also developed methods for combining spin density image data with T_i-weighted image data using post-acquisition processing to produce high-contrast, edited-quantitative images. This procedure is termed *segmentation* in the literature, and a recent example can be found in reference 3.[3] Thus, relaxographic images are *naturally segmented* images.[4] The segmentation process usually assumes that all the ^1H_2O signals from the spins in a segment - say white matter - have the same relaxation time. Our results suggest that this is not really true.[5] Also, the extent to which relaxographic peak components (like white and grey matter) do actually overlap puts a natural constraint on the success that the segmentation procedure can achieve. Mr. Li has just begun work on ways to achieve curve resolution of relaxograms. Mr. Sammi and Dr. Levy are pursuing post-acquisition MR image segmentation.

In any case, it is relaxographic (or segmented) MR image data that should be combined with PET data for the same slice. This maximizes the quantitative nature of the resulting image. There are two general ways that the PET and MR image data can be combined: in the *real-space domain*, to produce what we call a PETAMR image, or in the *Fourier-space domain*, after which a Fourier transformation produces what we call a PEMR image.

The first step in either of these procedures is the co-registration of the data from the two different imaging modalities. Real space data from analogous PET and MR image slices have been co-registered using literature methods, as well as the new GALAXY technique developed by Drs. Levy and Logan, along with other members of the BNL PET group.[6]

Mr. Sammi has been working to produce PETAMR images. In the last fiscal year he has made tremendous progress. He has determined that if a rational color-scale is used to encode the PET data, true hybrid PETAMR images can be produced that

retain the information of both PET and MR. The quantitative PET information is encoded as mostly the *hue* of the color. Since this is reasonably independent of the *value* (brightness) of the color, the latter can then be replaced with the intensity of the MR image for each of its pixels. Now, the PETAMR image has the pixelation (resolution) of the MR image, but retains the exquisite PET tracer sensitivity. If the MR image also has high contrast (as above) that matches that of the PET, the MR image also "edits" the PET image so that the high-resolution of the PETAMR image becomes evident.

Exciting results obtained by Sammi are seen in the Figure. The images in the left column are PET, and in the middle column MR, maps of axial brain image slices for each of four different subjects (rows), and have already been co-registered. The PET images were made with the ^{18}F-labeled deoxyglucose (FDG) tracer. Since this is a metabolically-incompetent glucose surrogate , the intensity of pixels in such an image is proportional to the metabolic activity of cells in the voxels represented by those pixels. It is known that FDG is trapped to a considerably greater degree in grey matter (GM),[7] and this is evident in the contrast seen in the PET images at the left of the Figure. (The Figure presents the PET intensity as the hue of the rainbow color-scale - so that the redder the pixel color, the more FDG trapped. In fact, the hue magnitude is a linear measure of the glucose metabolic rate in these cases.) However, because of the relatively poor resolution of the PET images [nominally $(3.6\ mm)^2$ for the top three images, $(6.7mm)^2$ for that in the fourth row], the grey matter anatomy is not very evident. In comparison, the MR images in the middle [nominally $(0.94\ mm)^2$ resolution for the top three, $(0.78\ mm)^2$ for that in the fourth row] display GM in considerable detail. These MR maps are relaxographic images (the bottom one is conventionally segmented), quantitatively representing GM water.

Mr. Sammi combined the real-space data of these PET and MR image pairs. The right column of the Figure shows the resulting PETAMR images. These beautifully combine the metabolic information of the PET images, in their pixel colors, and the high spatial definition of grey matter evident from the MR image. The approach employed by Sammi, and described above, essentially uses the PET pixel hue to "color" the underlying MRI pixels, which were originally rendered in gray-scale tones.

It is obvious that, with this technique, if an MRI pixel is black the corresponding PETAMRI pixel is black, even if the overlying PET pixel had some color. The information contents are combined in a multiplicative manner. Thus, the PETAMR images seen in the Figure are *"grey matter-edited" FDG images* - maps of only the GM FDG. The small amount of PET intensity not arising from GM has been discarded from these images. It is not irreversibly dispensed with, however. The relaxographic imaging technique also yields quantitative white matter (WM) water MR images of the same slices. In work not shown, these were also combined with the PET FDG images to produce "WM-edited FDG" PETAMR images.

The images in the first two rows of the Figure represent axial periventricular slices at the level of the *caudate* and *putamen* structures in the *basal ganglia*, and of the *thalamus*. The perspective of these views is such that the front of the brain is at the top, and the left side of the brain is the right side of the image. The first row represents a healthy male volunteer while the second row

a healthy female volunteer. Since the slice in the top row is very slightly oblique, the left caudate and right putamen interior brain structures are slightly more intense than their contralateral counterparts. In the second row, all of these are particularly bright, as well as are the two thalamus structures. In each case these structures are more sharply demarcated in the PETAMR images than in the PET images. Particularly striking is the clear definition of the cortical grey matter in the PETAMR images. The individual sulci and gyri are quite distinct. If one wished to quantify the glucose metabolic activity occurring in a particular gyrus, it would be quite possible using a PETAMR image. One could compare this from state to state in a given subject, or from subject to subject in a given state. The third row represents a slightly more superior axial slice in the brain of a male volunteer with a history of substance abuse (a major research area at BCIN). Moreover, the FDG PET image was acquired during the presence of a pharmacological level of ethanol in the subject's brain. For these many reasons, the total FDG activity in the brain slice is considerably reduced. Nonetheless, there is excellent correlation with the GM water MR image (obtained when no ethanol was present), and the PETAMR image displays the same sorts of enhancements as seen in the two rows above. The last row presents an oblique slice of a different male volunteer. In this case the slice is parallel to the canthomeatal line in the brain. Thus, it is more superior in the frontal regions of the brain, and more inferior in the back. In fact, in this case, it intersects the top portion of the *cerebellum* in the rear, and this is quite visible in the MR image. Nonetheless, there is little glucose metabolism in the cerebellum in this resting state and thus the FDG intensity is weak. Therefore, the cerebellum is not very evident in the PETAMR image. This demonstrates a rather elegant manifestation of our approach.

Drs. Logan and Levy have also begun to implement the new method outlined in the original proposal - the PEMRI of the title. This involves combining the data from the two experiments at a fundamental stage of image representation. Specifically, the Fourier-space images are convolved. These are the Fourier transforms of the real-space images. (The MR Fourier-space image is often called the k-space image.) The Fourier-space images are types of interferograms that exhibit only diffraction-type patterns, not the objects of real space. In the PET Fourier-space image, the PET inculcates metabolic information in the low spatial frequency components.[8] The MRI $^{1}H_2O$ intensity, however, supplies the high spatial frequency components not present in the PET data. The convolution is carried out following the general principles underlying the Constrained Reconstruction Methods.[9] After the appropriate convolution of the PET and MRI Fourier-space images, a back Fourier transformation produces a *hybrid* real-space image that contains information from both basis images. We call it a *positron emission magnetic resonance image* (PEMRI) and, in principle, it also can present PET tracer mapping with a spatial resolution approaching that of MRI. As stated above, the latter is (generally speaking) about an order of magnitude greater than the spatial resolution of PET. If the MR image used is a relaxographic, or segmented, image, however, the PEMRI process concentrates all of the PET intensity into only the regions illuminated in the MR image, even if is not located there in reality. Dr. Logan is exploring the consequences of this aspect using computer simulations and data from a phantom sample. Her early results are encouraging, and she is about to

begin work with some of the brain image data shown in the Figure.

Thus, PETAMRI and PEMRI represent the synergistic enhancement of *both* the PET and MRI images. A SPECT analog could be called SPEMRI (single photon emission magnetic resonance image). Of course, this approach can be applied to the combination of ultrasound, or x-ray (CAT scan) image information with MRI information (USOMRI, CAMRI ?). The analogous data from any pair of imaging techniques can be convolved according to these fundamental principles. This also includes data from MR spectroscopic (MRS) images as well. These often have spatial resolution similar to those of the nuclear medicine methods. In fact, Mr. Sammi has made some initial effort on this. The PEMRI method will also be useful for the data set pairs acquired from a combination PET/MRI instrument. Though we are not convinced of the wisdom of the latter approach, at least one group is involved in constructing and testing a prototype device for small animal models.

REFERENCES:

1. C. Labadie, T. M. Button, W. D. Rooney, J-H. Lee, and C. S. Springer *Proc. Soc. Magn. Reson. Med.* **10** 1218 (1991).

2. C. Labadie, J-H. Lee, G. Vetek, and C. S. Springer *J. Magn. Reson., B* **105** 99-112 (1994).

3. Y-H. Kao, J. A. Sorenson, and S. S. Winkler *Magn. Reson. Med.* **35** 114-125 (1996).

4. I. Palyka, J-H. Lee, K. Ugurbil, M. G. Garwood, and C. S. Springer *Proc. Int. Soc. Magn. Reson. Med.* **4** 1642 (1996).

5. I. Palyka in *Relaxographic and Functional Magnetic Resonance Imaging*, Ph.D. Dissertation, State University of New York, Stony Brook, New York (1997).

6. A. V. Levy, D. L. Alexoff, F. Hode, M. Denis, D. Bertollo, A. P. Dhawan, J. Logan, A. B. Andrews, and N. D. Volkow *Proc. IEEE/EMBS*, **18** 452 (1996).

7. J. C. Mazziotta, and M. E. Phelps, Chapt. 11 in *Positron Emission Tomography and Autoradiography: Principles and Applications for the Brain and Heart*, Ed. by M. Phelps, J. Mazziotta, and H. Schelbert, Raven Press, NY (1986), pp. 493-579.

8. A. V. Levy, F. Gomez-Mont, N. D. Volkow, J. F. Corona, J. D. Brodie, and R. Cancro *J. Nucl. Med.* **33** 287-295 (1991).

9. Z-P. Liang, F. E. Boada, R. T. Constable, E. M. Haacke, P. C. Lauterbur, and M. R. Smith *Rev. Magn. Reson. Med.* **4** 67-185 (1992).

PAPERS/JOURNALS/PUBLICATIONS:

We have described the relationship between relaxographic and segmented MR images.

- "'Natural' Segmentation in Efficiently Computed Relaxographic Images" I. Palyka, J-H. Lee, K. Ugurbil, M. G. Garwood, and C. S. Springer *Proc. Int. Soc. Magn. Reson. Med.* **4** 1642 (1996).

Dr. Levy and his co-workers have described their registration approach.

- "The GALAXY Method for the 3-D Spatial Registration of PET Images to Talairach Brain Atlas" A. V. Levy, D. L. Alexoff, F. Hode, M. Denis, D. Bertollo, A. P. Dhawan, J. Logan, A. B. Andrews, and N. D. Volkow *Proc. IEEE/EMBS*, **18** 452 (1996).

We have submitted a large paper describing the PETAMR approach, and are preparing another describing PEMRI.

- "The Intimate Combination of Low- and High-Resolution Image Data: I. Real-Space PET and ^1H_2O MRI, PETAMRI" M. K. Sammi, C. A. Felder, J. S. Fowler, J-H. Lee, A. V. Levy, X. Li, J. Logan, I. Palyka, W. D. Rooney, N. D. Volkow, G-J. Wang, and C. S. Springer *Magn. Reson. Med.*, submitted for publication.

- "The Intimate Combination of Low- and High-Resolution Image Data: II. Fourier-Space PET and ^1H_2O MRI, PEMRI" J. Logan, A. V. Levy, J-H Lee, F. Hode, C. Felder, D. Alexoff, J. S. Fowler, and C. S. Springer, in preparation.

LDRD FUNDING:

FY 1996	$ 100,208
FY 1997	$ 169,224
FY 1998	$ 174,052

PET IMAGE MR IMAGE PETAMR IMAGE

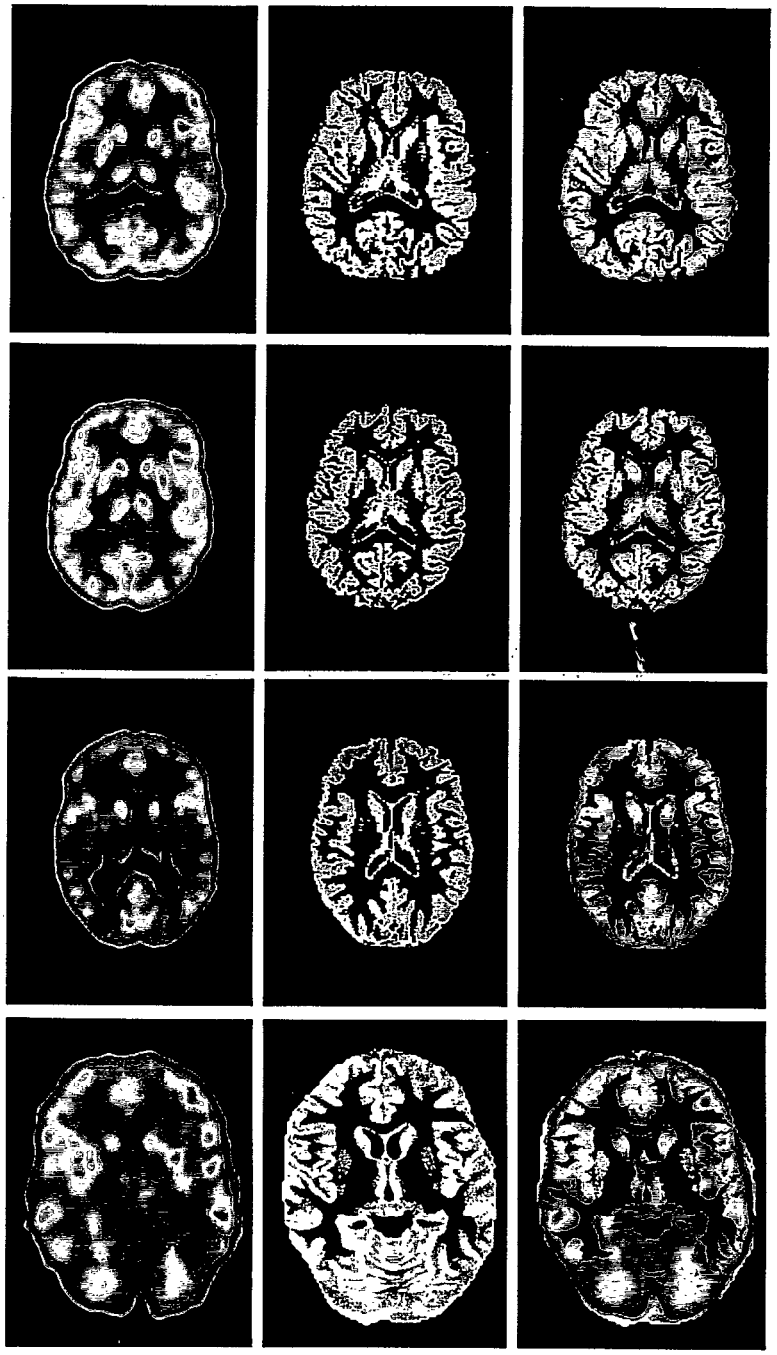

Research into New Database Methodology Based on the Object Protocol Model

Enrique E. Abola 96-26
Joel L. Sussman

PROJECT DESCRIPTION:

The scheduled completion in 2003 of efforts to sequence the human genome has generated increased interests in identifying and understanding the biological role of gene products. Attempts are now being made to develop protocols that will allow for large-scale studies to identify the functions of proteins encoded in the genome. Dubbed *Structural Genomics*, these studies along with rapid developments in structural and molecular biology have resulted in dramatic increases in the size and complexity of data that must be captured in biological database systems. Researchers need immediate access to these data using query systems that are powerful, intuitive, and allow questions to be cast using natural language constructs.

This project addresses computational and data management needs of structural genomics through the construction of database systems that can access all data and knowledge inherent in structural and sequence studies. It includes the development of tools and protocols that identify, access, and return data related to Protein Data Bank (PDB) objects which reside in other biological and chemical databases.

We address issues such as data representation and data access in structural biology using the contents of the PDB.

Results of the study will help in understanding of what is required to build systems that addresses user demands, expected to increase dramatically in the near future.

TECHNICAL PROGRESS AND RESULTS - Fiscal Year 1998:

Purpose: The project has several objectives culminating in the installation of a database available on the Internet:

a) Development of a web-based query system with support for searches using ad-hoc queries,

b) Development of tools and auxiliary data resource for describing and managing chemical and structural information on biologically and medically important ligands that bind to proteins,

c) Development of tools for deposition of data into the database,

d) Development of 3DBase, a structural database based on the contents of the Protein Data Bank.

The primary objective of this study is to build a database system capable of answering complex ad-hoc queries on biological systems. For example, large-scale studies that are aimed at defining the structural folds of approximately 100,000 proteins in the human genome will require answers to questions on the relationships among sequence, structure, and function across genomic lines. The database query system that can support these queries will require access to programs that do homology building, threading, sequence and structure comparison, molecular viewing, etc.

The system must be capable of answering these diverse questions. It must be highly flexible, easily extended or modified to reflect our changing understanding of biological processes. It must be interconnected to other databases. It also must be capable of using new computational tools as they arise.

Approach: Data modeling work needed to support the activities described above were done using the Object Protocol Model (OPM) developed by Dr. Victor Markowitz at Lawerence Berkeley Laboratory (LBL) and Data Logic Inc. OPM provides a complete database design and data management toolkit. The database itself was implemented on a SYBASE engine. A description of OPM is accessible via: (http://www.genelogic.com/opm.htm)

Programs for data deposition, *AutoDep ver. 2.1,* and for data browsing, *3DB-Browser,* were developed for use on the Web. This deposition system is a crucial component of 3DBase as data loading tasks are facilitated by its use.

The web browser *3DB-Browser* was developed in collaboration with Dr. Jaime Prilusky from the Weizmann Institute of Sciences. This form-based query system is capable of linking information stored in the PDB with those found in other relevant databases. It uses both the *Glimpse* text retrieval system and SYBASE SQL queries in answering questions entered through a form.

Finally, we collaborated with Dr. Manfred Hendlich from University of Marburg to adopt his ligand database, RELIBASE, and his program, *Bali,* for use in this project. RELIBASE and Bali provide a powerful environment for describing and managing chemical and structural information on small organic molecules (e.g. inhibitors, cofactors, etc.) that bind to proteins.

Technical Progress and Results:
Development of Data Deposition Tools:
A new version of PDBís deposition tool, *AutoDep 2.1*, was released last July 1998. This new version supports PDBís layered-release protocol that allows for the immediate loading of a well-defined and automatically validated set of newly deposited entries without staff intervention.

The new version represents a major rewrite of the deposition tool and is now the test-bed for analyzing the effects on data quality and data processing throughput rates of entries released without staff participation. This new data deposition protocol is crucial for bioinformatics resources as the expected growth in information and knowledge is projected to be exponential in size and complexity while operating funds for these resources are expected to decrease.

Since its release the new deposition tool has proven to be a popular tool with over 90% of depositions to the PDB now being done using AutoDep. In addition, new data release mechanisms provided by the layered-release protocol has dramatically reduced the number of entries being placed on-hold for a year. Most depositors now opt to have the data released immediately after publication of their paper.

The deposition tool is available via the internet- (http://www.pdb.bnl.gov/pdb-docs/submit_page.html)

Development of tools for handling ligands in PDB entries:

A new tool was developed for entering into PDB archives information related to ligands bound to protein molecules. This new tool developed in collaboration with Dr. Hendlich and Dr. Prilusky performs automatic searches in PDB databases for matches to ligands included in newly deposited entries. Candidate hits are returned to users via an html page. Users are then requested to verify the exact identity of the new group through a choice list. Groups not currently in PDB entries are characterized using software developed as part of this work. An alpha version was demonstrated last July and work is underway to integrate the product with AutoDep.

Database Development: The current implementation of the database, 3DBase and its query system can be accessed via

(http://bach.pdb.bnl.gov:5000/pdb-docs/.proposal/OPM-Java.html)

The OPM schema for 3DBase is accessible via the URL given above. The database contains all the information needed to manage the PDB resource, as well as data describing the molecular contents of a PDB entry. The database supports not only user queries but also all functions related to acquiring, annotating, and managing data. We are using new features of OPM, such as Application Specific Data Types (ASDT), that associate methods to object classes and provide PDB with the necessary features to construct the database.

The database contains five major types (class hierarchies) of objects:

1. objects containing information on the experimentally determined 3-D structures,
2. objects containing meta-information on the complete MSD/PDB system,
3. objects containing meta-information on external information resources on the Internet,
4. objects containing meta-information on MSD/PDB users, and
5. objects containing meta-information on underlying application domain of structural biology.

Type (1) objects correspond to annotated PDB entries. They contain basic information on the 3-D atomic model; the underlying experimental procedures and results (raw data); the individuals and institutions who produced and deposited the entry; related publications and linked data-objects in relevant electronic resources such as protein sequence or function databases; notable structural or other domains and features that can be mapped to the 3-D model; and other physical, chemical, or biological annotations.

Examples of Type (1) objects are descriptions of molecular and chemical contents described by the 3DBase object class *oAggregate*, or secondary structure assignments based on depositors' judgement, or secondary structures algorithmically assigned using programs such as STRIDE or DSSP described in the object class *oHelix*.

Type (2) objects collectively provide the complete declarative definition of what the archive is and what it does. They capture the structure (syntax), behavior (methods), and meaning (semantics) of all Type (1) objects, and all archived components (3DB-AutoDep, 3DBase, 3DB-Browser) and their parts. Items in the AutoDep data dictionary, such as program prompts and data validation methods, are Type (2) objects. Another notable example is workflow-associated objects used in processing and managing entries.

Type (3) objects capture necessary information on external resources referenced (*via* links) by Type (1) objects (archive entries). For each external resource, Type (3) objects typically contain a description, Internet addresses and access protocols, and data-access methods. Type (3) objects provide semantic links to other databases such as Swiss-Prot and GenBank.

Type (4) objects contain names, addresses, passwords, and other information on the depositors, as well as characteristic information on different end-users (data consumers). The latter will enable us to present different views of the archive to different types of end-users. For example, crystallographers and chemists may want to see entries at different level of detail than gene mappers and evolutionary biologists. Finally, Type (5) objects will capture the referential semantics of all aspects of the Type (1) objects. These objects constitute a glossary that associates all items from the archive entries with specific domain terms (e.g., an asymmetric unit or active site); each will have sufficient definitions, descriptions, and examples that their usage in the database is completely and unambiguously understood by investigators and other users knowledgeable of the application domain.

PAPERS/JOURNALS/PUBLICATIONS:

J. L. Sussman, D. Lin, J. Jiang, N.O. manning, J. Prilusky, O. Ritter and E. E. Abola, "Protein Data Bank (PDB): Database of Three-Dimensional Structural Information of Biological Macromolecules," *Acta Cryst.*, (1998). D54, 1078-1084

LDRD FUNDING:

FY 1996	$ 14,394
FY 1997	$ 98,792
FY 1998	$ 94,249

Tailored Pulse UV/XUV Photon Source Development

Louis F. DiMauro and *96-27*
Erik D. Johnson

PROJECT DESCRIPTION:

The arbitrary shaping of temporal laser pulses at visible and ultraviolet wavelengths is being studied. Applications include the design of an optimal pulse shaped for efficient photoemission from an ejector rf-electron gun for linear accelerators. Additional investigations are also proposed on the production of high harmonic radiation above 10 eV photon energies for use as a seed pulse in the DUV-FEL project at the Source Development Laboratory.

PREVIOUS TECHNICAL PROGRESS:

The initial stage of this LDRD was focussed upon the design, setup and installation of a laser laboratory at the Source Development Laboratory (Bldg 729). The laser laboratory provides high-powered light for photocathode operation and future DUV-FEL demonstrations. A 400 sq. ft., class-1000 clean room housing 115 sq. ft. of optical table space became operational in August 1997. A 10 Hz, high-powered titanium sapphire laser system underwent initial installation at the end of September 1997.

Concurrent with the SDL effort, an atomic beam source was installed into the P.I.'s laboratory in the Chemistry building (555A). This apparatus was designed to generate high harmonic (HHG) radiation as a potential injector source for the DUV-FEL. During the construction phase, initial experiments were performed in collaboration with Dr. Pierre Agostini (Saclay, France) using the Saclay facilities. The objective was to test the use of a doughnut spatial mode in the fundamental beam to produce a uniform harmonic beam while accommodating the simple separation of the fundamental beam after the HHG source. This scheme worked very successfully. Figure 1 shows a CCD camera image of the 17^{th} harmonic (25 eV photon energy) produced by this experimental geometry. The harmonic beam is circular and bright, containing approximately 10^9 photons per shot.

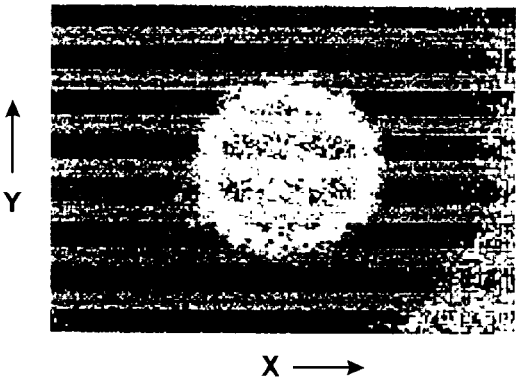

Figure 1 Spatial profile of the 17^{th} harmonic beam produced by excitation of argon gas by a titanium sapphire beam.

TECHNICAL PROGRESS AND RESULTS - Fiscal Year 1998:

Purpose: BNL has launched several accelerator-based initiatives in recent years which rely upon the production and control of intense, short pulse, UV and VUV/XUV radiation. The 10 MeV Pulsed Radiolysis Facility (CRCR), the Accelerator Test Facility and the Source Development Laboratory (SDL) are all based on photocathode electron guns which require a short wavelength (UV) drive laser, with the latter having the additional requirement of a synchronized VUV/XUV injector beam for

the DUV-FEL project. Optimization of these experiments can be achieved in part by direct control over the temporal profile of the radiation pulse. One aim of this project is to develop strategies of efficient production and control of arbitrary pulse shaping in the UV-XUV range. Sources of this type will also be valuable tools for optimal control methods in atomic, optical, chemical and materials science. The second objective is directed at the development of a high harmonic source of coherent XUV radiation as a primary and sub-harmonic injector beam for the DUV-FEL project. This development can be pivotal in extending the advantages of the seeded beam approach to FELs into the soft x-ray regime. The research proposed in this document remains a necessary and vital "missing" component for numerous BNL initiatives.

Approach: Rapid advances in optical engineering, such as the advent of chirped pulse amplification (CPA) to generate intense, ultra-short visible laser pulses and progress in the optical telecommunication sciences, has provided the tools necessary for the production of arbitrarily shaped pulses of coherent radiation. The experimental challenge is to synthesize these techniques and create intense, encoded UV-XUV coherent pulses. The fundamental principle is that an ultra-short laser pulse is governed by a simple transform relationship that connects the pulse duration with its bandwidth. The shorter the pulse is in time, the larger is the bandwidth associated with the laser's central frequency. Chirped pulse amplification makes use of this simple relationship for amplifying ultra-short pulses to gigawatt or greater peak powers while minimizing the potential for optical damage to critical amplifier components. The actual implementation of the CPA technique is accomplished by the use of dispersive optical elements, i.e. gratings, prisms, before and after amplification and is illustrated in Figure 2. A *weak*, ultra-short pulse first enters a stretcher apparatus which elongates the pulse in time by at least a factor of a thousand. This enables the efficient extraction of gain from the amplifier medium by lowering the peak power of the pulse by the same factor. Once the gain has been extracted the *amplified* pulse is ejected into the compressor which reconstructs the temporal shape of the input pulse but with increased power (by a factor of 10^6). Thus, the stretcher and compressor provide the proper mathematical optical transform function for performing this operation.

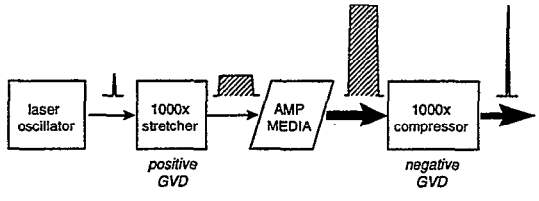

Figure 2 Chirped pulse amplification scheme.

The physical arrangement of the stretcher allows the incorporation of additional optical components which permits the controlled alteration of the input spectrum. The spectrum is altered in such a way that it transforms after the compressor gives the desired pulse shape which differs from the original input pulse. For instance, proper modulation of the frequency spectrum of a temporal gaussian input pulse in the stretcher will transform it into a temporal square wave pulse following compression. It is easy to imagine that illumination of a photo-cathode with a square pulse will produce a more uniform electron beam as compared to a standard gaussian envelope. The technical development involves the extension of known shaping techniques and

principles used for low powered visible beams into the high powered, UV range.

Technical Progress and Results: A Spectra-Physics/Positive Light laser system purchased by the NSLS was used as the initial platform for producing 800 nm light at the SDL building. Implementing the CPA approach outlined above, 100 fs pulses with 25 mJ energy at a 10 Hz repetition rate was produced. A number of issues were immediately apparent for successful SDL operation. These included (1) synchronization to the 81.6 MHz external rf clock of the LINAC (2) transverse mode quality (3) shot-to-shot energy stability (4) third harmonic generation for photocathode operation and (5) implementation of adequate diagnostic systems.

Synchronization of the titanium sapphire oscillator was accomplished by active feedback of the laser oscillator's cavity length to a sub-harmonic at 81.6 MHz of the LINAC's rf-source. An optical isolated 3 dbm rf-line was installed into the laser laboratory. The external reference replaced the local oscillator of the titanium sapphire oscillator. The phase stability was determined by cross-correlating the output of the titanium sapphire oscillator with a Nd:YLF oscillator located in the Chemistry department. The measurement showed that the phase stability was equal to or less than the 3 ps resolution of the instrument. This value equates to an upper limit of 2.5° stability in the LINAC operation.

A number of significant mechanical and optical modifications were implemented on the CPA amplifiers to improve both spatial mode and energy stability. Mode quality was improved by a hard spatial filter placed at the beam waist of the regenerative amplifier section. This minimized the long term drift of the mode quality produced by thermal lensing in the regenerative amplifier's pump laser. Stable lowest order mode operation is obtained on a daily basis. Energy instabilities in the system were introduced by two sources. Mechanical instabilities resulted in amplitude fluctuations due to poorly designed optical mounts in some of the commercial components. Replacement of these components with high quality mounts resulted in improved energy stability and better daily reproducibility of the optical beam path. Fluctuations in the amplifier's pump beam energy also resulted in significant instabilities. By running the amplifier into saturation by modifying the optical design, fluctuations were minimized to the shot noise of the pump laser. Currently, this noise is higher than desirable but could be improved by the manufacturer.

The production of UV light for illumination of the rf-photocathode was accomplished using nonlinear optics. Using a series of phase-matched nonlinear crystals, the 800 nm output of the titanium sapphire fundamental was frequency tripled to 266 nm. This wavelength exceeds the work function of the magnesium cathode material for producing photoelectrons and is similar to operational electron guns at other facilities. The third harmonic output exceeds 3 mJ pulse energy and easily meets our initial requirements for illumination of the rf- gun photocathode. The efforts described above for improved fundamental performance significantly increased the mode quality of the third harmonic beam. Pulse shaping is accomplished by the introduction of an amplitude mask into the stretcher section of the CPA. Final shaped light characterization was not possible due to lack of adequate diagnostics for the UV pulse. A frequency resolved optical gating instrument has been ordered by the NSLS.

This instrument will allow full determination of the UV pulses amplitude and phase. However, significant optical diagnostics of the titanium sapphire fundamental was constructed and incorporated into the system.

A high priority was place over the last year in the design and construction of an optical transport system and gun hutch optical system for delivery of the 266 nm light to the gun hutch. This scheduling plan was in preparation for delivery of the gun assembly from Stanford in early 1998. The designs for a vacuum transport line assembly was completed and constructed at the NSLS. These components are awaiting installation at the SDL building. A optical table has also been received and is undergoing placement in the gun hutch. Preliminary design of an optical relay system has been modeled. The design incorporates both spatial shaping and wave front correction of the 266 nm light for optimum emittance performance of the rf-photocathode.

A future requirement for the UP-FEL project is the need for a coherent VUV/XUV source of seed radiation in the 100-50 nm range. Generation of high harmonic radiation from high-density inert gas jets produced by intense field irradiation is one viable seed source. The major engineering issue is the effective coupling of the high harmonic radiation into the experimental target chamber, i.e. the DUV-FEL wiggler. Optimization of the harmonic throughput onto a target depends upon a number of experimental parameters, i.e. optics, phase matching. One key problem hampering the efficient extraction of the harmonic radiation was solved in the previous year. We have demonstrated an efficient method for separating the collinear harmonic radiation from the more intense, fundamental drive laser beam using a novel excitation geometry.

The harmonic apparatus designed in FY 1997 based on the Saclay design was installed in the chemistry building. The vacuum and detection system was characterized and found to give adequate performance. Gas target densities exceeding the Saclay design allowed for the production of high harmonic radiation from inert gas clusters. Cluster targets have been reported in the literature to produce ten times more harmonic photons than the single atom. We have not independently verified this result but are in the process. Space has been designed into SDL laser room to accommodate this apparatus for DUV-FEL seeding of the NISUS wiggler. Currently we are evaluating the use of hollow core optical fibers for producing phase-matched VUV/XUV radiation.

LDRD FUNDING:

FY 1996	$ 71,570
FY 1997	$ 114,097
FY 1998	$ 119,319

BNCT for Leukemia Through *Ex Vivo* Purging of Bone Marrow

Jeffrey A. Coderre *96-38*
and John D. Glass

PROJECT DESCRIPTION:

The overall objective of this project is to experimentally determine the feasibility of using boron neutron capture therapy (BNCT) to purge bone marrow *ex vivo* prior to autologous bone marrow transplantation.

TECHNICAL PROGRESS AND RESULTS - Final Report:

Purpose: Many leukemias and lymphomas respond, initially, to chemotherapy, then become resistant to the therapeutic drugs. At this point, the patient can be saved only by eradicating his hemopoietic tissue and replacing it with healthy, genetically compatible marrow through a transplant.

Genetic matching for a marrow transplant is exacting: a match with a high probability of compatibility is often not available. The transplant recipient is a perfect genetic match with himself, but his own marrow is the source of his disease. The concept of an autologous transplant is, 1) to remove some of the patient's own marrow from his body, 2) eradicate the remaining diseased marrow from his body, 3) selectively remove the malignant cells from the harvested marrow, then 4) return the purged marrow to the donor /recipient. So far, the third step in this process is not very well perfected: a high percentage of autologous transplants result in recurrence of the original disease. Our objective is to selectively remove malignant cells from bone marrow with BNCT.

Approach: Our approach to cleansing bone marrow of malignant cells is to selectively deliver boron-10 to the malignant cells using boron-containing analogs of metabolites. Irradiation of the bone marrow sample would then selectively kill the boron-loaded malignant cells while sparing the normal bone marrow stem cells.

Milestones in the development of BNCT for bone marrow purging include: 1) synthesis of boron compounds; 2) demonstration that the boron compounds selectively accumulate in leukemia cells; 3) *in vitro* BNCT of leukemia cells with the new boron compounds; 4) measure survival of normal bone marrow stem cells under BNCT conditions; 5) BNCT *in vitro* of bone marrow mixed with leukemia cells; 6) *in vivo* rescue experiments, bone marrow transplant in mice injected with leukemia cells. Milestones 1-4 were completed under this LDRD funding. NIH grant support will be sought to complete milestones 5 and 6.

Results:
An asparagine analog: 3-boronoalanine: In the first year of the project, the principle metabolite analog being considered was 3-boronoalanine, an analog of asparagine. Many leukemia and lymphoma cells have an unusual requirement for exogenous asparagine (Broom, 1963). This is exploited in the clinical setting by adding the enzyme asparaginase to blood or culture medium to deprive the tumor cells of asparagine. 3-Boronoalanine is a structural analog of asparagine, or more precisely, a structural analog of a transition-state intermediate in the hydrolysis or transamination reactions at the asparagine side-chain. We reasoned that 3-boronoalanine might be a tight binding inhibitor of enzymes in the asparagine-requiring leukemia cells. The compound was prepared by a published procedure (Kinder, 1987). Using methodology to measure the

intracellular boron content following incubation in boron containing medium (Capala, 1996), we showed that 3-boronoalanine delivered boron more efficiently to asparaginase-sensitive (asparagine-requiring) cells than to asparaginase-resistant (asparagine-sufficient) cells (Figures 1 and 2). This is consistent with our understanding of 3-boronoalanine as an asparagine analog.

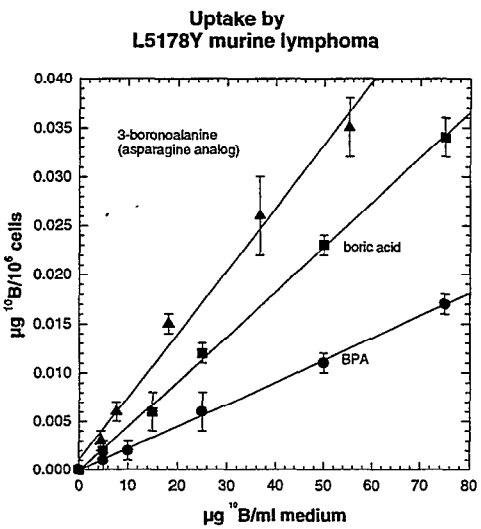

Figure 1. Asparaginase sensitive L5178Y murine leukemia cells concentrate the asparagine analog, 3-boronoalanine, compared to metabolically inactive boric acid which is uniformly distributed in cells and the medium. *p*-Boronophenylalanine (BPA), which is strongly concentrated in melanoma and glioma cells, is actually excluded by L5178Y cells, showing lower accumulations than the boric acid control.

3-Boronoalanine did show selective accumulation in both leukemia and lymphoma cells, but the degree of selectivity was not great. In addition, the synthesis, although published, was long and difficult. Making large amounts of this compound will be difficult.

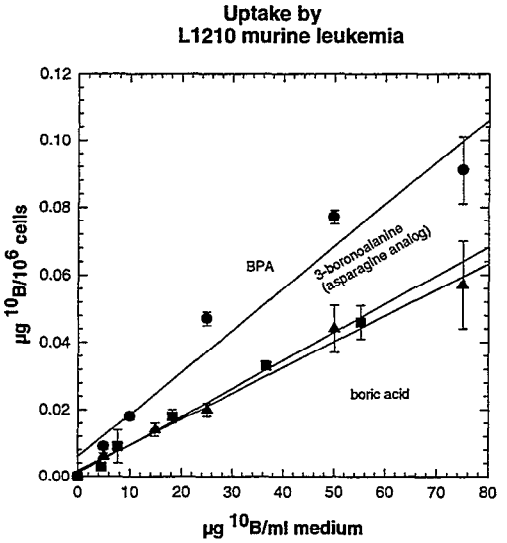

Figure 2. Asparaginase-insensitive L1210 murine leukemia cells do not accumulate the asparagine analog, 3-boronoalanine, compared to the boric acid control.

A melphalan derivative, BSMel: In the second year of the project, we synthesized a new boron-containing amino acid analog. It is much easier to prepare than 3-boronoalanine and is avidly taken up by a number of malignant cell lines, including leukemias and lymphomas. The analog is based on a widely used metabolite analog and chemotherapy agent known as melphalan (a nitrogen mustard derivative of phenylalanine, 4-[bis(2-chloroethyl)amino]-L-phenylalanine) that kills tumor cells by alkylation (cross-linking) of double-stranded DNA. Melphalan was converted to a metabolite analog (BSMel) containing a high B-10 content for use as a boron delivery agent for neutron capture therapy. BSMel is a new compound, a patent application was filed.

Synthesis of ^{10}BSMel: ^{10}BSH (880mg) was dissolved in 30 mL 5% sodium bicarbonate. Melphalan (213 mg) was added and the solution was stirred vigorously in a stoppered tube. Within about 2 hours, most of the melphalan had dissolved and a fine white precipitate began to form. At the end of 48

hours the reaction mixture was placed in the refrigerator overnight to complete separation of a fine white solid. The precipitate was collected by centrifugation and dissolved in 30 mL water with heating to the boiling point. The hot solution was left to cool to room temperature and a small amount of insoluble material was removed by centrifugation. Acidification to pH 2.7 with HCl caused heavy precipitation of the product, which was completed by storage in the refrigerator overnight. The product was collected by centrifugation and washed with water resuspension and centrifugal sedimentation. The washed centrifugal pellet was frozen and dried by lyophilization to yield 120-160 mg of ^{10}BSMel. The compound contains a single dodecaborane cage rather than the two cages that would result from substitution of both arms of the nitrogen mustard group. From the known propensity of BSH to undergo dialkylations and from the symmetry of the proton NMR spectrum of the product, we tentatively conclude that BSMel is probably the bicyclic compound resulting from alkylation of a single BSH molecule by both arms of the nitrogen mustard group of a melphalan molecule.

BSMel, biological testing: The most significant biological results relate to the uptake of BSMel into a number of malignant cell lines. Both the asparaginase-sensitive L5178Y mouse lymphoma cells and the asparaginase-resistant L1210 mouse leukemia cells, for example, readily accumulate high concentrations of boron in the presence of BSMel (Figures 3 and 4).

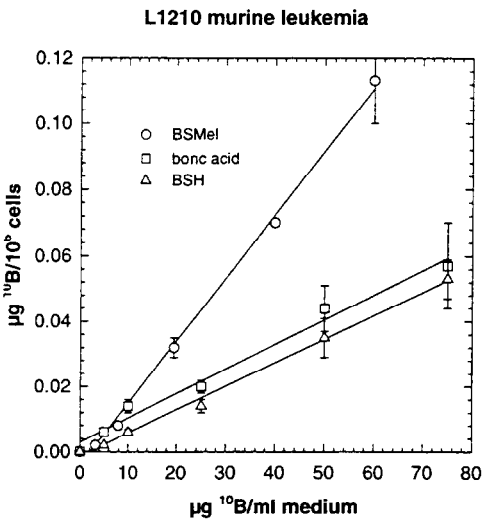

Figure 3. The melphalan-sensitive L1210 murine leukemia cells strongly accumulate the boron-containing melphalan derivative BSMel. Contrast this result with the failure of these asparaginase-insensitive cells to concentrate the boron containing asparagine analog, 3-boronoalanine, as shown in Figure 2. Note, also, that BSH is not accumulated by these cells: the uptake of BSMel can not be easily attributed to trivial mechanisms such as adsorption of the dodecaborane anion to cells or cellular components.

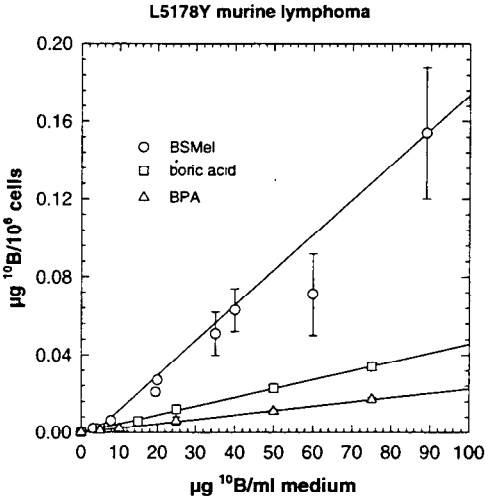

Figure 4. The melphalan-sensitive L5178Y murine lymphoma cells strongly accumulate the boron-containing melphalan derivative, BSMel. Note, again, that BPA is excluded by these cells, compared to the boric acid control.

Clonogenic assays: In year three the focus of research shifted to a demonstration that BNCT *in vitro* can selectively kill leukemia cells and not damage the normal bone marrow. The work with bone marrow is complicated by the fact that only a very small fraction of bone marrow is the critical stem cell population: the population that must be spared during BNCT. The objectives in year three required the development of new techniques in the BNCT tissue culture laboratory to grow and assay the leukemia cells and the bone marrow stem cells.

Clonogenic assay of leukemia cells in soft agar: Both the L1210 murine leukemia and the L5178Y murine lymphoma cell lines grow in suspension. To perform colony forming assays, it is necessary to plate the cells in medium mixed with (0.26 %) agar to form a three dimensional "soft agar" matrix. After 2 weeks growth, the colonies are counted and compared to controls. Experimental points are normalized to the plating efficiency of the controls. Each data point is the mean ± sd of 5 replicate dishes per point.

We have established the methodology for assaying murine leukemia and lymphoma cells in soft agar. A pilot study was carried out using boric acid. Boric acid is a non-specific boron compound and is present at equal concentrations inside and outside the cells (Capala, 1996). Murine L1210 leukemia cells were exposed to boric acid at a concentration of 25 μg ^{10}B/ml (5 mM), for 2 hours. The cells were then exposed to increasing fluences of thermal neutrons as previously described (Coderre, 1993). Figure 5 shows the survival curves for cells exposed to the thermal neutron beam of the Brookhaven Medical Research Reactor in the presence or absence of boric acid. The plating efficiency of non-irradiated L1210 cells was approximately 30%. The beam + boric acid experiment was repeated twice, both sets of points are shown. This experiment will serve as a reference when we begin the thermal neutrons + BSMel irradiations.

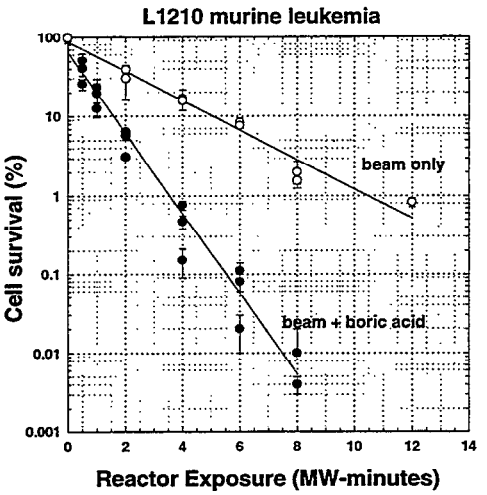

Figure 5. Survival of murine L1210 leukemia cells exposed to thermal neutrons in the presence or absence of boric acid. Reactor exposure is expressed in units (MW-min) that are the product of time and reactor power and are proportional to dose.

Clonogenic assay of bone marrow stem cells: Bone marrow consists of a variety of terminally differentiated cells that are irrelevant in a bone marrow transplant situation. It is the stem cells that have the potential to give rise to these cell populations that must be assayed. A special medium is required for the assay of these stem cells (Methocult, StemCell Technologies, Inc). This medium also forms a soft matrix. Methocult contains all of the growth factors and cytokines to specifically grow the murine bone marrow stem cells. Colonies greater than 50 cells are counted after 2 weeks of growth.

Fresh bone marrow was isolated from

C57/Bl6 mice. The mice were euthanized, the four femurs were removed and adherent tissue was dissected off. The bones were washed with alcohol. Using sterile techniques, the ends of the femurs were removed with a razor blade. A syringe filled with sterile saline solution was used to extrude the bone marrow from each femur. The cells were counted in a Coulter Counter. The yield was approximately 20 x 10^6 cells per mouse (all 4 femurs). Plating 3 x 10^5 cells in a well containing 10 ml of Methocult medium resulted in approximately 30 colonies at 2 weeks. This is the plating efficiency of the bone marrow stem cell assay: 0.1%.

SUMMARY:

The first stages in the development of a new BNCT modality, *ex-vivo* purging of bone marrow, have been accomplished. A boron containing analog of the anti-cancer agent melphalan has been synthesized. BSMel retains specificity for the targeted tumor cells: leukemia and lymphoma. Experiments to determine the effectiveness of BSMel-based BNCT against leukemia cells *in vitro*, and to measurement of the sensitivity of bone marrow stem cells to BSMel-based BNCT are underway.

ACCOMPLISHMENTS:

A patent application was filed on the new boron compound BSMel.

A poster was presented describing the BSMel work at the Eighth International Symposium on Neutron Capture Therapy for Cancer, 13 - 18 September, 1998, La Jolla, California. A manuscript will appear in the conference proceedings. Title: "BSMel: An Aromatic Amino Acid Analog Of High Boron Content, Easily Prepared From B-10 Enriched And Stereochemically Pure Precursors" Authors: John D. Glass, Michael S. Makar, and Jeffrey A. Coderre.

A collaboration has been established with Amitabha Mazumder, MD, Chief of the Bone Marrow Transplant Unit at the University Hospital, State University of New York at Stony Brook. Dr. Mazumder provided the methodology for bone marrow stem cell culture in Methocult medium. He will participate in the bone marrow rescue experiments.

REFERENCES CITED:

Broome, J.D., Evidence that the L-asparaginase of guinea pig serum is responsible for its antilymphoma effects. J. Exp. Med., 118, 99-120, 1963.

Capala, J., Makar, M.S., and Coderre, J.A., Accumulation of boron in malignant and normal cells incubated in vitro with boronophenylalanine, mercaptoborane or boric acid. Radiat. Res., 146, 554-560, 1996.

Coderre, J.A., Makar, M.S., Micca, P.L., Nawrocky, M.M., Joel, D.D., Slatkin, D.N., and Amols, H.I. Derivations of relative biological effectiveness for the high-LET radiations produced during boron neutron capture irradiations of the 9L rat gliosarcoma *in vitro* and *in vivo*. Int. J. Rad. Oncol. Biol. Phys., **27**, 1121-1129, 1993.

Kinder, D.H. and Ames, M.M. Synthesis of a 2-amino-3-boronopropionic acid: A boron containing analog of aspartic acid. J. Org. Chem., 52, 2452-2454, 1987.

NIH GRANT APPLICATION:

An NIH grant proposal entitled "Purging of Leukemic Bone Marrow Using BNCT" was submitted 5/23/97. It requested $ 185,243 in direct costs for the first year and $ 570,807 in

direct costs over a 3-year period of support. The grant was not funded. A resubmission is planned.

LDRD FUNDING:

FY 1996	$ 82,116
FY 1997	$ 86,342
FY 1998	$ 93,575

Autecology of the Peconic Bay Brown Tide Organism, *Aureococcus anophagefferens*

Julie La Roche *96-49*

PROJECT DESCRIPTION:

*B*rown tides, algal blooms of *Aureococcus anophagefferens*, have affected the living resources in many of the shallow bays on eastern Long Island. The brown tides first appeared in 1985 and they persisted for extended periods in 1986, 1987, and 1989. These blooms decimated scallop populations in Peconic Bay and Suffolk County began a brown tide monitoring program in 1986 to acquire hydrographic and biological data in Peconic Bay. The reoccurrence of brown tide blooms in 1995 sparked a renewed scientific interest. Based on an analysis of a time series data set collected by Suffolk County, several BNL researchers have recently proposed the "Groundwater hypothesis" to explain the bloom occurrence in the Peconic Bay. Our hypothesis postulates that brown tide blooms (>250,000 cells/ml) are caused by differences in the rate of supply of organic and inorganic nitrogen. This hypothesis has been widely endorsed by the broad scientific community but it remains to be tested experimentally in the laboratory and in the field. A combination of laboratory and field studies have been carried out to determine the role of macro-, micro-, and organic nutrients on the growth and photosynthesis of *A. anophagefferens*. A test of this hypothesis will start with demonstration that growth of *A. anophagefferens* can be supported by dissolved organic nitrogen (DON) compounds as a sole source of nitrogen and by demonstrating that DON from the Peconic Bay can be utilized by *A. anophagefferens*.

TECHNICAL PROGRESS AND RESULTS - Fiscal Year 1998:

Approach: This project was designed to test the Groundwater hypothesis put forward by La Roche et al. (1997). The approach was 3-fold:

1. A field component in direct collaboration with the Brown Tide Survey conducted by Suffolk County, Department of Ecology.

Our data consist of weekly (April to September) or biweekly (October to March) nutrient bioassays, bacterial counts (beginning in the summer of 1998), and identification of dominant phytoplankton species in addition to some nutrient measurements at 2 stations (170 and 119) within the Peconic Estuary system. The goal of this component is to identify the limiting nutrient for phytoplankton growth in brown tide and non-brown tide years. So far the results demonstrate that in years with no brown tide blooms, nitrogen is the limiting nutrient in the Peconic Estuary system throughout the year except during December and January. During those months, the inorganic nitrogen concentrations are in excess for a very short time but then are rapidly depleted by phytoplankton growth. We now have almost 3 years of data, and we expect to carry out those experiments until August 1999 with funds from a grant from Suffolk County, Department of Ecology. A manuscript is in preparation for submission to the journal Marine Ecology Progress Series and will include all of the data collected during this 3-year period.

In the context of this field survey, we have developed a rapid method to determine urea concentration using 96-well plates and plate reader (Appendix 1). This method allows the

determination of urea on fresh samples. The initial data set collected during 1997 and 1998, show low concentrations in the winter followed by slightly higher concentrations in the spring and summer. A similar method has been developed for ammonia measurements.

2. Characterization of the DON from the Peconic Estuary system.

We are investigating the potential for dissolved organic nitrogen (DON) to supply the nutrient requirements that allow *Aureococcuse anophagefferens* to bloom in Long Island coastal waters. We suggested that during the remineralization of organic matter in sediments, DON is released and transported to the overlying water column where it can be consumed by brown tide algae, thereby stimulating growth. To substantiate this hypothesis, we need to demonstrate there is sufficient DON in pore-waters to act as a nutrient, and that a fraction of this DON is metabolically available. This part of the work has been done so far in collaboration with Dr. Daniel Repeta of Woods Hole Oceanographic Institute. This work has progressed rapidly but is a long-term undertaking and it will be continued jointly with Dr. Julie La Roche after the completion of this LDRD, as part of a National Science Foundation award and a concurrent award from the Suffolk County Department of Health, Office of Ecology.

3. Utilization of DON by *Aureococcus anophagefferens*.

We have begun to characterize the utilization of nitrogen by *Aureococcus* at the biochemical level. In order to optimize the method of cell surface labeling, we have conducted a series of experiments with iron-, phosphorus- and nitrogen- limited cultures. From these experiments, we have determined the volume of cultures and cell density necessary for western blots, and we have established the sampling schedule necessary to see the induction of proteins during the course of nutrient limitation. Dr. Mine Gry Berg, a postdoctoral fellow who was involved in this work, will pursue similar experiments with various organic nitrogen sources as part of a NSF grant.

We have begun assessing methods for the partial purification of the enzyme urease from *A. anophagefferens*, as it is known that urea is one of the preferred sources of nitrogen for this species. The goal here is to produce an immunological probe to be able to detect urease from *A. anophagefferens* in the field.

Our axenic clone of *A. anophagefferens* was lost during an incubator failure last year and we have now prepared a new clone using the protocol described in Appendix 2.

PAPERS/JOURNALS/PUBLICATIONS:

Two manuscripts are in preparation. One manuscript describes the salinity/growth relationship for *A. anophagefferens* and will be submitted to the Journal of Phycology. The second manuscript will present the nutrient enrichment bioassays and will be submitted to the Journal of Plankton Research.

FOLLOW-ON FUNDING:

A three-year grant from NOAA for FY97-99 has been awarded to the PI as part of the Brown Tide Research Initiative (BTRI). The purpose of this project is to design probes to detect iron limitation in *A. anophagefferens* (Approximately $ 100,000 for 3 years). A two-year grant was also awarded from Suffolk County Department Health, Office of Ecology to pursue the testing of the Groundwater hypothesis (Approximately $ 200, 000 for 2 years).

Appendix 1. A modified method for determining urea in seawater using a 96-well plate reader.

The manual method for determination of urea in seawater using diacetylmonoxime reagent (Mulvenna and Savidge 1992) was modified for use on a 96-well plate reader. The foremost advantage of this method is that it is rapid and requires very little sample, 96 samples of 200-300 µl each can be read at once in less than 3 seconds. Secondly, the method is both precise and accurate. The coefficient of variation of triplicate standard samples typically ranged between 0.02 and 2 %. The lower limit of detection of the method was typically less then 0.1 µM urea. Because the analysis is a direct colorimetric analysis in which the diacetylmonoxime reagent forms a six-membered ring upon reacting with urea, the disadvantage of the indirect enzymatic method, in which the reaction of urease with urea may not go to completion, is avoided.

Method: The reagents (A and B) for the analysis of urea samples was prepared using the same concentrations as in Mulvenna and Savige (1992). The additions of the reagents were scaled down to a sample volume of either 200 or 250 µl. Samples and standards were added to the wells in the plate reader in triplicate. The reagents were then added sequentially with a 12-channel pipettor. Upon addition of each reagent, the plate was shaken immediately for 15 seconds in the plate reader. After the last shake, the plate was covered in foil and incubated in an incubation oven at 85°C for 50 min. Following incubation, the plate was immediately placed in the freezer to cool down for 10 minutes. The absorbance was read immediately at a wavelength of 490 nm using a MRX Microplate reader from Dynatech Laboratories. Reagents were mixed fresh with each analysis and standard samples were made from a primary stock solution of 10mM urea. A standard curve was measured for each plate. Optimal color development, sample precision, and linearity of the calibration curve were determined by experimentation with the incubation and the cooling times over a range of different periods.

Reference:

Mulvenna P.F., Savidge G. 1992 A modified manual method for the determination of urea in seawater using diacetylmonoxine reagent. Estuarine, Coastal and Shelf Science 34:429-438

Appendix 2. Production of an axenic culture of *Aureococcus Anophagefferens*

We have modified a protocol published by Cottrell & Suttle, C.A. (1995 J. Phycol. **29 385**-387) for the preparation of an axenic culture of *A. anophagefferens*. The antibiotic concentrations used in the protocol were determined by defining the upper limit of tolerance of *A. anophagefferens* to each antibiotic. Exponentially growing cultures were exposed to the following antibiotic treatment sequentially: Penicillin (1.0 mg ml^{-1}), Neomycin, (0.25 mg ml^{-1}), Streptomycin (0.10 mg ml^{-1}), Kanamycin (2.00 mg ml^{-1}), Gentamycin (0.25 mg ml^{-1})

For the penicillin treatment, a fresh innoculum of *A. anophagefferens* is grown in exponential phase for approximately 3 days in 8ml of f/2 nutrient artificial seawater (ASW). A sterile glucose solution (0.01% final concentration) is added to the culture 3 hours before the dark period to stimulate the growth of heterotrophic bacteria. Penicillin G is then added at the onset of the dark period. At the onset of the light period, the culture is diluted 10 fold with

fresh culture media in order to reduce the antibiotic concentration. Growth of the culture is monitored for 3-4 days by following chlorophyll fluorescence.

All the other antibiotics are added sequentially to the final concentrations listed above, following a 10-fold dilution with fresh medium and recovery from the previous antibiotic treatment. For each antibiotic treatment, an aliquot of the culture is taken to assess the bacterial contaminants. Approximately 1 ml of culture is transferred to a tube containing rich bacterial growth media and on petri dish (MB2216). Bacterial contaminants are also assessed by direct cell counts following DAPI staining.

LDRD FUNDING:

FY 1996	$ 98,405
FY 1997	$ 103,357
FY 1998	$ 107,191

The Development and Demonstration of Accelerator Based BNCT Capability

D. Raparia *96-50*

PROJECT DESCRIPTION:

Statement of work: To study the feasibility of producing neutrons for Boron Neutron Capture Therapy, BNCT, with an accelerator rather than with a reactor. If a small commercial proton accelerator based system to produce neutrons is found to be feasible, then BNCT could become a readily available clinical procedure.

PREVIOUS TECHNICAL PROGRESS:

A seven meters long beam line and RFQ/Linac accelerator was installed. The RF power supply had problems, still not functioning properly. Proof of concept experiments were done at RARAF (Navis Laboratories) for different configuration and had established that proton beam current needed for treatment was about 5 mA.

The $^{10}BF_3$ detector was used in phantom to produce benchmark curves which can be used in testing the thermal and epithermal components of the neutron spectrum.

TECHNICAL PROGRESS AND RESULTS - Fiscal Year 1998:

Purpose: To study the yield and energy spectrum of neutrons produced using a proton beam (<2.5 MeV) from an accelerator, as an alternative source for Boron Neutron Capture Therapy (BNCT). The major emphasis is to study the feasibility of various production target designs to optimize the yield and energy spectrum.

Approach: The neutron generator for BNCT is based on a low energy (1.9 - 2.5 MeV) proton beam impacting a Lithium-7 target to produce neutrons by the (p,n) reaction. The resulting neutron flux is a function of both energy and angle, with a maximum energy of 800 keV in the forward direction when one use 2.5 MeV protons impinging on the target. The filtering concept [1-4, 8] is based on slowing down of neutrons below 100 keV by inelastic scattering from fluorine. It is followed by an iron filter which takes advantage of minima in the scattering cross section at 25 keV, 70 keV, and 85 keV. Thus there should be peaks in the neutron energy spectrum at these energies. In a real therapy source the spectrum will be further tuned by the addition of hydrogenous material. Calculations indicate that the resulting neutron yield per mA of proton current is high enough that the accelerator becomes relatively straight-forward.

Technical Progress and Results: (1) More proof of concept experiments for softening the neutron spectrum were done at RARAF. Three configuration were test. This first geometrical configuration of the target, filter and reflector assembly is shown in Fig. 1. In the second configuration the Be reflector was replaced with two Teflon and Mo and Be reflectors were replaced with Fe disks, and in the third configuration both two larger Teflon and Fe disks. In addition there was about 1 mm thick water layer for target cooling purposes.

The unfolded neutron spectrum , for the case of Teflon, Fe filter, and the calculated one are shown in Fig. 2. The peak and valleys in the calculated spectrum follow the macroscopic cross section of the materials in the filter.

The calculated and measured epithermal neutron fluxes per mA of a proton current for different filters are summarized in Table 1. At present, the epithermal fluxes were measured from about 5 keV up to 35 keV and extrapolated to 1 eV by the ratio obtained from the Monte Carlo calculations.

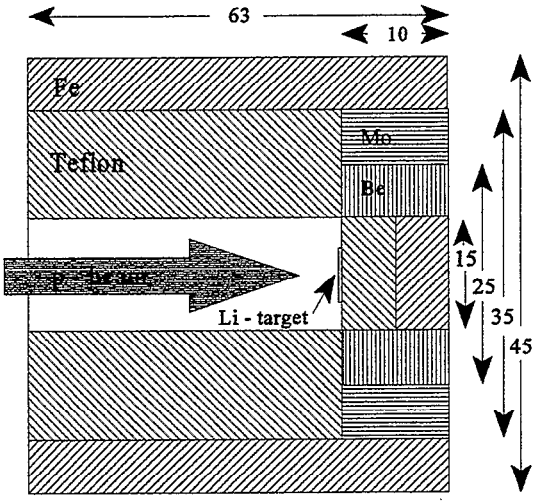

Figure 1. Schematic configuration of the filter assembly with the target. All the dimensions are in cm.

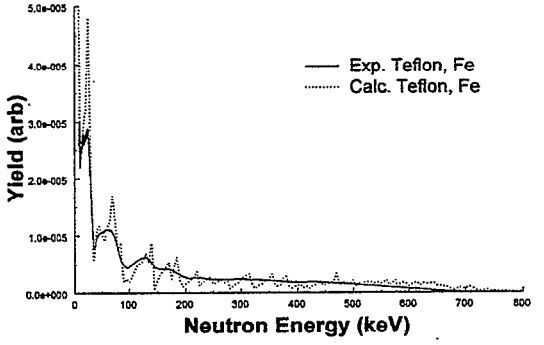

Figure 2. Comparison between an unfolded and calculated spectrum for the Teflon Fe filter at 2.5 MeV proton energy. The spectra were normalized to the same area between 35 and 200 keV.

Table 1. Measured and calculated epithermal fluxes per mA of 2.5 MeV proton beam.

Filter	Measured Flux ($n/cm^2/s/mA$)	Calculated Flux ($n/cm^2/s/mA$)
No Filter	0.22×10^8	-----
Teflon, Fe No Reflector	0.31×10^8	----
Teflon, Fe	1.25×10^8	2.17×10^8
Mo, Teflon, Fe	1.26×10^8	2.10×10^8
Mo, Be	1.71×10^8	2.09×10^8

(2) In depth measurements in phantom at the BMRR and RARAF facilities using a small $^{10}BF_3$ counter suggest that the accelerator produced neutron beams due to 1.9 and 2.5 MeV protons are harder than that from the reactor, resulting in a small shift of the thermal neutron peak into a deeper region in the phantom, Fig. 3. Based on the counts at the depth for maximum counting in the reactor the estimated current required to deliver the same count rate was about 1 mA for 2.5 MeV proton beam and about 6.8 mA for 1.9 MeV proton beam. In addition, lateral scans in air and in phantom, at the RARAF facility showed that the beam resulting from 2.5 MeV protons is wider and flatter than that from 1.9 MeV protons.

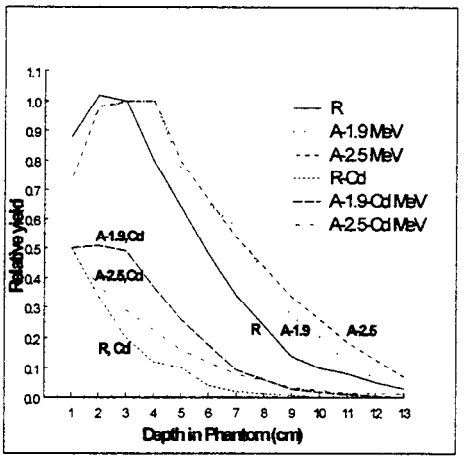

Figure 3 In phantom measurements using $^{10}BF_3$ counter, exposed to reactor beam and two accelerator beams at 1.9 and 2.5 MeV. Bare counter readings are normalized to one at 3 cm, and Cd covered counter readings are normalized to 0.5 at 1 cm.

PAPERS/JOURNALS/PUBLICATIONS:

[1] "NIFTI And DISCOS: New Concepts For A Compact Neutron Source for Boron Neutron Capture Therapy Application," J. Powell, H. Ludewig, M. Todosow, and M. Reich, BNL report 63605, June 1995.

[2] "New Concepts for the Compact Accelerator/target for Boron Neutron Capture Therapy," J. Powell, H. Ludewig, M. Todosow, and M. Reich, Proceedings of the 14th International Conference on the Application of Accelerators in Research and Industry, 1996, page 1309.

[3] "Target Studies for Accelerator-based Boron Neutron Capture Therapy," J. Powell, H. Ludewig, M. Todosow, and M. Reich, Proceedings of the 4th International Conference on Nuclear Engineering, 1996, page 493.

[4] "Target/Filter Concepts for the Accelerator Driven Boron Neutron Capture Therapy Applications," J. Powell, H. Ludewig, M. Todosow, and M. Reich, accepted for publication in Nuclear Technology.

[5] "Phantoms with $^{10}BF_3$ Detector for BNCT Application," D. E. Alburger, D. Raparia, and M. S. Zucker', Medical Physics, 25, 1735, 1998

[6] "Accelerator Based Neutron Spectra Analysis for the BNCT," L. Wielopolski, H. Ludewig, J. Powell, D. Raparia, J. Alessi, G. T. Danby. Y. Y. Lee, M. Zucker, D. I. Lowenstein, to be publish in the Proceedings of the 15th International Conference on the Application of Accelerators in Research and Industry, 1998.

[7] "Analysis of Accelerator Based Neutron Spectra for BNCT using Proton Recoil Spectroscopy," L. Wielopolski, H. Ludewig, J.R. Powell, D. Raparia, J.G. Alessi, and D.I. Lowenstein, to be published in Frontiers in Neutron Capture Therapy, 1999.

[8] "High Neutron Efficiency, Low Current Target for Accelerator Based BNCT Applications," J. Powell, H. Ludewig, M. Todosow, and M. Reich, submitted to Radiation and Shielding Topical Conference on Technologies for New Century, April 19-23 , 1998, Nashville, Tenn.

[9] "Thermal-Hydraulic Target Test," H. Ludewig, J. Brodowski, and J. Powell, BNL Memorandum. October 22, 1997.

LDRD FUNDING:

FY 1996	$ 188,449
FY 1997	$ 412,137
FY 1998	$ 201,230

Physics Goals for a New Intense Muon Facility

William J. Marciano *97-02*

PROJECT DESCRIPTION:

The focus of this LDRD project remained largely the same as originally proposed: To identify and scrutinize the most compelling physics studies that could be carried out at a new very intense muon source capable of delivering $10^{11} \sim 10^{13} \mu^{\pm}$/sec, 4 to 6 orders of magnitude beyond current facilities available at TRIUMF and PSI. Such a source could be developed in the near term at Brookhaven's AGS, be part of the front end of a future muon collider complex, or be coupled to an intense neutron spallation source.

The AGS is a particularly attractive muon source facility. It has been recently upgraded and has achieved record proton beam intensities, 6×10^{13} protons/pulse. Further intensity increases are also expected. Its utility as a muon (and antimuon) source for a future very high energy $\mu^+\mu^-$ collider has been investigated. In principle, it appears possible to produce a very clean secondary muon beam at the AGS with intensity approaching $10^{13}\mu$/sec. (The first dedicated effort would aim for $10^{11}\mu$/sec.)

A very intense muon beam can have important applications well before the full muon collider dream is realized. Indeed, we have advocated[1] the possibility of a low energy physics program at the AGS which would take advantage of the unique opportunities available at such a facility. The envisioned program would include its own forefront physics research while helping to advance R&D for future muon collider technology.

In our effort to motivate the new intense muon source, we have outlined a program of low energy physics experiments that could be carried out there. The program would initially concentrate on fundamental elementary particle physics studies, but later find applications in condensed matter via μSR, biology where μ^+e^- atoms could be used as probes and muon catalyzed fusion research. Some of the fundamental measurements envisioned include:

1. Precision Measurements of Muon Properties (τ_μ, g-2, e.d.m., muonium *hfs* etc.)
2. Muon Neutrino Studies (mass, oscillations...)
3. Searches for *P* and *T* violation in Muonic Atoms
4. Searches for Muon-Number Non-Conservation

Each of these topics is undergoing close scrutiny in an effort to assess how far such studies could be pushed as well as to determine their potential importance and likelihood for uncovering "New Physics."

TECHNICAL PROGRESS AND RESULTS – Fiscal Year 1998:

To date, much of the LDRD effort has been directed at studies of the muon-number violating reaction μ^- + Nucleus $\rightarrow e^-$+ Nucleus. The basic concept is simple, a stopped μ^- will quickly cascade into a 1*s* atomic orbit and reside in close contact with the nucleus. There it lives of order 10^{-6} sec. before either undergoing capture $\mu^- p \rightarrow \nu_\mu n$ or decay $\mu^- \rightarrow e^- \nu_\mu \bar{\nu}_e$. If, however, muon-number is not exactly conserved, the coherent reaction $\mu^- N \rightarrow e^- N$ becomes possible. Its signature, a monoenergetic e^- with $E_e \cong 105$ MeV is very distinct from backgrounds and relatively easy to identify.

Already, experiments have searched for that rare reaction and set an upper bound of 7×10^{-13} on its occurrence. With an AGS source capable of delivering $10^{11}\mu^-$/sec, one could probe the 10^{-16} level. Recognizing that fact, a proposal (P940, W. Molzon et *al.*) was submitted to BNL with the goal of searching for $\mu^- Al \rightarrow e^- Al$ to better than 10^{-16} and received scientific approval. If supported by the D.O.E., it would be the flagship experiment of the AGS 2000 program. Because such an experiment detects only one final state particle, it can take very high intensities without encountering accidentals. Hence, we believe it could ultimately be pushed to the $10^{-18} \sim 10^{-19}$ level. No other known rare decay or process can be probed at that level.

Preliminary feasibility studies of coherent muon-electron conversion were initiated at the 1996 AGS 2000 workshop and at a small but dedicated workshop held in July 1996 at the Institute for Theoretical Physics in Santa Barbara. Following those meetings, collaborative theoretical work with A. Czarnecki and K. Melnikov (Postdocs at Univ. of Karlsruhe) began. During FY97, the transition rate for muon-electron conversion in atoms was carefully examined and detailed computer calculations were carried out for arbitrary muon-number violating interactions. Relativistic atomic effects, Coulomb wavefunction distortions, finite nuclear distributions, etc. were taken into account for a broad range of stopping targets. The results have been shown at various conferences and recently published in "Coherent Muon-Electron Conversion in Muonic Atoms" A. Czarnecki, W. Marciano, and K. Melnikov, AIP Conference Proc. 435, Eds. S. Geer and R. Raja (1998). Follow-up FY98 studies included scrutiny of specific models and their predictions including supersymmetry, heavy neutrino mixing, multi-Higgs etc. Also, the background from $\mu \rightarrow e\nu\ \nu$ decay in orbit is being reexamined to see if 10^{-18} sensitivity is feasible. These efforts have been facilitated by the arrival of A. Czarnecki at BNL (starting Sept. 30, 1997), supported by LDRD funding and a long term visit by K. Melnikov during the summer of 1998, also supported by LDRD funding. Results of that collaborative work are being prepared for publication.

A second part of the LDRD effort has been studies of new sources of P and T violation that might be unveiled using muons. Predictions for the muon electric dipole moment (which violates P & T) were examined in a variety of models. Those studies were done with O. Vives, a postdoc from Spain who visited BNL for 6 months during FY98, supported in part by LDRD funding.

Effects of P and T violation in muonic atoms have also been examined. Discussions with M. Pospelov (an LDRD supported visitor during FY97) elucidated possible signatures of CP violation. With the help of A. Czarnecki (now a regular Research Associate with the BNL HET Group), we hope to expand that effort in the future.

In the area of precision muon measurements, several theoretical ideas were developed during FY98. The use of high precision measurements of the muon lifetime combined with the $W^{\pm}$ mass measurement was shown to provide a severe constraint on heavy gauge bosons (W. Maricano, WEIN Conference, Santa Fe 1998). Higher order contributions to g_μ-2 were refined (A. Czarnecki and M. Skrzypek, submitted to Phys. Lett. B) and a review of leptonic anomalous magnetic moments was prepared (A. Czarnecki and W. Marciano, BNL-HET-98/43 Report).

A related project carried out under some LDRD support involves muon collider physics and machine design studies. W.

Marciano in collaboration with B. Kamal (HET postdoc) and Z. Parsa (BNL CAP) examined Higgs resonance signatures and backgrounds at a $\mu^+\mu^-$ collider. Effects due to muon polarization and forward-backward asymmetries were scrutinized. Also, new ideas for intersecting $\mu^+\mu^-$ storage rings with large crossing angles were advanced as a means of reducing severe detector backgrounds and neutrino radiation. These results have been reported in "Workshop on Physics at the First Muon Collider and at the Front End of the Muon Collider," AIP Conference Proceedings 435 (1998) Eds. S. Geer and R. Raja, p. 657 and "Physics Potential and Development of $\mu^+\mu^-$ Colliders, AIP Conf. Proc. 441 (1998) Ed. D. Cline, p. 174 and p. 347. A related study (A. Czarnecki and W. Marciano, Int. J. of Mod. Phys. **A13**, 2235 (1998)) focused on the utility of high-energy lepton colliders including $\mu^+\mu^-$ for measuring $\sin^2\theta_W$ with extremely high precision as a means of uncovering "New Physics."

ACCOMPLISHMENTS:

The work reported above has led to several concrete developments. Elucidating the importance of μ-*e* conversion for uncovering "New Physics" and scrutinizing its theoretical underpinnings has helped lead to an approved experiment at the AGS (E940, W. Molzon Spokesman) with 10^{-16} sensitivity. Studies of the muon e.d.m. provided goals for a future effort at the AGS muon storage ring to push for 10^{-24} *e*-cm sensitivity. A letter of intent for such a measurement has been submitted by Y. Semertzides *et al.* Members of this LDRD have been and will continue providing theoretical support for those efforts.

The renewed interest in low energy muon physics, partially spawned by this LDRD, has also helped stimulate activities outside of BNL. The RIKEN-RAL muon collaboration under K. Nagamine has examined upgrading their laboratory to much higher intensities ~ $10^{11}\mu$/sec in an effort to probe fundamental elementary particle measurements such as μ-*e* conversion. The PSI laboratory in Switzerland has examined the possibility of searching for $\mu^+ \rightarrow e^+\gamma$ at 10^{-14} sensitivity.

Many seminars and conference presentations on muon physics and LDRD results were given by A. Czarnecki and W. Marciano during FY98. (See attached list.)

Muon Physics - Seminars, Conferences and Workshops FY98:

A. Czarnecki
(LDRD Supported Research Associate)

1. *Muon g-2: a theory update*, talk at the E821 Collaboration Meeting, November 1997.

2. *Coherent muon-electron conversion in muonic atoms*, talk at the Workshop on Physics at the First Muon Collider and at the Front End of a Muon Collider, Fermilab, November 1997.

3. *Higher order corrections to muon electric and magnetic moments*, seminar for the BNL High Energy Theory Group, December 1997.

4. *Using muons to probe for new physics*, seminar at the Physics Department, New York University, February 1998.

5. *Using muons to probe for new physics*, seminar at the Physics Department, University of Michigan, Ann Arbor, March 1998.

6. *Using muons to probe for new physics*, colloquium at the Physics Department, University of Western Ontario, London (Canada), April 1998.

7. *Unstable muon in an electric field*, seminar for the High Energy Theory Group, Brookhaven National Laboratory, May 1998.

8. *Methods for computing higher order quantum corrections (including muon electric and magnetic moments)*, seminar at the Physics Department, University of Valencia (Spain), September 1998.

9. *Electroweak corrections to muon g-2 and sensitivity to new physics*, talk at the 5th Intl. Workshop on τ Lepton Physics, Satander (Spain), September 1998.

W. Marciano (Senior Investigator)

1. *Muon g-2 and supersymmetry*, Brookhaven National Laboratory seminar, October 1997.

2. *Low energy physics and the first muon collider*, Fermilab, November 1997.

3. *Higgs resonance studies at the first muon collider*, Fermilab, November 1997.

4. *The physics of muon colliders: A perspective*, San Francisco, December 1997.

5. *Searching for supersymmetry with muons*, Princeton IAS, December 1997.

6. *Muon anomalous magnetic moment*, University of Pennsylvania, January 1998.

7. *Muon g-2*, University of Virginia, February 1998.

8. *Muons and kaons at the JHF*, KEK, Japan, March 1998.

9. *Supersymmetry*, Boston University, March 1998.

10. *Muon g-2*, Rutgers, April 1998.

REFERENCES:

1) W. Marciano, "The First Muon Collider and Low Energy Physics," BNL CAP Seminar 11/7/95.

LDRD FUNDING:

FY 1997	$ 91,434
FY 1998	$ 99,545

A Novel Curved Proportional Counter for X-ray Powder Diffraction Studies at NSLS

D.P. Siddons *97-08*
P.J. Pietraski
G.C. Smith
B. Yu

PROJECT DESCRIPTION:

There exist many areas where X-ray diffraction studies can reveal structure information that is unobtainable by other techniques. X-ray powder diffraction, in particular, is most effective when very large scattering angles can be covered by a single detector. The only device presently available for such studies is a commercial detector, which uses large signal amplification in a gas. This detector covers an angle of 120°, but operates with both limited counting rate capability and about 1mm position resolution; it does not make full use of intense synchrotron X-ray beams. This project involves the construction of a new, prototype gas-filled detector, operating in a lower signal amplification mode and equipped with a large number of electronic readout channels. These features significantly increase the counting rate capability and improve the position resolution to one tenth mm. The recent discovery in our laboratory of a new electrode on which controlled electron multiplication can be sustained, and which can easily be curved to cover 120°, formed the basis for the original proposal.

TECHNICAL PROGRESS AND RESULTS – Fiscal Year 1998:

Purpose: It is the intention of the proposed work to investigate a range of anode-cathode geometries, using a new electrode structure based on electron multiplication along the sharp edge of a blade. This new technique was proven to work in earlier studies which sought a solution to the instability problem that exists in microstrip gas detectors. A geometry which permits high counting rates with utmost electrical stability will be found, and incorporated into a prototype position sensitive detector, covering just under 50°, and implemented with high resolution encoding electronics also developed specifically for the device. Proof of principle will be established by tests on existing NSLS beam-lines. The long-term objectives are to show significant improvements of this new detector and electronics over existing devices, in order to justify requests for additional funding from outside agencies for a full sized, fully implemented device. Such an instrument would be in demand at powder diffraction lines at all of the world's major synchrotron sources.

Approach: Our strategy focuses on the utilization of developmental radiation detector hardware already in existence in our laboratory, the purchase of machining time to fabricate specialist electrodes, and the investigation of the electrical characteristics of these electrodes with standard techniques developed with our previous gas-filled wire chambers. A parallel effort has been launched to develop hybrid multi-channel electronics for readout of a prototype detector; funding has permitted the hiring of an electronics engineer for this purpose. Consideration will be given at a later stage in the project to the possibility of converting to monolithic electronics, which will be appropriate for a full-size detector and would take advantage of similar work already being carried out in this laboratory for LHC and RHIC detectors.

Technical Progress and Results: In the second year of the program, we have continued the test chamber studies of the various operating parameters for the blade anode. A curved blade detector with 45° angular coverage has been constructed using the optimized parameters obtained from the test chamber studies. A complete set of readout electronics of 16 channels has been constructed. The curved detector has been tested both with conventional delay line readout as well as the new digital centroid finding electronics.

Continuing studies on the optimization of the operating parameters in a gas proportional counter with blade anode have been carried out using the test chamber constructed earlier. Fig. 1 shows the schematic cross-section of the chamber, together with the definitions of several key geometrical parameters.

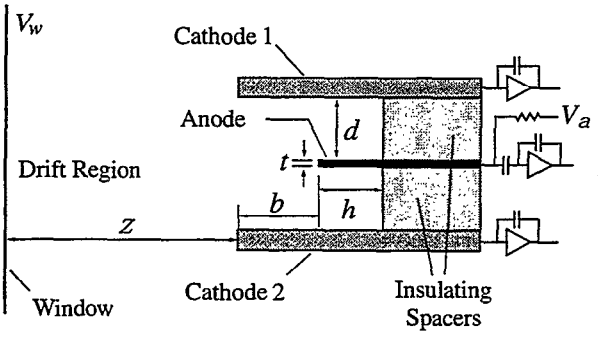

Figure 1. A schematic cross-section of the test chamber with blade anode.

The recess, b, of the tip of the anode blade, with respect to the cathodes, influences the gas gain at a given anode voltage and the uniformity of the gain in the direction across the anode. It also affects the acceptance aperture in the drift region. Gain variation across the anode blade was investigated by scanning a collimated beam at right angles to the blade direction. A deeper recess improves the gain uniformity, but decreases the acceptance aperture. Many synchrotron experiments require an acceptance aperture of typically 10 mm in a one-dimensional detector. It is also desirable that the anode maintains a fairly uniform gain across this aperture. Since b = 4mm satisfies both of these criteria reasonably well, this value was selected to make further studies.

A convenient way to extract avalanche position information from this electrode configuration is to use an interpolating technique to sample the induced cathode charge, as is common in various types of proportional wire chambers. Using printed circuit board, a test cathode was fabricated that consisted of a continuous plane of copper except for two sets of strips that run along and across the blade length; this replaced one of the metal shim cathodes. The induced cathode charge profiles across and along the blade direction were measured by sampling the charge on these two sets of strips. These charge profiles provide the information required for designing position interpolating cathode structures with low differential non-linearity.

Based on the results from the test chamber studies, a 1-D position sensitive x-ray detector has been constructed with a blade anode. In order to eliminate parallax errors at large diffraction angles, the anode blade and other electrodes are curved. Fig. 2 shows a photograph of all major parts in this detector's assembly. It covers an angle of 45°, has an arc length of about 20cm with a radius of curvature of 25cm. The blade is fabricated from a 25μm thick stainless steel sheet using electric discharge machining. The blade recess and anode cathode spacing are set at 4mm and 2.4mm respectively. In addition, drift field defining electrodes are used to ensure that field lines from the window are more effectively focussed onto the anode. This has the effect of reducing gain variation across the blade and therefore improving energy resolution. The two

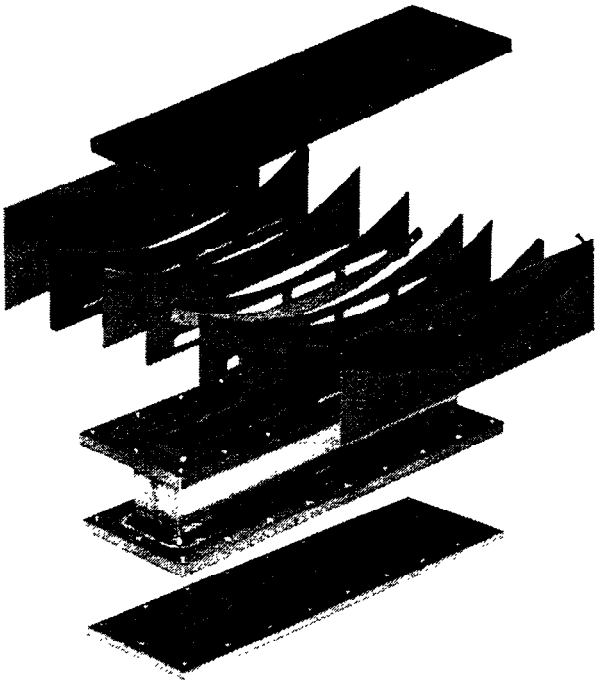

Figure 2. Exploded view of the prototype detector with 45° angular coverage.

cathodes are made of printed circuit boards, with 40 copper zigzag shaped strips running radially on each cathode facing the anode blade. Corresponding facing cathode strips are electrically connected together as a single readout node (thus virtually all the cathode charge is utilized for position encoding). These readout nodes can be connected to either a conventional delay line readout system or a newly developed digital centroid-finding system, which is described later in this report. The delay line readout system has been used in many 1D and 2D MWPC based position sensitive x-ray detectors developed by our group. Since the behavior of the delay line readout system is well understood, its results serve as a good reference to understand the behavior of the digital system.

The linearity of the detector's position response is measured using the detector's uniform irradiation response. As shown in Fig. 3, the differential non-linearity is about 10%, with a 1μs delay line readout system.

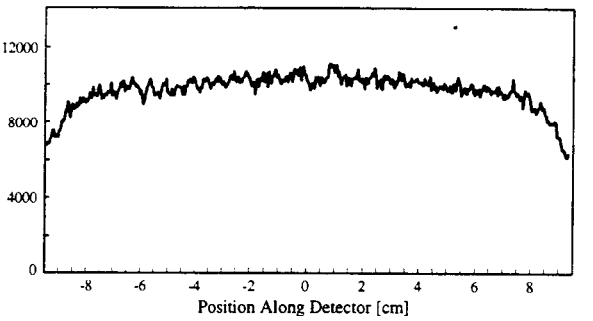

Figure 3. Detector's uniform irradiation response using a 1μs delay line readout. The fall-off at the ends of the detector is due to the x-ray source.

During the course of 1998, a prototype Digital Signal Processor (DSP) based fast centroid-finding readout system has been designed, constructed and tested. A block diagram of the readout system is shown in Fig.4.

The custom designed surface mount daughter-board contains 32 charge preamplifier circuits on a module 76x38 mm^2. It is mounted directly on the detector printed circuit board. A separate board holds 48 standard BNL bipolar amplifiers in hybrid technology (number IO533) with 250ns peaking time.

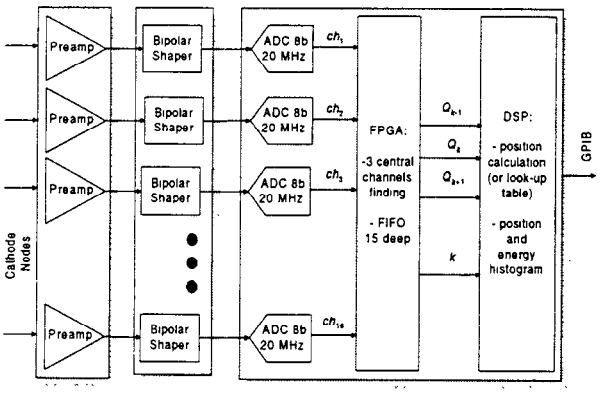

Figure 4: Block diagram of the detector readout system

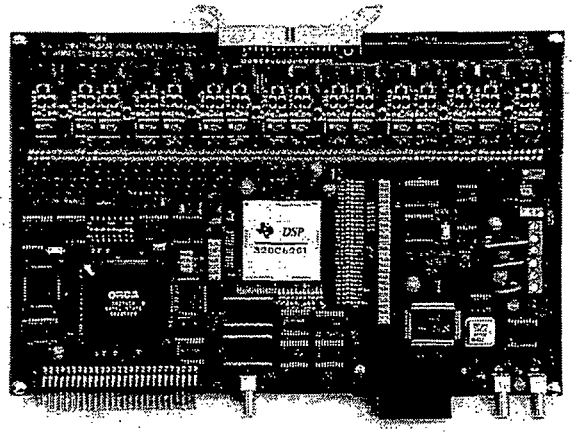

Figure 5: Photograph of the prototype PCB which contains 16 ADCs, FPGA, DSP and a GPIB interface.

The prototype printed circuit board (Fig.5) contains 16 analog to digital converters (ADC). The ADC is a 10-bit AD9200 with parallel output (8 bits of information are used). ADCs are free running with a 20 MHz clock. The advantage of this approach compared to the usual triggering on the anode signal is in the possibility of treating multiple hits. The system has no common dead time.

The digital outputs of all 16 channels of one segment are connected to a Field Programmable Gate Array (FPGA). Fig. 6 shows its simplified logic diagram. The central channel is found by first forming all the adjacent 3 way sums of the digital ADC outputs. A channel k is qualified as the central channel at sampling instant t_i if the following conditions are met:

1) The sum $S_k(t_i)$ of the sampled bipolar shaper signals $ADC_k(t_i)$, $ADC_{k-1}(t_i)$ and $ADC_{k+1}(t_i)$ must exceed a threshold in order to discriminate against the noise background.
2) The sum $S_k(t_i)$ must exceed $S_{k+1}(t_i)$ and must not be exceeded by $S_{k-1}(t_i)$. In addition to partially qualifying channel k, channels k-1 and k+1 are disqualified from being central channels.

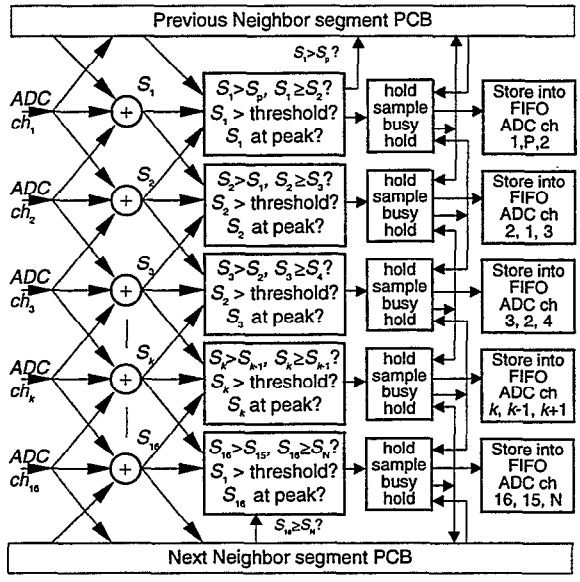

Figure 6: Simplified central channel finding logic realized in the FPGA

3) The sum $S_k(t_i)$ must exceed $S_k(t_{i+1})$. This identifies the sampling instant nearest the peaks of the analog bipolar signals involved, in the sense that their sum has peaked.

When all of the above conditions are satisfied, the ADC data on channels k, k-1 and k+1, at time t_i, are stored in a buffer as Q_k, Q_{k-1} and Q_{k+1}. The central channel sensing electronics for all 3 of these channels are then disabled until the shaper pulse dissipates, 16 samples in this case, providing post-pileup rejection. 16 such buffers (one for each possible central channel) are scanned sequentially for new data. Any new data, along with the number of the central channel, is subsequently written to an on chip First-In First-Out memory (FIFO). Each element of data (32 bits) listed in the FIFO represents one event and contains all the information needed by the DSP to perform the centroid computation. The FIFO can store up to 15 events. The FPGA logic is fully pipelined, and can give one output for every clock cycle.

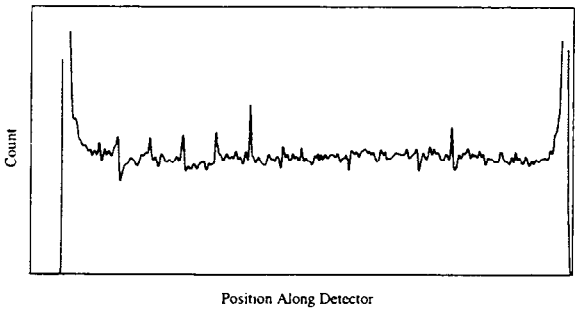

Figure 7: Uniform irradiation localization response using center-of-gravity algorithm.

A Digital Signal Processor (DSP) is a processor optimized to execute fast multiply-accumulate instructions. For this project we have chosen the Texas Instrument TMS320C6201. In a 5 ns clock cycle it can execute eight 32-bit instructions. The DSP has 128 Kbytes of internal static memory, accessible in one clock cycle and can use 16 Mbytes of dynamic memory on the board (7 - 42 clock cycles for single access). The DSP program is written in assembler and fully optimized. It performs the following tasks: extraction of 3 charge signals and of the central channel from the single 32 bit FPGA output, pedestal subtraction, gain correction and center-of-gravity calculation on 3 strips. The ADC quantization error is corrected by addition of 8 random bits to the original values and continuing calculation with 16 bit data. The execution time is less than 100 clock cycles. The event rate is therefore limited to around 2×10^6 per sec. Histogramming is performed directly in the DSP internal memory. Each histogram update consumes only 5 clock cycles and does not affect significantly the maximum count-rate.

A GPIB interface, realized using the National Instrument GPIB-TNT4882 chip, permits the read-out of the histogram results by a host computer.

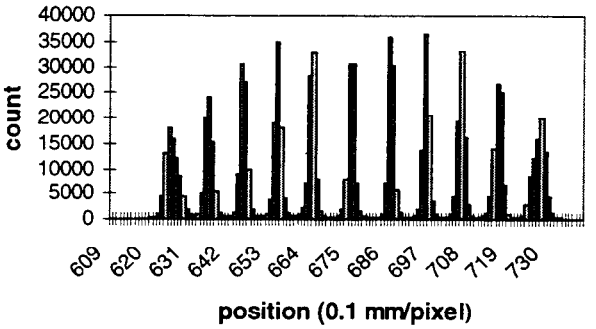

Figure 8: Collimated beam irradiation (1mm steps) response using Gaussian fit (anode charge 0.2 pC). The broadening of the peaks at both ends are the result of parallax errors caused by the parallel translation of the collimated beam across curved blade.

Because the induced charge distribution on the cathode spreads to more than the 3 strips used in the centroid finding electronics, a proper position reconstruction algorithm is needed to reduce the systematic non-linearity. Two of such algorithms have been studied in detail. One is a Center-of-Gravity method: Let the charge collected on the central channel k be Q_k, and the charges to the left and to the right be Q_{k-1} and Q_{k+1}, and w be the distance between two readouts. The position is then given by:

$$x = kw + w\frac{Q_{k+1} - Q_{k-1}}{Q_{k-1} + Q_k + Q_{k+1}} C_3 .$$

C_3 is a correction factor that depends on the detector geometry. The UIR for the curved proportional detector using the center-of-gravity algorithm is presented in Fig. 7. The detector response is very uniform except for a few local spots. Corrections to those will be studied further.

The other algorithm is called the Gaussian Fit. The reconstructed position is given by:

$$x = kw - \frac{w}{2}\frac{\ln(Q_k/Q_{k+1}) - \ln(Q_k/Q_{k-1})}{\ln(Q_k/Q_{k+1}) + \ln(Q_k/Q_{k-1})}$$
$$= kw + \frac{w}{2}\frac{\ln Q_{k+1} - \ln Q_{k-1}}{2\ln Q_k - \ln Q_{k-1} - \ln Q_{k+1}}$$

This method largely eliminated the local spikes exhibited in the center-of-gravity method. However, as the actual distribution of the cathode charge is not a Gaussian function, another kind of systematic error still exists. The detector response to a stepped collimated beam is shown in Fig. 8. Position resolution measurement of a collimated beam shows a resolution of 59 μ m in the center of the readout channel and 65 μm near the inter-channel connection using the Gaussian fit algorithm.

To summarize, this project has resulted in the development of an advanced, prototype detector, and fast analog and digital electronics, suitable for high resolution, high rate powder diffraction at the National Synchrotron Light Source, and at other synchrotron facilities. The work has led to a better fundamental understanding of gas proportional multiplication along the thin edge of a metal sheet, permitting a new type of robust 1D X-ray detector to be constructed. New techniques for fast, low noise digital centroid finding have been developed for this position sensitive detector. Results from the entire prototype system indicate clearly that the goal of a device with a full 120 degree coverage is achievable. The work has resulted in three presentations at International Conferences, generating considerable interest from participants in the same field. One report is already published, with two pending.

PAPERS/JOURNALS/PUBLICATIONS:

1. B. Yu, G.C. Smith, D.P. Siddons and P.J. Pietraski, "Studies of anode blades for gas proportional detectors," *Nuclear Instruments And Methods* A419 (1998) 519-524.

2. B.Yu, G.C. Smith, D.P. Siddons, P.J. Pietraski and Z. Zojceski, "Position Sensitive Gas Proportional Detectors with Anode Blades," submitted to *IEEE Transactions on Nuclear Science.*

3. P.J. Pietraski, Z. Zojceski, D.P. Siddons, G.C. Smith and B. Yu, "Digital Centroid-Finding Electronics for High-Rate Detectors," submitted to *IEEE Transactions on Nuclear Science.*

LDRD FUNDING:

FY 1997	$ 96,666
FY 1998	$ 99,509

Plasma Window for Transmission of Synchrotron Radiation

A. Hershcovitch *97-16*
E.D. Johnson and
P.M. Stefan

PROJECT DESCRIPTION:

*P*rior to the initiation of this project it was demonstrated that the presence of an atmospheric arc plasma increased the effectiveness of differential pumping structures by a factor of nearly 230 [A. Hershcovitch, J. Appl. Phys. 78 (1995) p. 5283]. The plasma establishes a vacuum-atmosphere interface without any intrusive solid structures, i.e., the plasma acts as a window which separates vacuum and atmosphere. Inherently, such a plasma window is also transparent to a wide range of the electromagnetic spectrum, from the ultraviolet out into the hard x-ray regime. The present project was designed to develop and test a prototype window system for use at synchrotron beamlines. The objectives were to extend the prior technology to improve the pressure differential and reduce the size of the apparatus.

As the project proceeded, additional applications were pursued in collaboration with other groups. For example, BNL-ATF personnel proposed utilizing plasma windows for their CO_2 laser amplifier and in an electron beam plasma accelerator. For a project at MIT, separation of a high pressure gas target from accelerator vacuum has been proposed. At the APS, a fast igniting plasma window to act as a fast valve is being developed.

Approach: Before proceeding with plasma window development, it was crucial to ensure that plasma windows do not generate electromagnetic interference, which would adversely affect any NSLS experiments. Therefore, a series of electromagnetic interference tests had to be conducted.

No external magnetic fields were incorporated in the early window configuration, since it was designed for various applications like non-vacuum electron beam welding, electron beam melting, and non-vacuum ion material modification. For transmission of synchrotron radiation, magnetized plasma windows can be used. In principle, these plasma windows should out perform the original window, since higher pressure plasmas with lower densities can be generated with confining magnetic fields. Therefore, initial experiments with magnetized plasmas were conducted.

Until a plasma window that can operate in oxygen is developed (arc housing made of special material), external gas feed is required. By feeding the gas through a venturi, assistance in differential pumping is expected.

To further enhance window performance, perpendicular (to window axis and to each other) electric and magnetic fields can be added in such a way that the **ExB** drifts guide escaping ions and electrons back into the window. Early MHD plasma thrusters were based on this principle.

TECHNICAL PROGRESS AND RESULTS:

A small test stand was assembled in the basement of building 535. The original plasma window, which was damaged during an electron beam transmission experiment,

was repaired and mounted on a vacuum system.

A series of Electro-Magnetic Interference (EMI) experiments revealed that rf emission from the arc is negligible. In these experiments, no EMI or electromagnetic noise was detected on: a radio, a "Walkman", or a computer (PC) operating adjacent to the plasma window. Quantitatively, an EMI probe in the range of 30 - 300 MHz detected rf noise of up to 0.7 mW/cm^2 on the arc power supply, and up to 0.9 mW/cm^2 on the arc circuit. However, on the plasma window itself, only 0.05 mW/cm^2 could be measured. The reason may be due to the fact that plasma frequency is so high that only EM radiation with a frequency higher than IR can escape. Finally, the "acid" test for rf noise was passed; The proportional counter electronics (belonging to Kirz and Feser) functioned well while the plasma window operated. These electronics are from the X-1A beamline, which would be a good candidate for utilization of a plasma window.

The plasma window coupled to a venturi operated successfully. The addition of the venturi resulted in enhancement of window performance by a factor of about 3 (i.e., the enhancement of vacuum separation over differential pumping reached a factor of 600). Additionally, the venturi seems to reduce the required plasma arc power level by 25%.

At MIT, record results for vacuum separation by a plasma window were obtained. That plasma window, which operated with arc currents of up to 90 Amperes (compared to 50 A at BNL), was successfully used to separate vacuum from atmosphere, and a 3 atmosphere gas target from an accelerator vacuum. With two small differential pumping sections, a pressure of 1.44×10^{-6} Torr was obtained at the accelerator (it represents more than an order of magnitude improvement over previous results). These MIT results prove the feasibility of using a plasma window for neutron tomography in particular and for internal targets in general.

A newly designed and fabricated plasma window was successfully operated at ANL. It fired on the first try without any breakdown problems (which is rather unusual for such a new design). This plasma window has a rugged construction, and it can be compatible with UHV operation. Additionally, the design ensures that water will leak to atmosphere in case of any puncture in the water cooling system. This plasma window may become the preferred prototype design.

Since gas rushing out from a venturi may be objectional to some users, experiments were performed to reduce axial gas flow with a funnel and by deflection. A combination of the two yielded a factor of 30 reduction in axial pressure.

Motivated by interest and assistance from ATF, the plasma window was also successfully used to separate between a high-pressure (82 psi) chamber and atmosphere. A laser beam (5 mW with a 543 nm wavelength) was readily passed from that chamber through the plasma window to atmosphere.

X-ray transmission experiments were performed at the X-6 beamline at NSLS. In these experiments, x-ray transmission (through a plasma window operating in argon) was measured for x-rays with energies of 3.2 KeV (an argon resonance) and 9 KeV (off resonance). Although these results have not been analyzed quantitatively yet, a qualitative observation indicates that,

as expected, x-ray transmission off resonance is excellent, while strong absorption occurs at resonance.

IMPENDING ACTIONS AND LONG TERM BENEFITS:

Plasma windows can be used to greatly improve five beam lines. At U-11 & U-13, two plasma windows can be used for vacua interface to contain an argon gas filter to remove higher order diffracted light. With a plasma window at X-1, microscopy can be greatly improved since absorption (in an inhomogeneous window) is eliminated. Finally, since plasma windows can not have scratches, spatial coherence effects will no longer be a problem at X-13 & X-25 for experiments like intensity correlation spectroscopy.

In addition to the obvious benefits to the NSLS, ATF and the sciences and technologies they foster, plasma windows can greatly enhance the laboratories' capability to conduct research in nuclear and high-energy physics, as well as medical and life sciences. BNCT based on recirculating proton beams can be realized with two plasma windows on either side of a lithium cell. Plasma windows offer the only viable scheme for maintaining a highly localized, high pressure, lithium vapor cell inside a high-energy proton storage ring. Additionally, high energy and nuclear research, would also benefit from various internal targets, plasma strippers and plasma lenses, e.g., a plasma stripper/lens could enhance the stripping of heavy ions between the Booster and AGS, as well as, between the tandem Van de Graaff and the Booster. A plasma stripper/lens or an internal gas target "sandwiched" between two plasma windows could achieve the desired vacua separation.

LDRD FUNDING:

FY 1997	$ 60,475
FY 1998	$ 56,022

Development of New Techniques in Picosecond Pulse Radiolysis

James F. Wishart *97-29*

PROJECT DESCRIPTION:

Statement of Work: The Chemistry Department has commissioned the Laser-Electron Accelerator Facility (LEAF), a state-of-the-art picosecond electron pulse radiolysis facility based on the radio-frequency photocathode electron gun technology developed at the BNL Accelerator Test Facility. The new accelerator is the first of its type to be dedicated to the study of radiation chemistry. Similar facilities are planned or proposed at other laboratories in France, Japan and the United States. The facility itself owes its existence to a proposal which resulted from a workshop organized with LDRD funds in 1989 (#89-42).

The unique design of this accelerator offers several advantages over other existing accelerators for the study of physical and chemical processes on the picosecond and femtosecond timescale. In particular, the new system includes a picosecond-synchronized femtosecond laser source which can be used to probe radiolytically-generated transients by time-resolved spectroscopy. Even more unique is the ability to do femtosecond excitation of radiolytic transients to probe their excited state physics and chemistry, and to examine the reactions of radicals with excited states. These studies are important for understanding charge recombination processes and radiation damage phenomena, and they will help in trying to comprehend the reactions which occur in heterogeneous, highly energetic and radiation-filled environments such as the Hanford waste tanks.

This project supports one research associate, to assist in the construction of time-resolved femto- and picosecond excitation and detection systems which unite the capabilities of pulse radiolysis with flash photolysis, and to use the system to investigate the chemistry of radical species, charge recombination in hydrocarbons, and reactions of highly excited species.

PREVIOUS TECHNICAL PROGRESS - Fiscal Year 1997:

Dr. Sergei Lymar received a Senior Research Associate appointment on this project in January 1997. Based on his experience in peroxynitrite chemistry and the capabilities of the new facility, he and Dr. Wishart submitted a proposal to the Environmental Management Science Program (EMSP), which was the first BNL proposal to be funded under that program ($700,000 over three years). The EMSP studies concern the reactivity of peroxynitrite (which is formed in the Hanford tanks by radiolysis of nitrate salts) and related species.

In March 1997, the DOE authorized commissioning of the LEAF accelerator. During the remainder of the fiscal year the primary activity was establishment and refinement of accelerator settings to steer the electron beam to the experimental stations, focus it on the targets, and minimize the undesired dark current. A system for temporal and spatial electron beam diagnostics was designed and a computer-controlled, remote laser beam steering system was installed. A station for transient absorption and conductivity kinetic measurements on the nanosecond and longer timescales was built. Substantial effort was invested in sample cell development to

eliminate RF noise (inherent to the picosecond electron beam itself) so that clean signals can be obtained at the shortest timescales.

TECHNICAL PROGRESS AND RESULTS - Fiscal Year 1998:

In February 1998, the LEAF facility received DOE authorization for Routine Operation, allowing the experimental program to begin. LEAF's thousand-fold advantage in time resolution over our existing 2 MeV electron Van de Graaff was immediately evident in the transient conductivity data obtained by Dr. Richard Holroyd and coworkers.

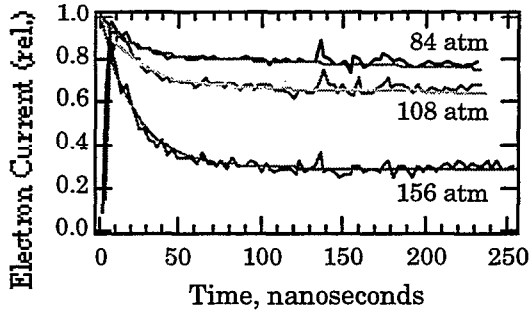

Electron capture by carbon dioxide in supercritical ethane was observed directly for the first time, increasing by a factor of three the amount of information gained about these remarkable reactions with activation volumes of liters per mole. One report on this work has been accepted for publication.

Electron and Laser Beam Diagnostics: An existing streak camera was upgraded (with capital funds) for use in characterization of the LEAF electron and laser beams. The temporal characteristics of the electron pulse were determined using Cerenkov light generated in a thin quartz plate. The electron pulse duration at Target "A" was observed to be approximately 30 ps. Direct measurement of the electron pulsewidth will permit us to optimize the accelerator characteristics to produce the shortest pulsewidth possible. Temporal jitter between the electron and laser pulses was within the resolution of the experiment (• 5 ps). The streak camera has also proven extremely valuable in tuning the characteristics of the 266 nm laser pulse which generates the accelerated electrons.

Picosecond Detection Station: An optical delay line for measuring the time-resolved absorption of transient species generated by radiolysis is now operational at the "A" target station. This station takes advantage of the picosecond-synchronized laser pulse for transient detection, which is a unique feature of the LEAF design. Software for remote computer control of the delay line, data acquisition, processing, and storage was written in LabView. Tests of the detection station were performed by monitoring radiolytic formation of solvated electrons in water. Rise-times of the observed transients agree with the accelerator pulse duration obtained with the streak camera. Further improvements in sensitivity and noise reduction are presently underway.

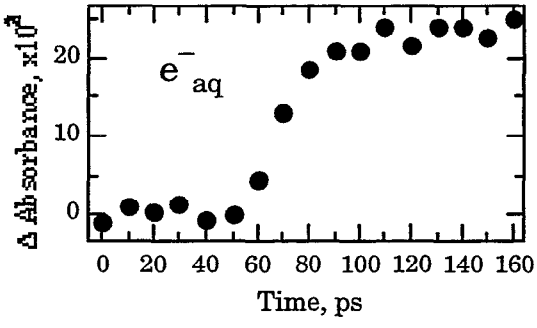

Transient absorption profile of 1.3 μM e^-_{aq} measured by the time-delay pulse-probe detection system.

LEAF-Related EMSP Activities: Utilization of LEAF's unique capabilities for studying reactions related to Hanford nuclear waste remediation is an integral part of an ongoing 3-year research project funded in FY1998 by

the DOE Environmental Management Science Program. A comprehensive study of radiation-induced peroxynitrite formation in solid nitrates and their concentrated solution was conducted in 1998. Quantitative information about radiation yields of peroxynitrite and their dependence on the reaction conditions was obtained. These results will be used in designing experiments for LEAF that can provide mechanistic information (such as the nature of the intermediates, their reactions and lifetimes) concerning peroxynitrite accumulation in the nuclear waste.

LDRD FUNDING:

FY 1997	$ 104,103
FY 1998	$ 114,120

X-ray Circular Dichroism of Biological Macromolecules

John C. Sutherland *97-39*
Erik D. Johnson
Chi-Chang Kao

PROJECT DESCRIPTION:

Conventional CD–MCD Spectroscopy: Circular dichroism in the ultraviolet, visible and infrared provides information on the structure of DNA, RNA, proteins, polysaccharides, and other molecules of biological interest in solution, hence complementing the structural information obtained from crystallography. Such measurements have been important in molecular biophysics, structural biology, drug design, and related fields for about 30 years. Magnetic circular dichroism in the same region has been used to study the electronic structure of absorbing species, particularly heme- and other metallo-proteins. Synchrotron radiation has been the source-of-choice for circular dichroism experiments in the vacuum ultraviolet ($\approx 105 \leq \lambda \leq \approx 190$ nm) since 1980, but the technology used in these experiments **cannot** be extended to shorter wavelengths.

X-Ray CD/MCD with Synchrotron Radiation: Interest in using circularly polarized x-rays generated by synchrotrons to measure CD extends back to the mid 1970's, however, usable beamlines are just becoming available. The most sensitive experimental arrangement presently in sight involves an elliptically polarizing wiggler that can switch between producing left- and right elliptically polarized x-rays at a frequency > 1 Hz. Such a device has been installed on beamline X13 at the NSLS, and preliminary testing has been performed. We recently obtained funds for a new monochromator to serve the elliptically polarizing wiggler on X-13 as part of the DOE facilities initiative. While other synchrotron sources are developing circular dichroism capabilities, there is a window-of-opportunity for BNL to begin a program leading to an x-ray CD/MCD research program and structural biology user facility at the NSLS.

We are testing the hypothesis that large circular dichroism signals occur when the wavelength of the circularly polarized light matches the pitch of the helix of a polymer such as DNA, RNA or proteins. Thus, unlike conventional circular dichroism, molecules containing different types of helical secondary structures with different pitches should also give maximal signals at different wavelengths, and the sign of the x-ray CD may indicate directly the handedness of the helix of the biopolymer. In collaboration with Eugene Stevens (SUNY-Binghamton), we will extend these observations to polysaccharides. In collaboration with Philip Stephens (University of Southern California) we will explore the MCD of the L-edge absorptions of metals in the active sites of metalloproteins. Such studies will be particularly important for proteins containing metals such as zinc, whose complexes do not absorb in the visible or near infrared and hence have not been subjected to analysis by conventional MCD. We shall also work with Patricia Snyder (Florida Atlantic University) in studies of x-ray MCD of atoms and CD/MCD of small molecules in the vapor phase. These experiments will improve our understanding of the fundamental mechanisms of x-ray CD and MCD and develop a strong user base, hence increasing the probability of obtaining extramural support.

TECHNICAL PROGRESS AND RESULTS – Fiscal Year 1998:

Purpose: The purposes of this program are to:

- construct a UHV beamline to receive soft X-rays (250 eV< h• < 1.25 keV) from the ellipsodailly polarizing wiggler at the National Synchrotron Light Source,
- develop new methods for extraction of circular dichroism signals with high sensitivity using phase-sensitive detection, and
- determine if helical macromolecules such as DNA exhibit differential absorption or scattering of X-rays when the pitch of the molecular helix is commensurate with the wavelength of the radiation.

Approach: This is a collaboration between the Ultraviolet Biophysics Group in the Biology Department and the Experimental Systems Group at the National Synchrotron Light Source. The project is divided into several modular sub-projects:

- Design and purchase (with funds from the 1996 DOE Facilities Initiative) of a UHV soft X-ray monochromator and articulated exit slit.
- Assembly of the beamline to include the new monochromator, exit and enterence slits, sample chamber and associated photon transfer and vacuum components.
- Design and construction of detector and signal processing systems, to include both mechanical and electronic components.
- Assembly and programming of a computer system for the acquisition and archival storage of experimental data.
- Evaluation of the performance of the beamline for the measurement of soft X-ray circular dichroism.
- Exploration of the circular dichroism of chiral biological molecules using the instrument described above.

Technical Progress and Results:

- The monochromator and articulated exit slit were designed by Dr. Erik Johnson, head of the Experimental Systems Group at the National Synchrotron Light Source. The monochromator was fabricated by Oxford Instruments Accelerator Technology Group (Osney Mead, Oxford, UK) and the exit slit by McPherson Instruments (Acton, MA, USA). Other major components (deflecting mirror, entrance slit, and sample chamber) and minor UHV components of the beamline were provided by the NSLS Experimental Systems Group. The configuration of the assembled beamline is shown in Figure 1.

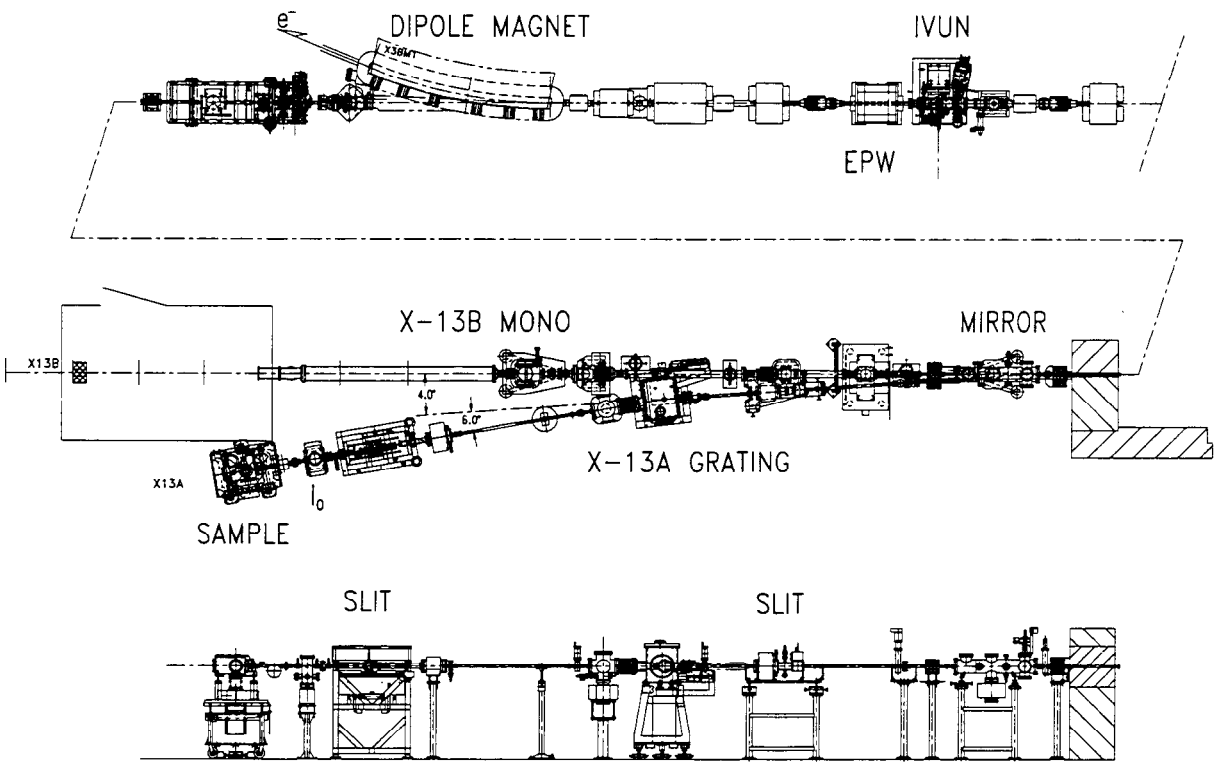

Figure 1 Diagram of beamline X13 at the NSLS. The top panel shows the straight section of the storage ring that the Elliptically Polarizing Wiggler (EPW) shares with another insertion device (an In-Vacuum Undulator, IVUN). The beam of electrons circulating within the storage ring enters this section from the right of the figure. The photon beam generated by either the EPW or the IVUN exits the storage ring vacuum chamber at a port located within the field produced by a dipole magnet that separates the electron beam circulating in the storage ring from the photon beam, which is traveling to the left in the figure. The vacuum chamber containing the photon beam passes through a series of shutters and valves and then through a radiation shield wall, which is the first element shown on the right-hand side of the center and lower panels. The center panel is a plan view of beamline X13 outside of the shield wall. A mirror located just outside the shield wall deflects the beam through 4° and focuses the photon beam towards either X13A, the soft x-ray beamline described here, or X13B, which is configured for experiments using higher energy x-rays. The experimental apparatus for X13B is contained within a radiation area exclusion structure (hutch) shown only as a rectangular outline. The lower panel is an elevation view showing only those components specific to X13A or common to both branches. The major components of X13A are, from right to left, the entrance slit, grating monochromator, exit slit, and sample chamber. A hutch is not required to contain the soft-x-rays reaching the X13A sample chamber. The electronics, computer system, and operator console are located to the left of the sample chamber.

- **Design of the beamline and signal extraction Electronics:** The design and construction of the beamline were described in a paper published in 1998 (Sutherland, Polewski et al. 1998). The novel design elements are the use of three lock-in amplifiers to extract simultaneously the circular dichroism and absorption spectra of a sample. The same system also operates in reflectance mode, and, as described in the paper, the sample and detector arm rotate about a common axis within the sample chamber. The three lock-in configuration are shown schematically in Figure 2.

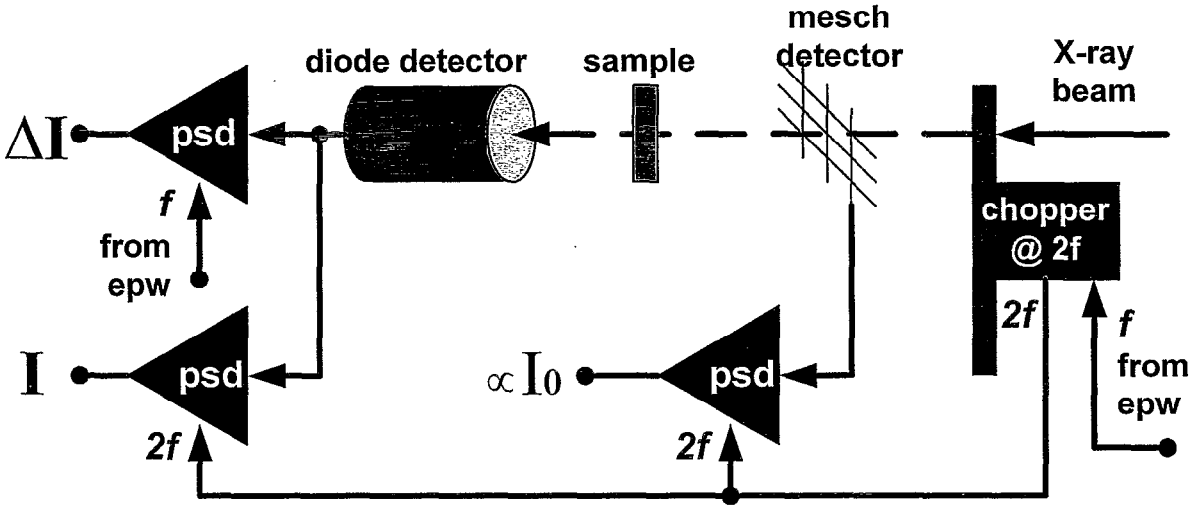

Figure 2 Schematic Diagram of the triple synchronous detection configuration for the simultaneous measurement of X-ray circular dichroism and absorption. A reference signal at frequency *f* is generated by the elliptically polarizing wiggler (epw) is applied to the rotating chopper and the phase sensitive detector (psd – also known as a "lock-in" amplifier) that detects the polarization induced difference intensity (ΔI). The chopper operates at twice the frequency of the epw, and generates a reference signal at this frequency, which is used by two other lock-ins to extract signals representing the time average intensity transmitted by the sample (I) and a signal proportional to the incident intensity (Io).

- **Sample Chamber.** The last component of the optical train is a sample chamber. As shown in Figure 3, the sample is mounted on a rotatable spindle so that the angle of incidence can be varied from normal incidence to grazing incidence under computer control. The detector (a photo diode at present) is mounted on the end of an arm, which rotates about the same axis as the sample. This configuration allows for four scan modes: photon energy is scanned while the orientations of the sample and detector are fixed, the orientation of the sample or the detector are scanned while the other component and photon energy are fixed, and the sample and detector are rotated synchronously such that the detector receives the specularly reflected beam, again with fixed photon energy.

- **Beamline Computer System.** A computer system that controls the stepping motors that move the monochromator grating, monochromator exit slit, sample angular position and detector position and acquires analog and digital data from the beamline was installed and programs that implement beamline operation and data acquisition were written. The operator interacts with the beamline computer *via* a graphical user interface (GUI). Data are stored on a server for subsequent recall and analysis on workstations connected to the BNL LAN or the internet.

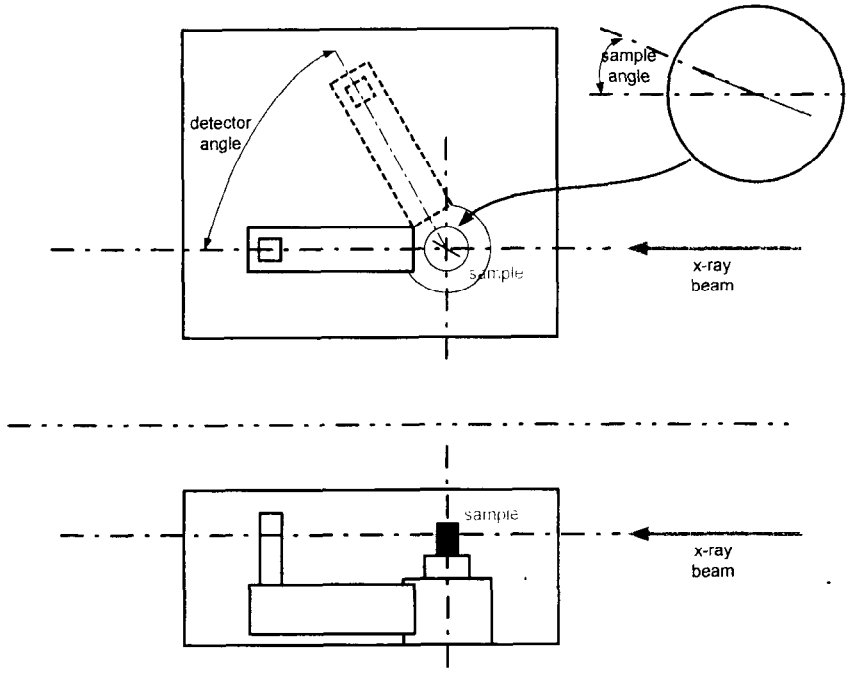

Figure 3 Sample chamber permitting independent or specularly correlated orientations of the sample and detector arm.

- **Results.** First successful operation of the beamline was achieved produce in late August, 1998, when the magnetic circular dichroism of a test sample of MnNiAs was recorded in the specularly reflected beam for an incident beam angle of 7° off grazing incidence. Typical data for differential reflectance are shown in Figure 4.

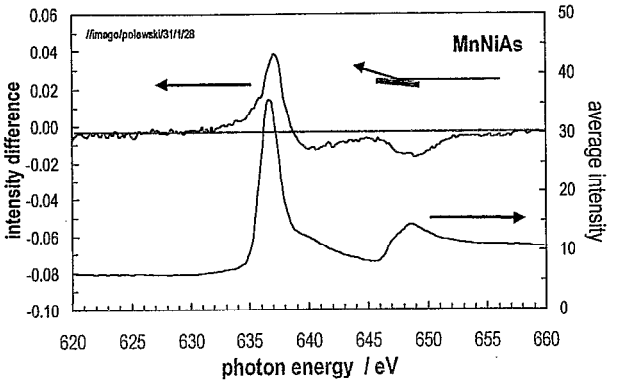

Figure 4 The difference in the reflected intensity of right- and left-circularly polarized X-rays (left axis) and the time average reflected intensity off a MnNiAs film at about 7° angle of incidence. The film had been magnetized by application of a magnetic field. We use such experiments to align and calibrate the electronics used for the extraction of CD (as shown in Figure 2).

- **Performance.** The use of phase sensitive detection increases the sensitivity for the detection of intensity differences (*i.e.*, CD signals) by at least a factor of 100 compared to previous experiments performed by scanning spectra with constant polarization, and switching polarizations or magnetic field between scans. This enhancement in performance is being used by solid state physicists in studies of the structure of thin films.

ACCOMPLISHMENTS:

Future Funding:

Biophysical Applications of X-ray circular dichroism are under development in collaboration with Adrian Parsegian, Head of the Laboratory of Physical and Structural Biology at the National Institutes of Health. We anticipate submitting a proposal to the Extramural Program of NIH as soon as preliminary data adequate to support a reasonable probability of funding are available.

PUBLICATIONS:

Sutherland, J.C., Polewski, K., Monteleone, D.C., Trunk, J.G., Nintzel, G.A., Carlson, D.G., Dong, Q.-L., Singh, O.V., Hulbert, S.L., Kao, C.-C. and Johnson, E.D. (1998). "Soft X-Ray Circular Dichroism and Scattering Using a Modulated Elliptically Polarizing Wiggler and Double Synchronous Detection." *Proceedings of the Society of Photo-Instrumentation Engineers: Advances in Optical Biophysics* **3256**: 2-14.

LDRD FUNDING:

FY 1997	$ 94,131
FY 1998	$ 106,038

X-Ray Schlieren Computed Tomography

F. A. Dilmania *97-44*
L.D. Chapman
B.A. Dowd
D.P. Siddons and
W.C. Thomlinson
In Collaboration with Z. Zhong, B. Ren, X.Y. Wu, and I. Orion

PROJECT DESCRIPTION:

*M*ammography is one of the most active fields of research among the different branches of radiography because while positive identification of each malignant tumor can save a life, existing methods of mammography still miss about 15 % of clinically obvious breast cancers [1]. A new method of mammography was invented at the National Synchrotron Light Source (NSLS) in 1986 by Chapman, Thomlinson, and their collaborators [2, 3]. The method was initially called X-Ray Schlieren Imaging [2], but now is referred to as Diffraction Enhanced Imaging (DEI) [3]. It uses synchrotron-generated, monochromatic, fan-shaped-beam x-rays for line-by-line imaging of the subject. At the heart of the method is an analyzer crystal, of the same type as used in the system's monochromator, that is positioned between the subject and the detector. This geometry detects only those x-rays that were transmitted through the subject with an angular deviation out of the plane of the fan beam that falls within the angular acceptance of the analyzer crystal. The curve that determines the shape of this angular acceptance is called the "rocking curve"; it modulates detection probability as a function of the deviation from the configuration in which the analyzer crystal is completely parallel to the monochromator's crystal (i.e., the "tuned" position). The information produced on the angular deviation of the transmitted x-rays are used to generate two new images of the subject: a) that of the x-ray index of refraction, and b) that of absorption in which the so-called "x-ray small-angle scattering" is suppressed. The first image is a natural "edge-enhancer" that accentuates the boundaries between different types of tissue, while, in the second image, contrast between different tissue types is typically enhanced remarkably because of lesser "smearing" effects from small-angle scattering. The first goal of the present LDRD was to implement DEI in the computed tomography (CT) mode at the NSLS. The advantage of the CT mode is that its cross-sectional view lacks the problem of overlying tissues that occurs in planar x-ray radiography. The goal was then to use these cross-sectional images to characterize DEI images of different types of normal and cancerous tissue in live mice and rats, in excised human tissues, as well as in normal tissues from chickens and cows.

The Statement of Work, revised slightly from that of our 1997 Interim Report, Statement of Work, is the following:

a. To develop a CT system for DEI at X15A
The emphasis will be on developing the monochromator/analyzer system. The monochromator will be a Bragg-Bragg device, while the analyzer will diffract x-rays either in the Bragg or in the Laue mode. The detector and the data-acquisition system (DAS) will be borrowed from the Multiple Energy Computed Tomography (MECT) program[4].

b. To develop the basic algorithms for reconstructing DEI CT
The CT projection data is acquired at three data points over the rocking-curve: at the peak, and at the half-maximum points.

The data then are processed to produce separate images of the x-ray index of refraction, and of absorption in which small-angle scattering is suppressed. The latter is called "the apparent absorption image." Besides these images, the slice is also imaged with the "conventional" method in which the analyzer crystal is removed and the detector positioned in the direct path of the transmitted x-rays.

c. To undertake a comprehensive set of tissue-characterization studies We will image normal and cancerous tissues in live mice and rats and in surgical specimens, and image normal animal tissues from chickens and cattle.

PREVIOUS TECHNICAL PROGRESS:

The first year's work (which was essentially 6 months because of the late start of the project) concentrated on preparing equipment for the system at the NSLS's X15A, which became available to the DEI program for 50% of its operating time in September 1997. In parallel, to understand the fundamental physics of the DEI process, experiments were carried out by Thomlinson, Chapman, Zhong, et al. in May and September 1997 at the Advanced Photon Source (APS), Argonne National Laboratory, and at the European Synchrotron Research Facility (ESRF), Grenoble, France. The following was accomplished as a result of these studies:

a) the DEI imaging hardware was developed to almost completely eliminate vibrations of the sample, monochromator, and analyzer. The key was learning how to rigidly tie together the monochromator and analyzer, while still retaining the full motion of the sample and detector. As a result of modifying the system, the analyzer is now held stable to about 0.1 μradian, which is sufficient for DEI at energies as high as 30 keV.

b) full quantitative calculations of the small-angle-scattering strengths were developed, and was compared with the measured "apparent absorption." The comparison was made at 18 and 30 keV, and provided confidence in our understanding of the basic physics of the process. The results clearly demonstrated dramatic improvements in image information that should be present in the CT images.

c) it was demonstrated that the index of refraction and DEI images depend only weakly on the beam energy. Normal absorption coefficient and its atomic-number dependence rapidly decrease as energy increases, thereby reducing conventional contrast. But the absorbed dose also decreases. Thus, if the image information is constant (and greater than conventional absorption) at higher energies and at lower doses, then DEI will have significant advantages over conventional imaging. In fact, the experiments confirm these expectations. DEI CT also should show the same advantage in dose/contras. We are confident that the experiment can be designed for higher energies for imaging of tissues and bones in anatomical specimens and in live animals.

TECHNICAL PROGRESS AND RESULTS - Fiscal Year 1998:

Purpose: The objectives of this program are to develop a DEI CT system and to use it to quantitatively characterize tissues. The following outlines the tasks in detail.

a. To develop or modify the following components of the DEI CT system:
   i. A Bragg-Bragg monochromator with 12 cm crystal width, using Si<333> (the existing system may be used as it

is, or may be modified).
ii. A Laue analyzer crystal, and its tangent-arm positioning system.
iii. An integral mechanical stand for both monochromator and analyzer.

b. To use the following components from the MECT program:
i. A subject-positioning system for rats.
ii. A modular CT detector with 0.9 mm element spacing. Images with a spatial resolution better that 0.9 mm can be obtained by slitting the detector to half or to a quarter of the actual element-spacing of the detector, and using it in conjunction with a data-acquisition method that employs sequential imaging with lateral shifts of the subject□s apparatus between collections.
iii. The data-acquisition system.

c. To develop the following image-reconstruction algorithms:
i. The conventional CT image (i.e. simple transmission in the Laue analyzer) will be handled as in regular CT.
ii. Sinograms for the "refraction image" and for the "attenuation image with suppressed small-angle scattering" will be prepared from projections using equations outlined in Refs. 2 and 3, and then reconstructed tomographically using the filtered backprojection method.

d. To carry out the following studies for tissue characterization:
i. Imaging human anatomical specimens, including different tumor tissues.
ii. Imaging normal live rats and mice.
iii. Imaging rats bearing intracerebral or subcutaneous 9L gliosarcoma tumors.
iv. Imaging the normal tissues of chickens and cattle.

Approach:

a. Monochromator development
The monochromator is the two-crystal Bragg-Bragg device developed by Thomlinson et al. The analyzer, a flat Bragg or Laue crystal, is mounted on a tangent arm so it can be stably and precisely positioned. A special tangent-arm device was designed and constructed to hold the crystal holder on both sides. Si<333> reflections will be used for high angular sensitivity. The maximum beam width is 12 cm, the maximum beam height is 2 mm, and the energy range will be 18-35 keV.

b. Routine development
Three sets of CT projection data are acquired, with the analyzer tuned at the rocking-curve's peak and at its half-maximum angles. The data then are analyzed (Refs. 2 and 3) to produce two sinograms, one for the refraction image, and one for attenuation with suppressed small-angle scattering. Those routines are linear mathematical operations, while the basic mathematical step in preparing CT projections are logarithmic [5].

c. System evaluation and tissue-characterization measurements
For continuation of our studies we plan to raise the beam energy to 35 keV for imaging larger subjects, and characterize the following tissues: a) normal live rats, imaged with transaxial slices along the entire body to characterize all major tissue types, b) live rats bearing subcutaneous 9L gliosarcoma and C6glioma tumors on their thighs, c) live nude mice, and perhaps nude rats, bearing human breast tumor MCF-7 on their thighs, d) cancerous and normal excised human breast tissues, and

e) normal tissue from chickens and cattle.

Technical Progress and Results:
Experiment at X15A were carried out in February, March, and July, 1998.

1. Hardware development: The X15A setup for planar mammography was developed in early 1997 (Thomlinson, Zhong, et al.). The steps for preparing the system for CT included a) adding a large platform to support the subject stage, b) adding a CT subject's stage, which was held by an elevator-stage from one side and a counter-balancing weight from the other, for precisely leveling it, c) equipping MECT's linear-array detector with a tantalum grid of the same pitch as the detector to limit the exposure of each detector element to 1/2 of its width (i.e. 0.46 mm) to improve spatial resolution, and d) developing a bi-axial "tangent arm" for positioning the analyzer crystal with high precision.

2. Algorithm development: The algorithm for CT image reconstruction was based on pre-reconstruction calculations that produced separate sinograms for the "refraction" and the "apparent absorption" images, followed by conventional filtered back projection to create CT images [5]. Four sets of data, obtained with the subject shifted laterally by 0.23 mm each time, were interlaced for a higher spatial resolution[4].

3. Phantom studies highlighting the "refraction" image: A 2"-diameter cylindrical acrylic phantom that included four non-axial cylindrical channels filled with oil was imaged at 22 keV [6-8]. Images obtained at the opposite shoulders of the rocking curve were subtracted and normalized to produce a CT image of the x-ray refractive index. This image was non-zero only at the points in the slice where the beam reached an angulated interface between two different media (Fig.1). These points were the radially opposite sides of the slanted oil channels. The CT image signal at these points was proportional to the tangent of the angle made by the channels with the rotation axis. The method was sensitive to minute changes in refractive index. Thus, it has the potential for use in radiology or in non-destructive testing as a natural "edge-enhancement" method.

4. Animal-tissue studies highlighting the "apparent absorption" image: A 3"-outer-diameter acrylic cup, filled with two pieces of bovine muscle surrounded by water, was imaged at 22 keV [9]. The pieces were tight fit, so that they did not move as the stage rotated. The muscle fibers were oriented vertically in one piece, and horizontally in the other. The images obtained at the peak of the rocking curve and normalized to conventional CT showed significant dependence on the orientation of the muscle fibers (Fig. 2). Since rocking-curve-top images are sensitive to subject-contrast arising from small-angle scattering (an effect called "extinction" contrast), this experiment demonstrates that muscle has a significant extinction contrast that is relevant to the radiography of soft tissues.

ACCOMPLISHMENTS:

Reference 5-9 below are direct products of this program; references 2 and 3 related to studies on the planar DEI CT; they led to the inception of this program and provided the basic algorithms for analyzing planar DEI images which were used as the first step in out CT reconstruction.

REFERENCES:

1. Baker, L.H. Breast cancer detection demonstration project: five-year summary report. CA 32(4), 194-225, 1982.

2. Chapman, D., Thomlinson, W., Arfelli, F., Gmür, N., Zhong, Z., Menk, R., Johnston, R.E., Washburn, D., Pisano, E., and Sayers, D. Mammography imaging studies using a Laue crystal analyzer. Rev. Sci. Instrum. 67(9): CD-ROM, 1996.

3. Chapman D., Thomlinson, W., Johnston, R.E., Washburn, D., Pisano, E., Gmür, N., Zhong, Z., Menk, R., Arfelli, F. and Sayers D. Diffraction enhanced x-ray imaging. Phys. Med. Biol. (In press, Oct./Nov. 1997 issue).

4. Dilmanian, F.A., Wu, X.Y., Parsons, E.C., Ren, B., Kress, J., Button, T.M., Chapman, L.D., Coderre, J.A., Giron, F., Greenberg, D., Krus, D.J., Liang, Z., Marcovici, S., Petersen, M.J., Roque, C.T., Shleifer, M., Slatkin, D.N., Thomlinson, W.C., Yamamoto, K., and Z. Zhong. Single- and Dual-energy CT with monochromatic synchrotron x-rays. Phys. Med. Biol. 42, 371-387, 1997.

5. Dilmanian, F.A. A CT reconstruction algorithms for Diffraction-Enhanced Imaging. Proceeding of the Workshop on Computed Microtomography, 1997 NSLS General Users Meeting. B. Dowd, Ed.

6. Dilmanian, F.A., Zhong, Z., Ren, B., Wu, X.Y., Chapman, L.D., Orion, I., and Thomlinson, W.C. Computed tomography using the diffraction-enhanced x-ray imaging method. Poster at the 6th International Conference on Biophysics and Synchrotron Radiation, Argonne, Illinois, August 4-8, 1998 (Conference Poster Abstract Book, p. 28).

7. Dilmanian, F.A., Zhong, Z., Ren, B., Wu, X.Y., Chapman, L.D., Orion, I., and Thomlinson, W.C. Computed tomography using the diffraction-enhanced x-ray imaging method. Abstract submitted to the 1998 Activity Report of the National Synchrotron Light Source, to be published in May 1999, E. Rothman and J.B. Hastings, Eds.

8. Dilmanian, F.A., Zhong, Z., Ren, B., Wu, X.Y., Chapman, L.D., Orion, I., and Thomlinson, W.C. Computed tomography of x-ray index of refraction using the diffraction-enhanced imaging method. (manuscript in preparation).

9. Zhong, Z., Dilmanian, F.A., Ren, B., Wu, X.Y., Chapman, L.D., Orion, I., and Thomlinson, W.C. Directionality in cow muscles imaged with the Diffraction-Enhanced Computed tomography. (manuscript in preparation).

LDRD FUNDING:

FY 1997	$ 59,792
FY 1998	$ 94,212
FY 1999 (est.)	$ 44,000

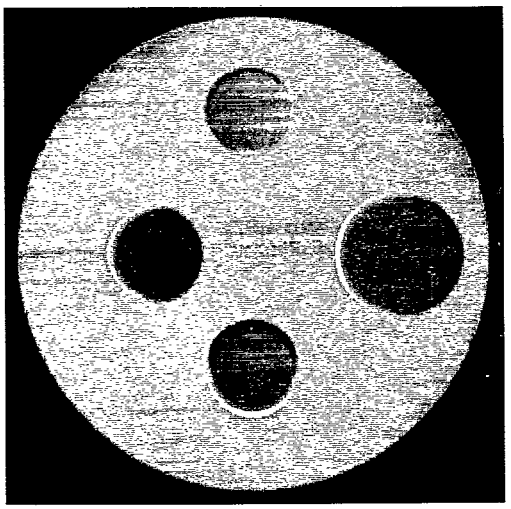

left image

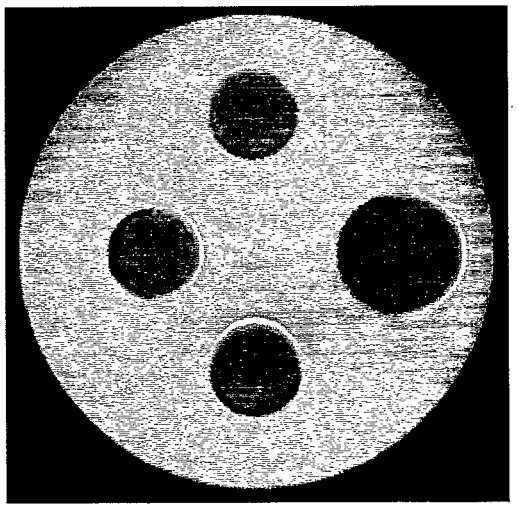

right image

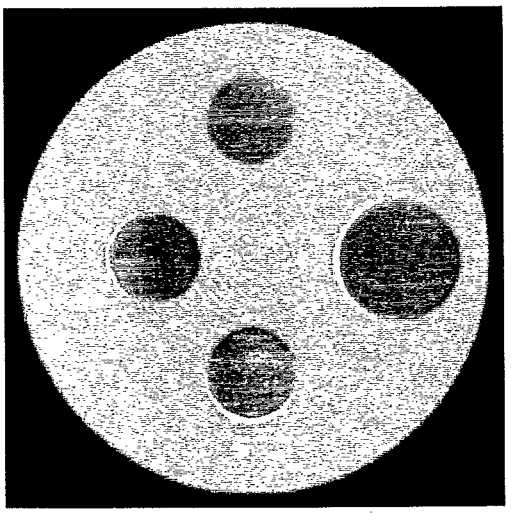

top image

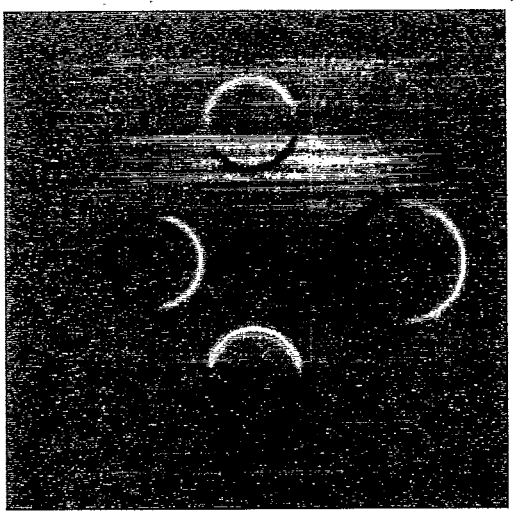

refraction image

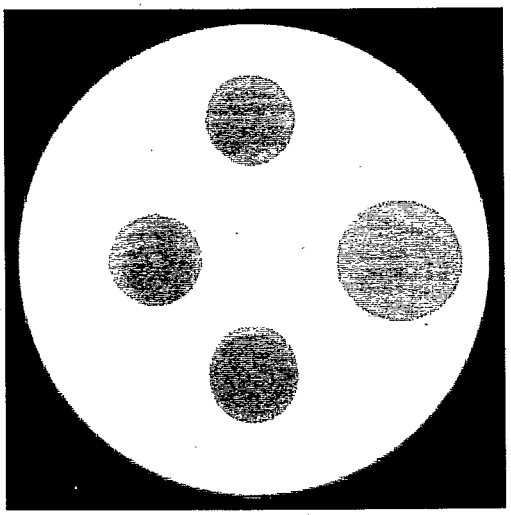

apparent absorption image

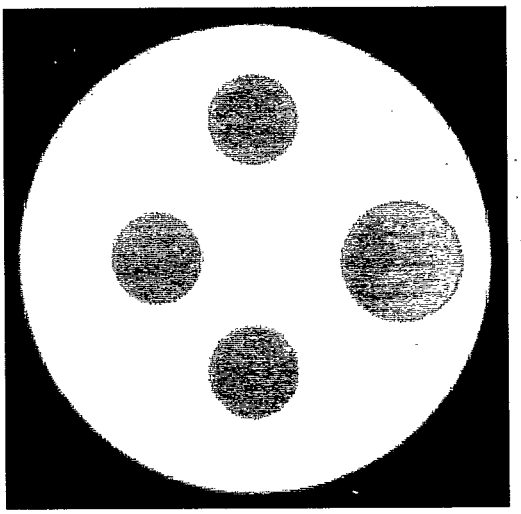

regular CT image

Fig. 1

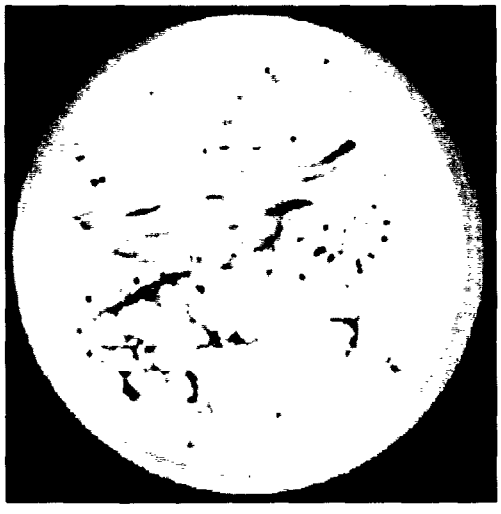

left image

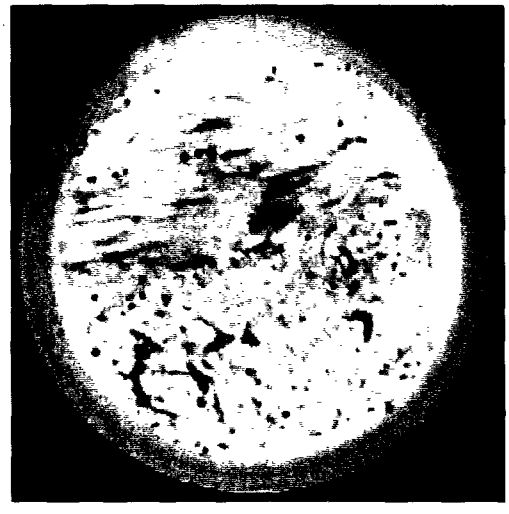

right image

top image

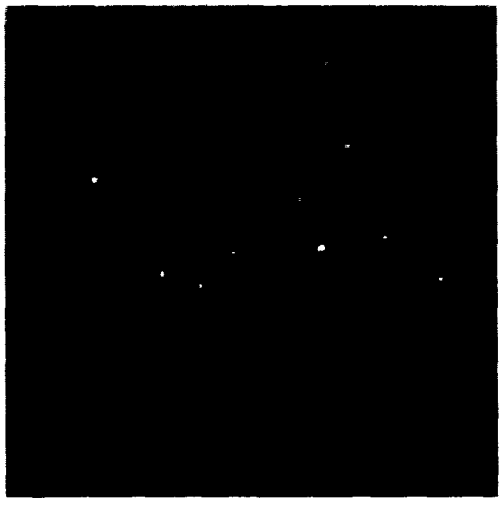

refraction image

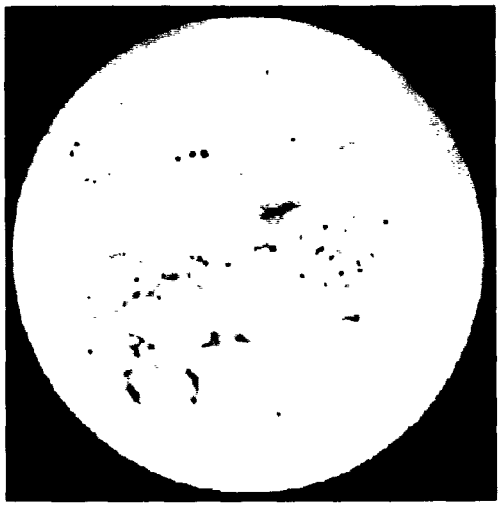

apparent absorption image

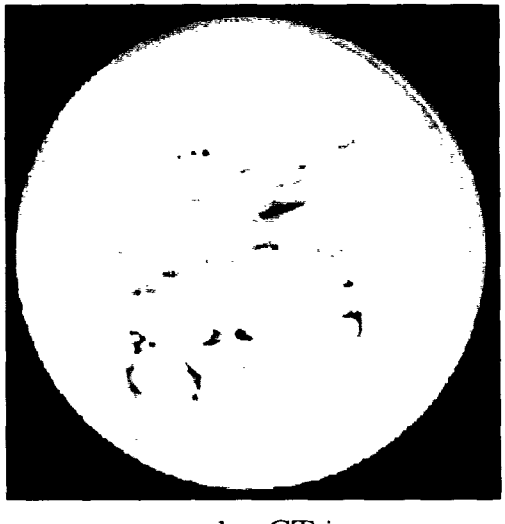

regular CT image

Fig. 2

Biodistribution, Toxicity and Boron Neutron-Capture Therapy in Animals Using Metallotetracarboranyl-porphyrins

Michiko Miura *97-45*

PROJECT DESCRIPTION:

Statement of Work:

1. To determine whether therapeutic tumor boron concentrations (>40 μg B/g) are achievable from boronated porphyrins in rats bearing 9L gliosarcomas as was shown in mice bearing mammary tumors. High tumor values should be attained with high tumor:blood and tumor:brain boron concentration ratios (each >5:1) and with minimal toxicity to improve boron neutron-capture therapy [BNCT].

2. To determine whether efficacy is possible by porphyrin-mediated BNCT using mice bearing leg tumors and rats bearing intracranial tumors using the optimal conditions determined in statement 1.

3. To determine whether imaging is feasible using single-photon-emission tomography [SPECT] of a copper-67 porphyrin or magnetic resonance imaging [MRI] of a manganese or gadolinium porphyrin.

4. To continue to synthesize boronated porphyrins including analogues of NiTCP, and other boron-containing compounds and to continue to test them for their biodistribution and toxicity properties in tumor-bearing mice.

PREVIOUS TECHNICAL PROGRESS:

BNCT is based on the production of high linear-energy-transfer ionizing radiation from the $^{10}B(n,^4He)^7Li$ reaction. It is therefore important that ^{10}B exists mainly in tumor tissue within the irradiation volume so that only tumor cells and their vasculature are selectively destroyed. For brain tumors, the critical normal tissues are blood and normal brain. It has been estimated that major advances in BNCT should be possible if ratios of ^{10}B concentrations in tumor to those in normal tissue were at least 5:1. Needless to say, the compound must not have unnecessary toxicities.

Large total doses (>200 μg/g body weight) are generally required for BNCT. Photodynamic therapy [PDT] is another bimodal cancer treatment that involves administration of photosensitizers, but requires <2 μg/g body weight of similar porphyrin or porphyrin-like compounds. Therefore, compounds that are not toxic at PDT doses can become toxic at BNCT doses.

NiTCP (Figure 1) was previously shown to be nontoxic to mice at doses that delivered 40-60 μg B/g to tumor tissue with tumor:blood boron concentration ratios >100:1 and tumor:brain boron concentration ratios >5:1. All other porphyrins tested prior to NiTCP had shown deleterious hepatic and renal effects, but the most notorious effect was thrombocytopenia.

Toxicity determinations are based on comparisons with control groups given solvent vehicle only. The observed parameters include: behavior, appearance, weight changes, and hematological, chemical, and enzymatic analyses of blood. In some

experiments, histological examination of coded hematoxylin/eosin-stained liver sections are carried out. Boron concentrations are determined by direct-current plasma atomic emission spectroscopy [DCP-AES] and by prompt-gamma spectroscopy.

A series of carborane-containing porphyrins were synthesized and their biodistribution and toxicological properties were determined in BALB/c mice bearing either KHJJ or EMT-6 mammary carcinomas for comparison with NiTCP. The nontoxicity of the porphyrins was not only limited to those that are lipophilic, but also appear be related to those with tetraphenylporphyrin structures. Certainly, all the water-soluble porphyrins tested elicited toxicity at BNCT-relevant doses.

One particular porphyrin, NiTCPH (Figure 1), showed outstanding properties and its copper analogue was selected for BNCT tumor palliation studies. NiTCPH delivered .100 Fg B/g to EMT-6 tumor tissue while maintaining, if not exceeding the tumor:blood and tumor:brain boron concentration ratios of NiTCP. If such concentrations of boron in this murine mammary carcinoma would translate to human carcinomas, NiTCPH or CuTCPH-based BNCT could potentially be used for the treatment of breast cancers in addition to brain tumors.

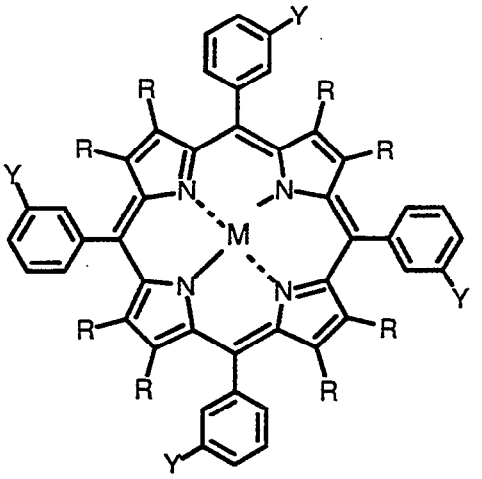

CuTCP: M = Cu, R = $CH_2CO_2CH_3$
CuTCPH: M = Cu, R = H

Y =

Figure 1. Structures of carborane-containing tetraphenylporphyrins.

TECHNICAL PROGRESS AND RESULTS – Fiscal Year 1998:

Purpose: *p*-Boronophenylalanine [BPA] is currently being used as the ^{10}B carrier in BNCT clinical trials for the palliative treatment of malignant brain tumors (glioblastoma multiforme) at the Brookhaven National Laboratory Medical Department. Although there is no toxicity associated with BPA, the normal brain and blood accumulate about one-fourth the amount of boron found in tumor, which could potentially limit the tumor dose. The treatment window for neutron-irradiation is only one to two hours after infusion since BPA clears out of tumor rapidly. A residence time of days in tumor would permit efficient fractionation of BNCT without reinfusion of compound. Borocaptate sodium [BSH], a sulfydryl boron hydride cage compound is being used in Japan and in Europe for BNCT. However, its tumor: normal tissue ratios are less than 2:1, with similar pharmacokinetics to BPA.

Therefore, the purpose of our work is to synthesize and test new compounds that could improve upon the efficacy of BPA- or BSH-based BNCT. The long-term objectives

are to improve current BPA- or BSH-based BNCT by supplementing or replacing them with another boron-containing compound that has higher tumor:normal tissue boron concentration ratios so that higher tumor doses can be delivered. If the boron carrier can be imaged by SPECT or MRI, then boron concentrations in all tissues within the treatment volume can be estimated.

Approach: New carborane-containing porphyrins including analogues of NiTCP were synthesized and tested in mice for biodistribution and toxicity. Compound administration was optimized for maximal tumor uptake with high tumor:blood and tumor:brain boron concentration ratios and minimal toxicity.

The most promising candidate from the biodistribution and toxicity study in the EMT-6 tumor model was CuTCPH. ^{10}B-enriched CuTCPH was administered to mice bearing EMT-6 tumors on the leg, which were then irradiated with thermal neutrons at the Brookhaven Medical Research Reactor [BMRR]. Controls for the BNCT group consisted of similar tumor-bearing mice that 1) received no treatment; 2) received thermal neutron irradiation only at different doses; and 3) received 100 kVp x-irradiation at different doses. Mice were closely monitored for tumor overgrowth and for any deleterious effects from excessive radiation. Comparison of the resulting survival data will determine efficacy of CuTCPH-based BNCT.

MRI studies on rats using manganese derivatives and SPECT studies using copper derivatives were planned to determine whether imaging is feasible using these techniques.

Technical Progress & Results:

BNCT STUDY:

Female BALB/c mice were implanted subcutaneously on the leg with EMT-6 tumor fragments. After ≈10 days, mice were sorted into 11 groups, each with a similar distribution of tumor volumes. Five groups received ^{10}B-enriched CuTCP-H at a total dose of 186 μg/gbw via serial ip injections (6 over 32 hr). Two days later, 4 groups were irradiated with thermal neutrons at the BMRR at 15, 20, 25, and 30 MW-min (≈39, 53, 65, 79 Gy). The 5th group was euthanized for determination of boron concentration in various tissues. Three groups of mice that were given no porphyrin, were irradiated with thermal neutrons only at the BMRR at: 30, 40, and 50 MW-min (≈7.0, 9.3, 11.6 Gy). Four groups that were given no porphyrin were irradiated with 100 kVp xrays (Philips RT-100 therapy unit) at doses of 21, 28, 35, and 42 Gy.

Tumors were measured twice a week and mice were euthanized when tumor volumes reached 500 mm^3 or when severe radiation damage was observed.

BIODISTRIBUTION:

Tissues of mice that were euthanized 2 days after the last injection, the same day the BNCT mice were irradiated, showed average boron concentrations of 85 $\pm$ 13 μg B/g in tumor, 13 $\pm$ 3 μg B/g in skin, and 4 $\pm$ 2 μg B/g in blood.

BNCT GROUPS:

The greatest tumor control was demonstrated by CuTCPH-mediated BNCT at 65 Gy (25 MW-min) where 5 of 7 mice treated showed no signs of tumor regrowth after more than 200 days after treatment (Figure 2a). The remaining 2 mice were euthanized within 90 days postirradiation due to tumor overgrowth. No mice in this group showed any signs of

2) a.

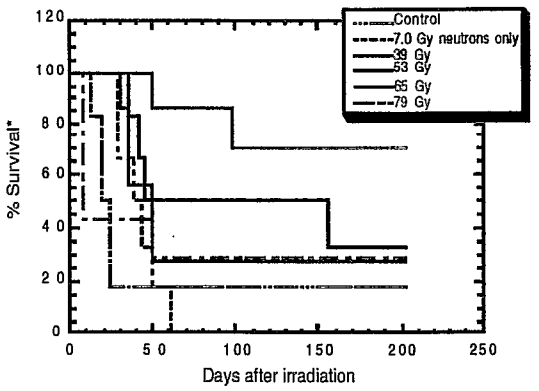

b.

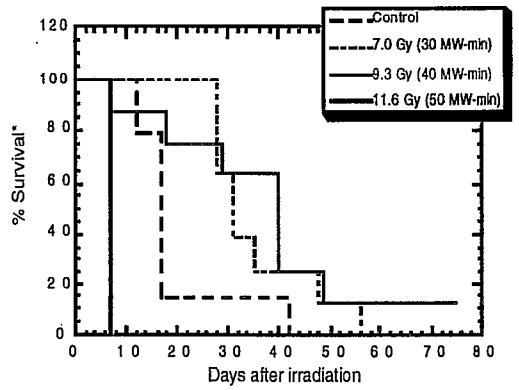

c.

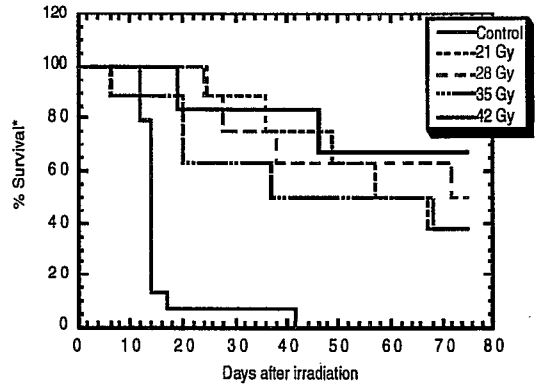

Figure 2. Survival curves for a) (top) BNCT-treated mice, b) (middle) mice treated with neutrons only, and c) (bottom) mice treated with 100 kVp xrays.

radiation syndrome. A 20% increase in the neutron-irradiation dose (30 MW-min, estimated 79 Gy) showed a dramatic whole-body dose response wherein 4 of 7 mice died within 1 week after irradiation, most likely from gastrointestinal radiation syndrome. When mice appeared ill ≈6 days postirradiation, they were given nutritional supplements (FreAmine and dextrose) by daily ip injections for about 1 week. A 20% decrease in the neutron-irradiation dose (53 Gy) showed a substantial increase in the number of mice euthanized for tumor overgrowth, allowing survival of only 2 in 7 mice.

The survivors of the 65-Gy BNCT group showed no signs of skin damage other than temporary alopecia. There were no signs of moist desquamation nor dermal necrosis in any of the BNCT-treated mice at follow-up times of ≈200 days.

NEUTRON-IRRADIATED GROUPS:

The lowest neutrons-only dose group given 7.0 Gy and the highest BNCT-treated group of 79 Gy correspond to the same total reactor exposure of 30 MW-min. By 56 days postirradiation, all mice in the 7.0 Gy group were euthanized due to tumor overgrowth (Figure 2b). At the same neutron-irradiation dose, but with the addition of ^{10}B-CuTCPH, the majority of animals died from gastrointestinal [GI] radiation syndrome. At 9.3 Gy, 1 mouse died of GI syndrome and 1 was euthanized due to extensive radiation damage to the leg. At 11.6 Gy, all 8 mice died from GI syndrome within 7 days after irradiation.

X-IRRADIATED GROUPS:

The highest dose group (42 Gy), showed survival comparable to the 65-Gy BNCT

group with 4 in 6 mice surviving (Figure 2c); however, the experiment has only progressed 80 days compared to >200 days for the BNCT groups. Moreover, radiation damage to the leg was observed in both the 42-Gy and the 35-Gy xray groups and no such damage was observed in any of the BNCT groups at any time.

Extrapolation of our data shows that 50% tumor control using CuTCPH-mediated BNCT corresponds to approximately 59 Gy.

Estimation of a compound-biological effect (CBE) factor takes into consideration the relative biological effect (RBE) of the high linear-energy transfer (LET) radiation from the neutron-capture reaction and the microlocalization of the compound in the cell, which is unique to the compound and its delivery vehicle. Using tumor control as an endpoint, and disregarding side effects to skin, the xray group at 42 Gy produced a tumor response similar to the 65-Gy CuTCPH-mediated BNCT group. The CuTCPH CBE factor in tumor appears to be less than 1. However, the CBE factors for skin and muscle also appear to be considerably less than 1, in addition to the fact that these tissues contain low boron concentrations (<20 μg B/g). Xray doses of 28 Gy and above, produced incidences of skin and muscle damage, whereas CuTCPH-mediated BNCT, at estimated doses of up to 79 Gy, did not. This difference in radiation sensitivity and the high tumor:normal tissue boron concentration ratios make it possible for CuTCPH-mediated BNCT to produce a significant improvement in therapeutic gain.

BIODISTRIBUTION IN RAT 9L GLIOSARCOMA:

Rats bearing multiple subcutaneous 9L gliosarcomas were given CuTCPH via a 50-hour intravenous (iv) infusion. Tumors and blood were sampled daily for 3 days starting from the end of infusion (0 hr).

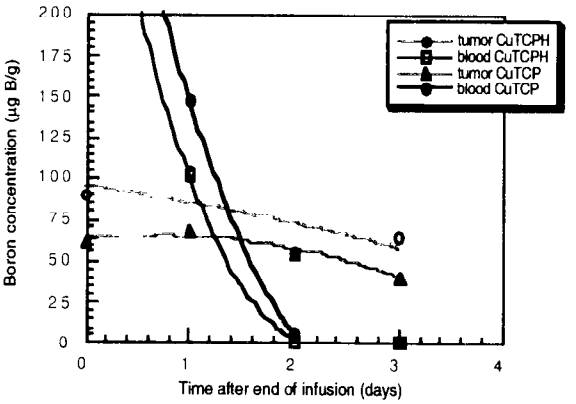

Figure 3. Boron concentrations in 9L tumor and blood from rats given either 195 mg CuTCPH/kg body weight or 214 mg CuTCP/kg body weight by iv infusion.

Somewhat higher concentrations of boron were maintained in the 9L tumors from CuTCPH compared with CuTCP as shown in Figure 3. While tumor values decreased from 55 to 41 ppm between day 2 to day 3 after infusion for CuTCP, they increased from 54 to 64 ppm during this same period for CuTCPH. Blood boron values dropped steeply for both compounds. As with mice, there were no toxicities observed in rats given either CuTCP or CuTCPH.

MRI STUDIES:

Manganese derivatives were synthesized for MRI studies. The solubilities of MnTCP and MnTCPH acetate derivatives were different from the nickel and copper analogues. After the saline was added, the compound appeared to precipitate out. Filtration was difficult and the resulting solution was about half that of the starting solution. This is probably due to

the +3 charge of Mn, which results in an axial ligand.

Four rats bearing multiple subcutaneous 9L tumors were imaged by T. Button at the SUNY Stony Brook MRI facility using a small whole-body coil. Two days later they were given ≈90 mg/kg body weight of CuTCPH by 45-hr iv infusion. One rat did not receive the full dose of porphyrin. Three rats were imaged at 0, 2, and 4 days after the end of infusion. After each image, the tumors were removed and blood was sampled for boron analyses. Unfortunately, the relaxation properties of MnTCPH in tumor were not sufficient for determination of subtherapeutic boron concentrations in tumor. The median tumor boron concentrations for 0, 2, and 4 days were 17, 11, and 11 μg B/g, respectively, assayed by DCP-AES.

Summary: BNCT using ≈200 μg/g body weight of CuTCPH and 25 MW-min of thermal neutron irradiation, which translates to approximately 65 Gy, palliated 5 of 7 EMT-6 tumors in mice with no damage to skin or muscle 200 days after BNCT. Neutrons alone could not control tumor without producing gastrointestinal radiation syndrome and 100 kVp xrays controlled the majority of tumors to 80 days but with some skin and muscle damage. CuTCPH-mediated BNCT appears to be superior to both neutrons alone and xrays in controlling tumors because of its high "advantage factor," which is the ratio of tumor dose to maximum normal tissue dose. In conclusion, given the low toxicity and efficacy of CuTCPH, further preclinical studies are warranted in order to seek FDA approval for the use of CuTCPH in humans in the treatment of glioblastoma multiforme and perhaps certain types of breast cancers.

The formulation of manganese derivatives requires further study if MRI is to become feasible.

PAPERS/JOURNALS/PUBLICATIONS:

M. Miura, D.D. Joel, M.M. Nawrocky, P.L. Micca, C.D. Fisher, J.C. Heinrichs, C.E. Rising, W. Walker, and D.N. Slatkin, Carborane-containing metalloporphyrins for BNCT. "Advances in Neutron Capture Therapy, Vol. 2." Eds. B. Larsonn, J. Crawford, and R. Weinreich, Elsevier, NY, 1997, pp. 56-61.

M. Miura, P.L. Micca, C.D. Fisher, C.R. Gordon, J.C. Heinrichs and D.N. Slatkin, Evaluation of carborane-containing porphyrins as tumor-targeting agents for boron neutron-capture therapy. *Br. J. Radiol.*, 71, 773-781, 1998.

M. Miura, P.L. Micca, D.T. Lombardo, K.M. Youngs, G.M. Morris, J.A. Kalef-Ezra, R. Ma, J.A. Coderre, Efficacy of Boron Neutron-Capture Therapy using a Carborane-Containing Tetraphenylporphyrin in Mice bearing EMT-6 Tumors, manuscript in preparation.

M. Miura, D.N. Slatkin and J.A. Shelnutt, Boronated porphyrins and methods for their use. U.S. Patent pending.

S. Cook was partially supported by the Associated Western Universities Summer Student Program during 6/98-8/98.

LDRD FUNDING:

FY 1997	$86,157
FY 1998	$108,857

Note: This project involves animal vertebrates or human subjects.

Development of Pump-and-Probe LIDAR for the *In-situ* Study of Fast Atmospheric Chemical Reactions

A. J. Sedlacek *97-50*
Mark Ruckman

PROJECT DESCRIPTION:

*I*n an effort to better understand and elucidate atmospheric chemistry and its dependence on microenvironments, the present LDRD was initiated to develop a novel differential absorption lidar technique. The technique, based on Raman spectroscopy and referred to as RaDIAL, offers the ability to monitor atmospheric species independent of the varying, aerosol burden (spatial and temporal) and laser energy pulse-to-pulse fluctuations. RaDIAL can be used to monitor a variety of trace atmospheric constituents like ozone (natural) or sulfur dioxide (natural or man-made). Since tropospheric ozone is central in the generation of the many important atmospheric free radicals, there exists an important need to completely and thoroughly understand the factors that influence the atmospheric chemistry of ozone. However, although our understanding of ozone chemistry is quite mature, very little work has been conducted on examining the sensitivity of ozone's short-term chemistry on microenvironments, such as near-factory emission stacks, or over large bodies of water where the aerosol burden can be quite high.

Trace atmospheric components play a major role in the greenhouse mechanism and contribute to global climate change. Lidar-based monitoring of greenhouse gases has technical and scientific advantages over point sensors and the "snatch-and-grab" sampling techniques presently employed. The LDRD has been used to conduct tests with the existing lidar equipment to determine what modifications are necessary to allow its use in greenhouse gas monitoring.

In addition, recent successes with a significantly smaller laser radar system being developed for the detection and identification of chemicals on surfaces and in cuvettes strongly suggests that the Optical and Remote Sensing group's existing Raman Lidar system can be used to detect liquid or solids at stand-off range. Consequently, the scope of the present LDRD was expanded to examine the potential capability of Raman lidar for liquid or solid detection and identification at ranges exceeding half a kilometer. If successful, this new platform will offer Hazardous Materials professionals a new tool for evaluating unknown chemical spills from a safe distance.

PREVIOUS TECHNICAL PROGRESS:

LDRD activities during FY97 focused on the development of the RaDIAL technique which exploits the inelastic Raman scattering returns from atmospheric nitrogen and oxygen as the two *in situ* probing wavelengths required for the differential absorption lidar (DIAL)-like measurement. In the RaDIAL technique, one of the Raman returns is tuned to the peak of the molecular absorption and the other to a non-absorbing region. By taking advantage of the constancy of the number density ratio of atmospheric nitrogen molecules to atmospheric oxygen molecules and knowing the nitrogen and oxygen Raman cross sections, the chemical of interest can be monitored and its concentration estimated

in a straightforward manner. Hence, the N_2 and O_2 Raman returns provide an *in situ* calibration standard. Furthermore, the N_2 and O_2 Raman beams for the differential measurement take place at the same time, in the same spatial volume and consequently the return signals are transmitted through the same atmospheric (turbulence) structure. The RaDIAL technique addresses traditional concerns of ranged-resolved DIAL such as atmospheric turbulence, aerosol burden and laser shot-to-shot energy variations since classical DIAL monitors only the elastically scattered return signals (which has three contributions: Mie scattering; Rayleigh scattering; and absorption). The new platform under development offers a superior stand-off sensing technique where range-resolved, open-path applications are required.

The RaDIAL platform, housed in a 33-ft recreational-type vehicle, was used to measure atmospheric ozone and detect other gases released into the atmosphere. Results from work done at the Nevada Test Site (NTS) showed that the RaDIAL technique could detect tens of parts per billion ozone concentrations and monitor the change in ozone concentration which varies with time during daylight hours. RaDIAL results compared favorably to concurrent measurements taken with a Dobson spectrometer. The RaDIAL measurements taken at the NTS showed a $\pm$15 % standard deviation about an average value of 62 ppb. In addition, a vapor release of acetone and gas release of sulfur dioxide at distances ranging from 1.4 to 3.3 km was also undertaken. The sensitivity of RaDIAL was found to be sufficient to monitor changes in the rate of acetone evaporation from an evaporation pan due to evaporative cooling at a range of 1.37 km.

TECHNICAL PROGRESS AND RESULTS - Fiscal Year 1998:

Purpose: The goals in fiscal year 1998 were: (1) an examination of noise sources/issues associated with the RaDIAL platform and (2) an exploratory evaluation of the RaDIAL systems towards the detection of liquid and solid ground/surface contamination or *in-vivo* studies of chemical or biologically important processes at ranges exceeding half a kilometer. The work focusing on ground/surface contamination (both liquid or solid) complements related developmental work for a mini-Raman Lidar system (MRLS) which is currently on an accelerated development schedule for the short-range, non-contact detection of surface contamination. The MRLS is sponsored by DOE-NN office.

Background: Of the physical phenomena exploited with active open-path sensors (i.e., lidar), the differential absorption technique DIAL (**Di**fferential **A**bsorption **L**idar) has routinely achieved detection sensitivities on the order of low ppm to high ppb levels, depending on the absorption cross-section, albedo variation, atmospheric make-up (i.e., aerosol burden), laser pulse-to-pulse energy stability, and atmospheric turbulence. In a typical application of DIAL, two probing laser lines are directed to the area of interest and their elastic return signals are monitored: λ_1 located at a highly-absorbing wavelength for the chemical species of interest and λ_1 in a non-absorbing spectral region. Elastic return of each outgoing laser line (λ_1 and λ_2) is provided through either a combination of Rayleigh scattering off of air molecules and the aerosol/ particulate-based Mie scattering or, if range-resolved mapping is not important, a retroflector [e.g., corner cube or sand-blasted aluminum as a back-drop].

However, despite the great sensitivity that the range-resolved DIAL platforms offer, they suffer from complex data reduction and error analysis complications due to real world complexities. This difficulty is a genetic one because the classical DIAL technique derives the molecule absorption information from the elastic-return channel mentioned above. Consequently, there is uncertainty in distinguishing variation in the return signal amplitude that is due to the presence or absence of the chemical species of interest from the spatial and temporal variations in the aerosol burden, or from laser power fluctuations. Although a variety of hardware and software techniques have been developed and implemented to confront these problems, the end result is typically an increase in the complexity of the DIAL platform. In an effort to address this significant short-coming, we have developed a novel lidar platform, referred to as RaDIAL, that combines the strengths of two existing lidar techniques to produce a system that can potentially achieve DIAL sensitivities without the complex data and error analysis thereby increasing the accuracy of the desired measurement.

The RaDIAL technique uses the strong molecular nitrogen and oxygen Raman returns generated whenever laser beams are propagated through the atmosphere as the two laser lines required for the DIAL measurement. The LIDAR technique permits the detection of N_2 and O_2 Raman returns from a parcel of atmosphere between a range R and R+ΔR. Since atmospheric nitrogen and oxygen are well mixed and the N_2/O_2 ratio (3.728) constant to ~100 of ppm level. Any deviation observed in this ratio is a measurement of the preferential absorption at either the nitrogen or oxygen return wavelength. RaDIAL overcomes a number of well known shortcomings of the DIAL technique including: (1) changes in atmospheric structure along the path of beam propagation; (2) elastic scattering by aerosols; (3) laser power and beam structure fluctuations; and (4) simultaneity of measurement. Proof-of-principle experiments on this new chemical sensing scheme have been carried out both at BNL and the Nevada Test Site (NTS).

Most applications of lidar involve studies of returns from soft targets like clouds, chemical plumes, turbulence and atmospheric gases. Studies of lidar returns from "hard" targets are less common although laser-radar systems are being increasingly used for target identification, and imaging. In 1998, Ray and Sedlacek assembled a miniaturized Raman lidar system using a diode-pumped, 266 nm Nd-YAG laser and 5-inch mirror-based receiver telescope. This system is being developed as a new chemical sensor for Hazardous Material (Haz/Mat) professionals who are confronted with unknown chemical spills. The goal of this mini-lidar system is ground/surface contamination assessment at distances ranging from meters to 10s of meters. The MRLS was demonstrated last November during a New York City sponsored emergency services exercise where the system successfully detected acetone at a distance of 5 meters in a driving rain. It has been estimated that once completed, the system will have a detection sensitivity towards surface contamination down to 0.25 gm/cm^2. Due to the incredible interest that the MRLS generated during FY98, the PI elected to expand the present LDRD to include proof-of-principle experiments using the RaDIAL platform for longer range detection/identification of liquid chemical spills.

Long-term Objectives: The LDRD has provided the opportunity to develop and understand a new chemical sensing

technique (RaDIAL) for measuring atmospheric gases and emissions into the atmosphere and conduct proof-of-principle experiments to assess the utility of the lidar for non-conventional applications. This was done using a lidar platform in the field and a tunable laser system in the laboratory. The data produced by this research is being used to attract follow-on funding and new interest from outside R&D or commercial entities. There are applications that address DOE mission needs in the environmental, security and safety areas as well. It is intended to seek support to develop the technique and technology in one or more of those mission areas and position BNL to participate in such projects.

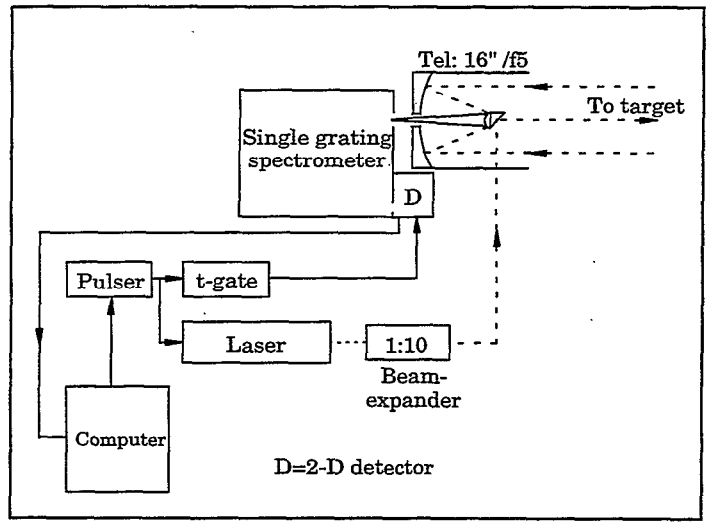

Figure 1. Schematic of Open-Path RaDIAL System

Approach: Research carried out in FY98 employed the lidar system developed for the CALIOPE program to acquire N_2/O_2 Raman spectra and Raman returns from "soft" gas phase and "hard" solid or liquid phase targets. Shown in Figure 1 is a schematic of the lidar platform used for those experiments.

The lidar system is composed of three main subsystems: (*i*) a laser system and beam transport optics, (*ii*) signal receiver telescope and spectral fingerprinting detection unit, and (*iii*) equipment control and data acquisition/processing subsystem. The laser system for the experiments was a Spectra-Physics GCR170 Nd:YAG-pumped dye laser system (Quanta Ray PDL-1).

Following expansion of the laser beam, to insure that the outgoing beam is eye safe before exiting the unit, the laser beam was directed to the area of interest. The return signals are collected by a 16-inch Cassegrain telescope and focused onto the slits of a single-grating spectrometer (2400 grooves/mm) and then detected by Oriel's Intaspec V intensified CCD (charge-coupled device) detector for spectral fingerprinting. The collected probe lidar return signals were curve fit to a Voigt lineshape so that the N_2/O_2 ratio could be computed. All timing aspects for distance ranging a specific target is based on a single-master oscillator (clock) which provides triggering to the lasers and gate delay timing to the detector circuitry.

Technical Progress and Results: Previous work during FY97 showed that RaDIAL measurements could be made with the lidar system developed under support from the DOE-sponsored CALIOPE program and that ozone and chemicals such as sulfur dioxide and hydrocarbon vapors were detected. The system showed significant sample-to-sample variations of as much as 15% about an average value that, in the case of the ozone measurements, were calibrated by a second technique. Ozone has a strong absorbance in the ultraviolet below 290 nm (Hartley band). The absorption of ozone or sulfur dioxide proved to be sufficiently strong that systematic fluctuations from interrogating the CCD detector did not obscure the signal which is a ratio of the N_2

and O_2 Raman returns. However, measurement-to-measurement variations in the intensity of the N_2 and O_2 Raman returns proved to be too large to permit RaDIAL measurements of the OH radical whose absorption (~ 10^{-16} cm^{-1}) lies at 308 nm. This variation has been attributed to the intensifier portion of the ICCD detector. It is believed that the intensifier increased the nominal noise level thereby reducing the dynamic range of the overall detector. During the course of the year, potential candidates for replacement of the ICCD have been evaluated. Some of these other detectors have included liquid-nitrogen cooled CCD, thermoelectrically cooled CCDs and near-UV acousto-optical tunable filters (AOTF) coupled with photomultiplier tubes (PMT). The PI has been interacting with Professor Robert Canahan (Northern Illinois State University) who has shown that quartz-based AOTFs offer the requisite narrow linewidths, and when used with PMTs offer the ability to exploit photon counting techniques, thereby increasing the detection sensitivity. In FY99, a two quartz-based AOTFs each coupled to a respective PMT will be incorporated into the RaDIAL platform. The advantage of AOTFs over narrow bandpass filters is the ability of AOTF to be tuned. Consequently, one AOTF can be used to cover an entire spectral region. However, the reason for incorporating two AOTFs is to allow the simultaneous measurement of the Raman returns from atmospheric nitrogen and oxygen.

Shown in Figure 2, is an example of data collected demonstrating the ability of the RaDIAL chemical sensing scheme to correct, to first-order, the degrading effects of turbulence. As can be seen, the two lower traces are the individual Raman returns from atmospheric nitrogen and oxygen. At a little after 10:00 am, the outgoing laser power was tweaked and held constant to ~ 5%. However, over the course of the next few hours, it can be clearly observed that the power return from nitrogen and oxygen decreases by over 50%. This degradation is due to atmospheric turbulence breaking up the outgoing laser beam and causing beam wander in both the outgoing and return signals. However, as shown in the upper trace, the RaDIAL sensing scheme can correct this effect since the approach is ratioing two correlated signals. They each represent about a minute of integration and a stand-off distance approximately 1 km.

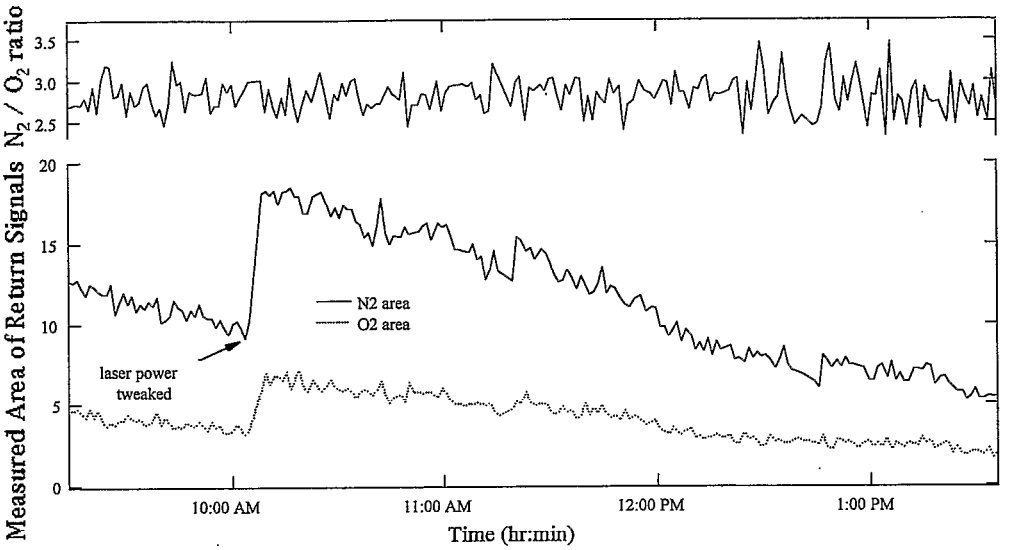

Figure 2: Ability of RaDIAL to self-correct turbulence-induced signal degradation

However, the data shown in Figure 2 also show great sample-to-sample variation. Far greater then is expected based on the number density stability of atmospheric N_2 and O_2. Consequently, measurements of the stability of the *observed* N_2/O_2 returns were repeated at Brookhaven on a lidar test range established at the RHIC site. Representative data showing the N_2/O_2 ratio is shown in Figure 3. It was found that the intensity of the N_2/O_2 Raman returns varied with atmospheric conditions and time of the day. Factors such as turbulence from daytime heating or winds blowing on or off-shore, mists, fog and low clouds, dust or smoke reduced the intensity of the Raman return.

As seen in the figure, sample-to-sample variability of the N_2/O_2 ratio varied as much as 20% or greater. It is likely that noise induced by signal intensification and charge integration account for these fluctuations and suggest that improved low noise detectors are necessary to realize the full potential of the RaDIAL technique towards trace gas detection and flash-photolysis atmospheric chemistry. This experience is consistent with work by others who have succeeded in improving DIAL platform sensitivity through incorporation of low noise photomultiplier tubes. Such a detector has been purchased and will be integrated into the RaDIAL platform and tested in FY99.

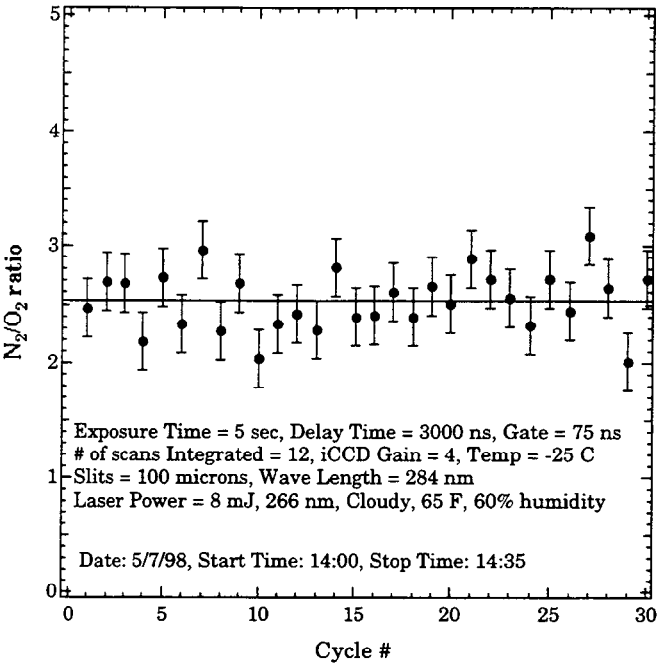

Figure 3: Variation in observed N_2/O_2 ratio

As alluded to above, the current LDRD was expanded to include an evaluation of exploiting the Raman returns from liquid and solid targets for the long range detection and identification of ground contamination. These experiments were carried out using a quartz-based windowed cell capable of holding a 12-inch diameter 3/8" thick liquid target. The cell was typically placed on a fixed target approximately 533 meters from the Raman lidar system. Range gating was used to maximize the relative return from the target. The outgoing laser beam was expanded to approximately 8-inches prior to exiting the van. Figure 4 shows the Raman return from a piece of Teflon at the above mentioned 533 meter range. The signal-to-noise factor easily exceeds a factor of 20 and the Raman components are comparable to their counterparts taken from the laboratory.

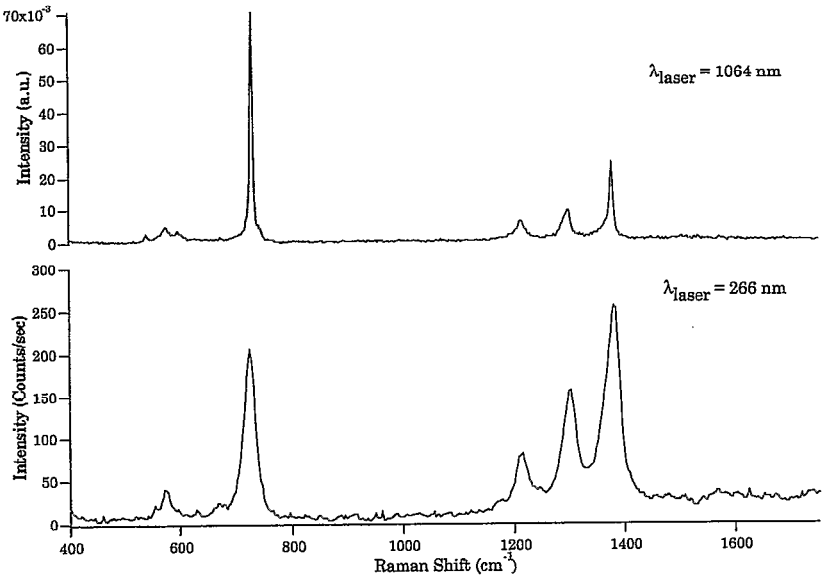

Figure 4: Raman spectra of Teflon collected by Raman lidar at a stand-off distance of 533 meters. Upper trace is library spectra of teflon for comparison

In contrast, Figure 4 shows data collected from a liquid target using the quartz-windowed cell described above. The bottom curve shows Raman components from pure cyclohexane and the top curve shows results for a cyclohexane mixture containing 1%, by volume, carbon disulfide (CS_2). Based on the strength of the cyclohexane returns and knowledge of the cross section for this chemical, it is estimated that the LIDAR system can detect kilogram quantities spread over a 1 m^2 target area. This shows the capability of Raman lidar to spectrally interrogate chemical spills (e.g. transportation-related) at safe stand-off ranges.

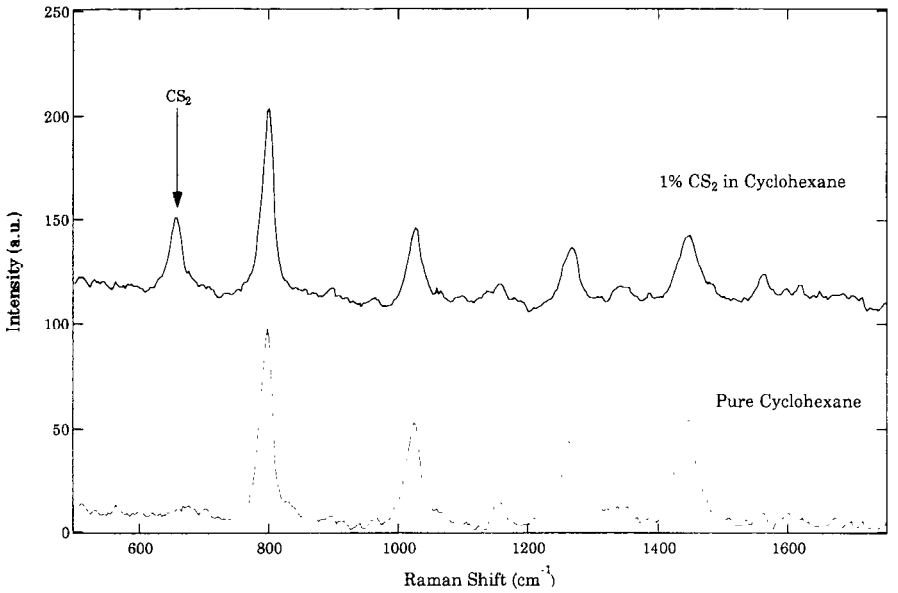

Figure 5: Raman spectra of pure cyclohexane and 1% CS_2 in cyclohexane collected with Raman lidar system. Stand-off distance is 533 meters

In addition, Raman returns some chemicals can also undergo resonant enhancement above the ν^4-enhancement at shorter wavelengths. CS_2 shows such enhancement and the Raman components expected between 500 cm^{-1} and 1750 cm^{-1} Raman shift is clearly visible. This demonstrates the potential of resonance Raman scattering for detecting selected chemical contaminants that possess resonance enhancement in the ultraviolet. In the present case of CS_2, its detection limit is at least a factor of 100 times lower than cyclohexane due to resonance enhancement. The LIDAR system was used to detect Raman returns from other solvents commonly encountered in industrial settings. These include nitrobenzene, acetonitrile, acetone, methanol, isopropyl alcohol, carbon tetrachloride and a mixture of acetonitrile and CCl_4.

ACCOMPLISHMENTS:

During the course of this first year of funding, the PI approached DoE/NN-20 to discuss the potential applications of the RaDIAL technique towards the detection of trace effluents and received $200,000 towards conducting a series of field tests out at the Remote Sensing Test Range (RSTR) on the Nevada Test Site (NTS). In addition a patent on the idea of exploiting the Raman returns from ground contamination for chemical detection and identification has been submitted. The results obtained from the trip out to NTS were presented at the 18th International Laser Radar Conference held during the week of July 6th at Annapolis, Maryland. From this meeting, both positive feedback and potential collaborations were established. In addition, the manuscript describing the RaDIAL technique, along with results from the proof-of-principle experiments carried out at NTS, is nearing completion and will be submitted to the Journal of Applied Optics. Finally, although a proposal based on this idea and submitted to DOE's Office of Health and Environmental Research in response to the Atmospheric Chemistry Program's call for proposals (OER Notice 97-12) was not

funded, solicitation for outside funding of this proposal has continued. In addition, the RaDIAL technique can also be exploited to measure Global Greenhouse gases (CO_2, CH_4, NO_x, etc.) and the PI has begun discussion with those colleagues in the Department of Applied Science who are taking the lead in the Environmental Carbon Observatory (ECO) institutional plan.

PAPERS/JOURNALS/PUBLICATIONS:

A.J. Sedlacek and M.D. Ray; Raman–Dial: Application to Areas Characterized by Varying Aerosol Burden, 19th International Laser Radar Conference Proceedings, 293 (1993) NASA/CP-1998-207671/PT1)

M. D. Ray and A. J. Sedlacek; Mini-Raman Laser-Radar System for In-Situ, Stand-off Interrogation of Surface Contamination, 19th International Laser Radar Conference Proceedings, 677 (1998) NASA/CP-1998-207671/PT2.

LDRD FUNDING:

FY 1997	$ 99,066
FY 1998	$ 99,778
FY 1999 (est.)	$ 100,000

Center for Imaging in Drug Abuse Research

Nora D. Volkow *97-68*

PROJECT DESCRIPTION:

A new PET camera as well as funds from NIDA and ONDCP were provided under an agreement that BNL would also provide with funds that would help launch the Center. These funds were to be provided via this LDRD. In turn the resources of this Center will be dedicated to gaining the knowledge required to advance the prevention and treatment of addiction and alcoholism while taking advantage of the imaging resources at BNL i.e. PET, SPECT and MRI.

TECHNICAL PROGRESS AND RESULTS - Fiscal Year 1998:

The effort for this LDRD has been to initiate clinical studies with the MRI and to evaluate the potential of imaging technologies to detect disruption of the Blood Brain Barrier.

The MRI studies required that we develop the programs that enable to acquire either relaxographic or spectrospic information. The results from these efforts are summarized below. The scientists involved with these MRI studies include: J.S. Fowler, Y.-S. Ding, D. Franceschi, J.S. Gatley, H. Hetherington, J.-H. Lee, X. Li, P. Molina, J. Pan, W.D. Rooney, M Sammi, D. Schuhlein, F. Telang, N.D. Volkow, G.-J. Wang, C.S. Springer, Jr.

Spectroscopic Studies: P.I. H. Hetherington

Purpose: One of the mechanisms by which alcohol conveys its intoxicating effects is hypothesized to be through its interaction with membrane lipids. As such the NMR visibility of alcohol in the human brain and its relationship to the pharmacological effects of alcohol have been an area of considerable interest. It has been reported that the visibility of brain alcohol is increased in alcohol tolerant subjects in comparison to non-tolerant subjects. Additionally, the effects of acute tolerance to alcohol consumption have been correlated with increased alcohol visibility in a two-drink paradigm. Despite these initial investigations of the effects of alcohol and NMR visibility, measures of the visibility of alcohol in the in vivo brain have varied widely ranging from 21% to 100%, depending upon the NMR acquisition method used. To date, with the exception of one study carried out in three volunteers, these studies have used single voxel measurements and have acquired little or no kinetic data. We therefore have focused our efforts on: 1) developing an in vivo NMR imaging method which minimizes artifacts and can be used in a kinetic mode (10 minute time resolution); and 2) have using this method to evaluate the regional kinetics of ethanol uptake and visibility in human brain.

Approach: We have completed studies in seven individuals who received 0.5g/kg of ethanol while in the magnet. Spectroscopic images of alcohol content and measurements of venous blood alcohol levels were obtained both before drinking, and at ten minute intervals after drinking for 90 minutes. Due to the predominant partitioning of alcohol to aqueous compartments, and differences in water content between white matter (WM), gray matter (GM) and cerebral spinal fluid (CSF), the tissue content of each spectro-

scopic imaging voxel was determined using a quantitative T1 imaging method.

Technical Progress and Results: In contrast to previous reports NMR studies, but in agreement with animal data, the brain alcohol concentration exceeded the blood level during the first thirty minutes after drinking. Using the final three time points, when the absorption phase has concluded and venous blood levels are in near equilibrium with arterial and brain levels, the visibility was measured to be 1.00 ±0.20. These studies showed that peak concentrations of alcohol in brain were reached 45 minutes after its oral administration at which time points the levels reached a plateau for the remaining period of scanning (85 minutes). These initial studies indicate that contrary to previous NMR studies, brain alcohol is 100% visible. This suggests that the previously reported alterations in visibility are most likely due to pulse sequence artifacts and changes in relaxation effects in detectable ethanol pools.

Long Term Objectives: We want to apply this methodology to investigate if there are differences in alcohol bioavailabilty between the genders that could help clarify the allegedly high susceptibility for the higher toxicity of alcohol effects in females than in males.

Relaxographic Studies: P.I. W.D. Rooney

Purpose: Previous studies have reported that brain water proton T_1 values are decreased during acute ethanol intoxication. This is a potentially important observation since it could indicate that either brain water content decreases during acute ethanol intoxication, or that ethanol interacts with brain macromolecules to catalyze water proton T_1 relaxation. Previous studies have not examined the regional distribution of changes in water proton T_1. If they exist, regional T_1 changes could be important in elucidating details of ethanol's mechanism of action in the central nervous system. We therefore have focused our efforts 1) to determine the spatial distribution of changes in brain water proton T_1 values during acute ethanol intoxication, and 2) to establish the reproducibility of T_1 measurements in normal human brain at 4T.

Approach: We have completed studies in five individuals who were scanned with the MRI in four different sessions: a) baseline (day 1), b) pre-EtOH (day 2), c) EtOH (day 2), and d) 24 hr post-EtOH (day 3). The EtOH session was started 60 minutes after drinking 0.75g/kg ethanol. During each MRI session a 3D anatomical image set with full brain coverage and a T_1 relaxographic imaging set from a single para-axial plane were acquired. Sixty-four images were collected at times that ranged from 0.027 to 17.1 sec following a non-selective adiabatic inversion pulse. Water proton T_1 maps were synthesized using the equation, $S(\tau) = S(\tau = \infty)[1-\beta \bullet \exp(-R_1\tau)]$; where, $S(\tau)$ is the measured pixel signal MRI intensity for inversion time τ, $S(\tau = \infty)$ is the steady-state value of the pixel MRI signal intensity, β relates to the efficiency of inversion, and R_1 $(=1/T_1)$ is the longitudinal relaxation rate constant. The T_1 maps had in-plane and through-plane resolutions of 3.5 mm and 10 mm, respectively. Regions-of-interest (ROIs) were manually selected from 12 bilateral brain areas; 1) peri-ventricular white matter, 2) frontal white matter, 3) thalamus, 4) caudate, 5) cortical-occipital gray matter, and 6) cerebral spinal fluid (CSF). T_1 values extracted from the ROI analysis were analyzed using a paired t-test. The reproducibility of the T_1 measurement was

estimated from the baseline and pre-EtOH MRI sessions.

Technical Progress and Results: Means and standard errors of water proton T_1 values for the six brain regions were found to be; 1) peri-ventricular white matter (890 ±11 msec), 2) frontal white matter (868 ±16 msec), 3) thalamus (1145 ±16 msec), 4) putamen (1180 ±25 msec), 5) cortical-occipital gray matter (1348 ±39 msec), and 6) CSF (3100 ±175 msec). There was no significant difference in water T_1 values for any of the MRI sessions or for any brain region. The T_1 reproducibility was excellent (95% confidence intervals were; precision: 0.959 ± 0.057, accuracy: 0.998 ± 0.003, and concordance: 0.951 ± 0.051). These results indicate that at the moderate level of brain ethanol studied in this project, water proton T_1 values were not changed by more than 17 msec (1.8% relative) in white matter structures, and 45 msec (3.8% relative) in gray matter structures.

Long Term Objectives: We will not continue these studies since they did not show evidence of water changes in during alcohol intoxication. Instead we plan to redirect our effort to develop functional MRI studies with the 5 Tesla Magnet.

Imaging Studies of the Blood Brain Barrier: P.I. F. Telang

Purpose: Recent studies provided evidence that stress could disrupt the blood brain barrier and that this in turn would enable the passage of compounds that are normally kept outside of the brain. This was discussed in the context of Pyridostigmine, a carbamate acetylcholinesterase (AChE) inhibitor, which is used prophylactically against chemical warfare agents that does not cross the BBB. It was postulated that during stress this compound could penetrate into the brain and exert CNS effects. Furthermore, it was hypothesized that the "central CNS" symptoms, (headaches, insomnia, drowsiness, nervousness, unfocused attention, and impaired capacity to conduct simple calculations) from soldiers during the Gulf War were due to entrance of Pyridostigmine into the brain.

Approach: To test if Pyridostigmine could enter the brain during experimental stress, we labeled it with C-11 and measure its uptake in control and in stressed rats (Swiss-Webster). The stress test used was the forced swimming test, which is a standard procedure for inducing stress responses in rodents. Pyridostigmine was labelled with C-11 in the methyl group of the quaternary nitrogen atom, by reaction of $[^{11}C]$-CH_3I with desmethylpyridostigmine. The stress protocol involved two separate 4 min. periods of forced swimming in water at 21 ° C in a 3 liter graduated cylinder with a 4 min. rest period in between the swim sessions. The second swim session was followed by a 10 min. rest period and then immediately by a tail vein injection of 1 mCi. of $[^{11}C]$-pyridostigmine. Animals were sacrificed 10 min. later and whole brain, the head (skull), tail, and sample of whole blood from each mouse were placed individually in scintillation vials and counted in a Gamma Counter (Packard, MINAXI 5000 series).

Technical Progress and Results: Contrary to expectations, stressed mice exhibited a slightly lower brain radioactivity than controls, possibly due to decreases in blood volume and brain interstitial fluid associated with hypercapnia from the stressful exercise. However, the decrease was not significant. The brain/blood ratios for C-11 (0.035) were consistent with the tracer being confined to blood vessels,

which account for up to 4% of total brain volume.

Long Term Objectives: We will not continue these studies since they did not show evidence of BBB disruption with stress. However, we will continue to develop PET ligands like Pyrodistigmine that may be beneficial in detecting BBB disruption on other conditions (i.e. multiple sclerosis, radiation into the brain). We have started studies to investigate the usefulness of iron nanoparticles to measure BBB disruption with the 4 T MRI.

ACCOMPLISHMENTS:

The manuscript reporting our results on the blood brain barrier is currently in press: Telang, FW, Ding YS, Volkow ND, Molina PE, Gatley JS. Tracer amounts of [^{11}C]pyrodistigmine do not cross the blood brain barrier in adult mice subjected to a force swim protocol. Biology and Nuclear Medicine (in press).

We are currently working on two manuscripts; one to report the results from the spectroscopic studies and the other to report the results for the relaxographic studies. We also plan to use the data from the spectroscopic studies to apply for a NIH grant. This study supported one postdoc.

LDRD FUNDING:

FY 1998	$ 332,828
FY 1999 (est.)	$ 350,000

Note: This project involves animal vertebrates or human subjects.

Molecular Biological Markers as Potential Prognostic Indicators for BNCT

Jacek Capala *97-70*
Jeffrey A. Coderre
Arjun D. Chanana
Aidnag Z. Diaz
Darrel D. Joel

PROJECT DESCRIPTION:

Forty-two patients have been treated with BNCT since September 1994. Although palliation of the tumor was achieved in all cases, the time to progression could not be correlated with clinical prognostic indicators. In this project we search for molecular markers that could be of use in predicting the course of the disease and to correlate their presence in samples of tumors (formalin fixed, paraffin embedded sections) obtained from BNCT patients with clinical outcome.

Studies by Hoshino, et al. (1) indicate that the survival of patients with intracranial glioma appears to correlate inversely with the proliferative potential (determined by *in-vivo* BrdUrd labeling) of the tumor. Another study (2) used a monoclonal antibody (Ki-67) to a non-histone nuclear matrix antigen. This antigen is present in late G1, G2, S and M phases of the cell cycle and is absent in Go and early G1 phases. Good correlation of the Ki-67 and BrdUrd labeling indices was demonstrated. Use of Ki-67 antibody requires frozen sections. However, another monoclonal antibody to this antigen (MIB-1) can be used on formalin-fixed and paraffin-embedded sections following the antigen retrieval by microwave heating (3).

Cytogenetic and molecular genetic studies of malignant gliomas have documented abnormalities in many autosomes especially the loss of heterozygosity for loci of chromosomes 10 and 17 (p53) and amplification of EGFR gene (chromosome 7). The amplification of the gene for EGFR protein is found over expressed in most malignant gliomas, especially in GBM (4). Patients expressing p53 protein (product of the tumor suppressor gene on chromosome 17) have significantly reduced survival. Both EGFR gene product and p53 protein can be evaluated on formalin-fixed, paraffin-embedded sections.

Apoptosis (active cell suicide controlled by gene expression) (5), combined with proliferative potential of tumor cells has been also proposed as a possible prognostic factor (6). Apoptotic cells in the available formalin-fixed, paraffin-embedded tumor samples can be identified by the detection of DNA breaks by terminal transferaze-mediated in situ end labeling (TUNEL) (7).

PREVIOUS TECHNICAL PROGRESS:

During fiscal year 1997, we accomplished several initial goals of this project:

1. A laboratory for immunohistochemical studies was established in Medical Department.

2. Antigens, such as Ki-67, p53 mdm2, EGFR, whose abnormal presence in tumor cells had been reported to correlate with poor prognosis were identified though literature studies and communication with leading scientist.

3. Protocols for immunohistochemical detection of Ki-67, p53 and EGFR were developed and tested on commercially available tissue samples.

4. Brain autopsies of two BNCT treated patients were carried out in collaboration with the Department of Pathology, Stony Brook University Hospital. Representative samples of tumor, normal brain and transition regions, where both tumor and normal cells are present, were obtained and prepared for immunohistochemical analysis.

TECHNICAL PROGRESS AND RESULTS – Fiscal Year 1998:

Purpose: The aim of this work is to evaluate the biological markers in formalin fixed, paraffin embedded, tumor sections obtained from BNCT patients and to study correlations of theses markers with the patient survival following BNCT. Markers shown to have significant correlations with patient survival could then be used prospectively to identify candidates for BNCT

Approach: The specific goals of this project for fiscal year 1998 were:

1. To identify which of the potential prognostic markers should be studied considering the limited number of available tissue samples.

2. To analyze the potentially most promising prognostic markers in all available tumor samples obtained at pre-BNCT surgery.

3. To correlate results of the immunohistopathological studies with the outcome of BNCT.

Technical Progress and Results: Based on literature studies, two biological features of the tumor have been identified as the most promising prognostic factors that could be studied using available tumor samples: 1) proliferative activity of tumor and 2) apoptosis. Proliferating and apoptotic cells were detected in the formalin fixed, paraffin embedded, tumor sections obtained from 23 BNCT patients, by immunohistochemical detection of Ki-67 and by TUNEL assay, respectively. Proliferative activity and the observed apoptosis varied significantly, both, within samples of the same tumor and from patient to patient, reflecting biological heterogeneity of the tumors subsequently treated by BNCT. The labeling indices (fraction of positive cells) for Ki-67 and TUNEL assay were in the ranges from 3% to and 76% and from 0% to 23%, respectively. However no significant correlation between these potentially prognostic markers and the outcome of BNCT was observed. These results may be due to the limited number of patients studied to date.

ACCOMPLISHMENTS:

Presence of two biological markers determining tumor growth: proliferative activity and apoptosis have been characterized in samples obtained form 23 GBM patients treated with BNCT. Results of this work will be used as a baseline for future studies comparing the pre- and post-BNCT characteristics of GBM.

REFERENCES:

1. Hoshino, T., et al. Int. J. Cancer 53, 550 (1993)

2. Shibuya et al. Cancer 71, 199 (1993)

3. Onda, K., et al. Cancer 74, 1921 (1994)

4. Jaros, E., et al. Brit .J. Cancer, 66, 373 (1992)

5. Kerr, J.F.R. et al. Br. J. Cancer, 26, 239 (1972)

6. Levine E.L. et al. Radiotherapy and Oncol., 37, 1 (1995)

7. Gavrieli, B. et al. J. Cell Biol., 119, 493 (1992)

LDRD FUNDING:

FY 1997	$ 99,822
FY 1998	$ 109,782

Note: This project involves animal vertebrates or human subjects.

Beam Enhancement in a High Brightness Electron Linac

Erik D. Johnson *98-23*
Ilan Ben-Zvi
Louis F. DiMauro
William S. Graves
Jerome Hastings
Richard Heese
Sam Krinsky
Xijie Wang and
Li-Hua Yu

PROJECT DESCRIPTION:

*B*NL has a leadership position in the development of concepts for the generation of vacuum ultra-violet radiation with Free Electron Lasers. We have reassembled the 230 MeV SXLS linac to be used with the long undulator NISUS in an Amplifier FEL, the Deep Ultra-Violet Free Electron Laser (DUV-FEL) located building 729, the Source Development Laboratory (SDL) [1,2]. The long-range target is to implement a Chirped Pulse FEL operating in the UV that would provide a sub-picosecond source of intense synchrotron radiation for a broad range of research. In this LDRD project, we undertake a program to develop some of the tools for production and characterization of a high current - low emittance electron beam suitable for driving the DUV-FEL.

Approach: In previous supported activities, we have developed strategies to meet the stringent requirements for the production and preservation of bright electron beams within the framework of existing hardware that can support our experiments. Although there are many aspects to the undertaking, a key element of our approach has been the development of a magnetic pulse compression system. A second element of our approach has been to develop suitable diagnostics for verifying the properties of the electron beam produced. In the course of this LDRD project, we have built prototypes for testing these concepts.

TECHNICAL PROGRESS AND RESULTS – Fiscal Year 1998:

Bunch Compressor Development:
In previous work the essential features for the bunch compressor were developed [3]. It is comprised of three major components: the dipole magnets, the vacuum vessel mounting the beam diagnostics, and the mechanical support system. The 4 dipoles are fabricated from solid blocks of 1006 low carbon steel. Each magnet uses eight air-cooled pancake coils of 16 turns. The maximum field strength is 4.5 kG, magnetic length is 19 cm, and the gap is 3 cm. The aluminum vacuum chamber is machined in halves and seam-welded at its periphery.

Two CCD cameras are used as electron beam and synchrotron radiation diagnostics. The electron beam probe is injected through the center of the vacuum chamber. It has a YAG crystal [4] and mirror to observe beam shape. It also has 3 slots 0.3, 0.6, and 1.0 mm wide, respectively, so that slice emittance may be studied. The slots may also be used to select a fixed energy bandwidth for transmission to the wiggler.

The local emittance and local energy spread are key determinants of single-pass FEL performance. In the DUV-FEL the compressor chicane is located after two linac sections where the electron beam energy may be as high as 80 MeV. The probe may be moved to any transverse position in the chamber by a stepper motor. The maximum displacement of the beam is 14 cm at 80

MeV. The compressor may be operated at any value from zero field to full strength.

Compressor Chicane Design

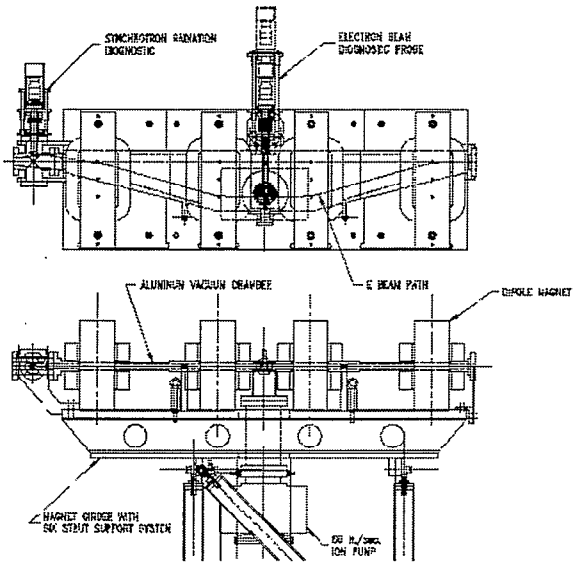

The synchrotron radiation monitor is used to observe emission as the beam passes through the final bend magnets. A variable position mirror is needed to accommodate potential magnet repositioning. The CCD mount is also moveable to accommodate variations in the direction of radiation emission.

Drift distances are 38 cm between outer magnets and 25 cm between the central magnets. For a given compressor length it is desirable to maximize these outer drifts (from magnets 1 to 2, and 3 to 4) in order to minimize the emission of coherent synchrotron radiation (CSR). The separated magnet configuration also reduces coupling between adjacent magnets.

Conservation of the longitudinal emittance requires that the uncorrelated energy spread of the bunch grow in inverse proportion to the bunch length reduction. The maximum energy spread that the FEL will tolerate sets a limit on the amount of compression that may be achieved. The input beam to the compressor is expected to have an uncorrelated RMS energy spread of .04% and a FWHM bunch length of 10 ps. The FEL will tolerate approximately 1% energy spread at the compressor (0.4% at the wiggler), hence we may compress the beam by a factor of 25 for a compressed FWHM of 0.4 ps. The beam current before compression is 200 Amps; after compression it is increased to 5000 Amps.

Compressor Installed in the DUV-FEL

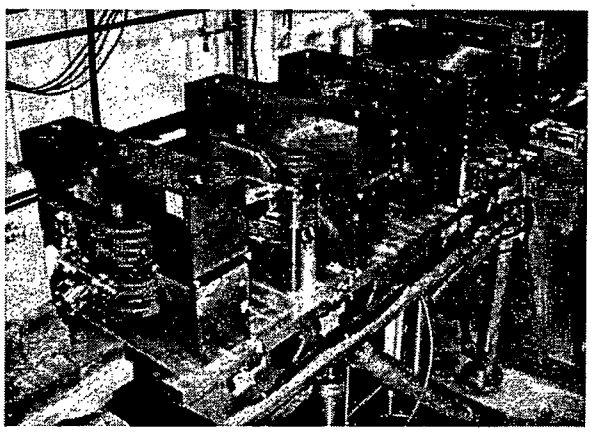

The substantially higher current provided by the compressor will have a profound impact on the performance of the FEL, and represents a major improvement in capability over the originally envisioned machine.

Electron Beam Diagnostic Development:

The high brightness electron beams now being produced for short wavelength FELs and high-energy colliders have focused sizes of a few microns in diameter. We have developed and tested a new beam diagnostic to measure transverse profiles down to this range using Yttrium:Aluminum:Garnet (YAG) crystals doped with a visible-light scintillator to produce an image of the transverse beam distribution [4,5,6]. The

advantage of this material over traditional fluorescent screens is that it is formed from a single crystal, and therefore has improved spatial resolution.

We have used the high resolution available from these crystals to test a compact three-screen emittance diagnostic [5]. Three screens displaced longitudinally are required to measure the beam's size and divergence. In the past, several meters of beamline were required for this measurement due to the poor resolution of each screen. The high resolution of the YAG screens permits a dramatic reduction of the required beamline length to a few centimeters. Three screens have been installed in the Smith-Purcell experiment at the ATF with a spacing of 6 cm. The beam image from each screen is transported by common output optics to a single video camera. This system allows rapid measurement of the emittance in a compact device.

We have also utilized this material as part of a pop-in periscope monitor for use in restricted spaces, such as the gap of the undulator for the High Gain Harmonic Generation (HGHG) at the ATF [6]. Modifications of this basic design are to be used for the DUV-FEL, both in the linac and in the undulators.

The probe is configured as a periscope which has the effect of displacing the image from the axis of the electron beam by a distance determined by the mirror spacing. Reproducible insertion of the probe is not required to maintain the precision of the monitor since the camera is firmly mounted to the undulator structure. As long as the probe length is stable and the camera does not move, the precision of the monitor is preserved, so a 'sloppy' actuator can be used. To provide fiducial reference marks, a fixed reticle is viewed through a beam splitter at a position for the YAG crystal.

Periscope Pop-in Schematic

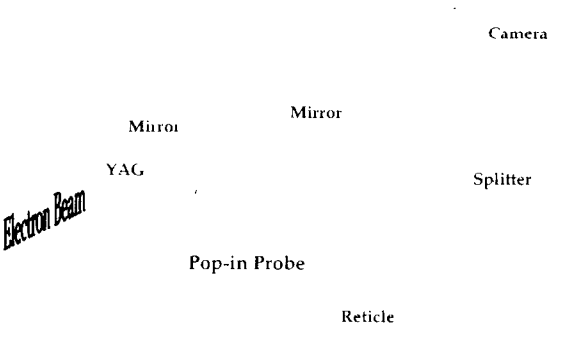

Periscope Pop-in Cross Section Drawing

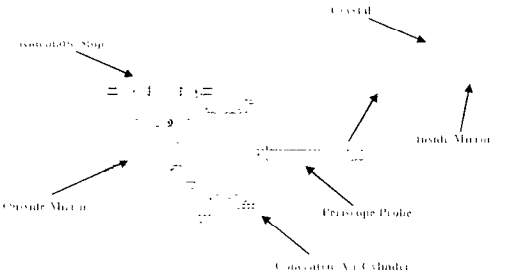

In this design the probe, actuator and optics are all on one side of the undulator. The light from the screen is collected through the hollow shaft of the probe. The actuator for moving the probe is a concentric air cylinder. Inner and outer cylinders capture the tubular piston so it is a double acting device. The piston carries the probe and overcomes the vacuum load provided by the bellows. We have installed five of these monitor systems on the HGHG experiment at the ATF.

Periscope Pop-in on the HGHG Experiment

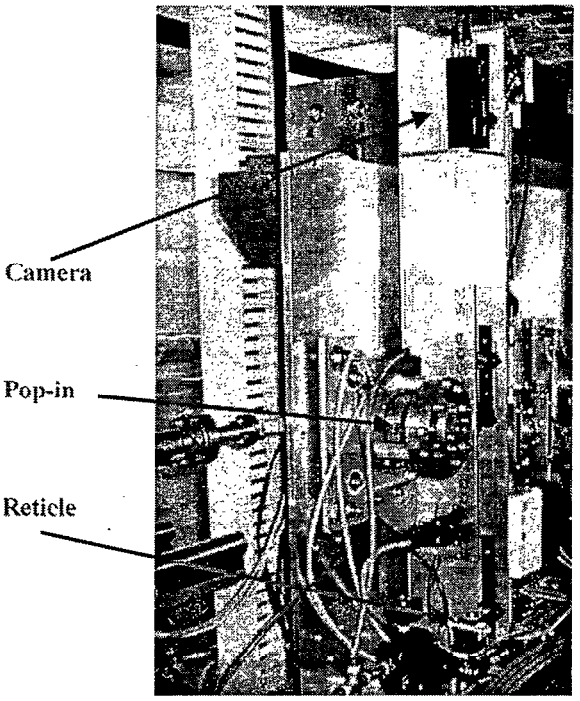

Monitors for use in the linac have also been developed that use many of the same design concepts as the undulator design described here. The probe does not need to be as compact in this application since the space restrictions are not as severe.

ACCOMPLISHMENTS:

Working from the established baseline parameters for our accelerator, we have developed some of the tools for electron beam preparation and measurement for the DUV-FEL. These techniques may be of broad utility to the accelerator community as well as being necessary components of our FEL project.

PAPERS/JOURNALS/PUBLICATIONS:

[1] "The BNL Source Development Laboratory," I.Ben-Zvi, E. Blum, W.S. Graves, R.N. Heese, E.D. Johnson, S. Krinsky, J.B. Murphy, L.-H. Yu, Presented at the FEL96 Conference, Rome Italy, August 26-31 1996. Nucl. Instrum. & Methods A393(1997) II-10.

[2] "The Source Development Lab Linac at BNL," W.S. Graves, E.D. Johnson, T.O. Raubenheimer, Proc. Linac-96 Conference, Geneva Switzerland, August 1996.

[3] "Design of the Source Development Lab Bunch Compressor," W.S. Graves, I. Ben-Zvi, E.D. Johnson, S. Krinsky, J. Skartika, M.H. Woodle, L.-H. Yu, and T.O. Raubenheimer, IEEE Particle Accelerator Conference, 1997.

[4] "A High Resolution Electron Beam Profile Monitor," W.S. Graves, E.D. Johnson, P.G. O'Shea, IEEE Particle Accelerator Conference, 1997.

[5] "A High Resolution Electron Beam Profile Monitor and its Applications," W.S. Graves, E.D. Johnson, S. Ulc, 1998 Beam Instrumentation Workshop, AIP Conference Proceedings Vol 451 p. 206, (1998).

[6] "Periscope Pop-in Beam Monitor," E.D. Johnson, W.S. Graves, and K.E. Robinson, 1998 Beam Instrumentation Workshop, AIP Conference Proceedings Vol 451 p. 479, (1998).

LDRD FUNDING:

FY 1998	$ 252,738
FY 1999 (est.)	$ 450,000

Novel Mechanisms of Hydroxy Fatty Acid Biosynthesis

John Shanklin *98-27*

PROJECT DESCRIPTION:

Plant fatty acids represent an $80 billion dollar a year market. However, the fatty acid compositions of crop plants contain a relatively small diversity of compared to the diversity found in nature. A goal of this laboratory is to increase this diversity. Crop plants vary in their fatty acid composition in terms of the degree of desaturation and in the chain length of the fatty acids. There are uncommon plants with unusual fatty acids such as hydroxy- and epoxy groups. These fatty acids are desirable because the functional groups are stereospecific and can be easily derivitized and therefore used for specific industrial starting materials such as lubricants and plasticizers which are currently obtained from petrochemicals. Much of the work in this laboratory has focussed on oxygen-dependent lipid modification enzymes that use diiron clusters for catalysis. While these systems constitute by far the most widespread class of lipid modification enzymes, there also exist a class of anaerobic enzymes that perform hydroxylation. The differences between these enzymes are that the aerobic class attack a saturated portion of the acyl chain, whereas the anaerobic hydroxylases hydrate an existing double bond.

Anaerobic hydroxylases or olefinic hydratases are found in both higher plants and in bacteria. Our goal is to clone the gene(s) encoding the hydratase and explore the possibility of using the system to modify plants to produce hydroxylated fatty acids via the anaerobic pathway.

TECHNICAL PROGRESS AND RESULTS - Fiscal Year 1998:

Purpose: The purpose of this R&D program is to define alternate metabolic pathways for the production of hydroxy fatty acids in plant seed oils. Objectives to be achieved during this research include: Identification of appropriate organisms that use anaerobic hydroxylases, isolation of the anaerobic hydroxylases enzyme, isolation of the anaerobic hydroxylases gene, biochemical characterization of the recombinant enzyme, and construction and evaluation of stable transgenic plants.

Approach: Several approaches were initiated, one using plants as a source of material, the other using bacteria.

For the plant approach we identified the indrajao, or *Wrightia tinctora* as a seed with approximately 60% isoricinoleic acid. Previous studies by others showed that developing seeds could synthesize 18:1 9-OH anaerobically. Our intent was to grow the plant and to harvest seed and use a conventional protein purification and enzyme assay analysis. For the bacterial approach, we undertook a genetic approach to directly identify the gene of interest. The idea was to identify species of bacteria that are related to *E. coli* such that expression of their genomic DNA would result in the accumulation of active anaerobic hydroxylase. This we could then assay if we could develop an assay to detect the hydroxylated reaction product.

Status:

1) Plants. We identified a seed source for plants that contain isoricinoleic acid, and purchased several pounds of indrajao seeds. Unfortunately the plants are rather slow

growers and we are still waiting for them to set seed that we can use as source material for the isolation of enzyme.

2) Bacteria. We successfully developed a visual screening technique that allows us to identify bioconversion in a mass format using ether extractions of the culture media that had been spiked with oleic acid and incubated for several days. The assay was verified using thin layer chromatography and gas chromatography/mass spectrometry. Many bacterial species that had been reported to perform the bioconversion of oleic to hydroxystearic acid were screened and it was confirmed that most of them indeed perform this function. Unfortunately the cell walls of *Nocardia cholesterolicum* were resistant to lysis. We therefore identified several other bacteria including *Flavobacterium* spDS5 that were able to perform the bioconversion, but these also contained nucleases that we were unable to inhibit. Thus, DNA purified from these organisms was susceptible to degradation, preventing us from making a genomic library. Finally, we were successful in isolating appropriately sized (40kbp) fragments of DNA from *Micrococcus leuteus*. This was cloned into a suitable host vector and the plasmid library cloned into *E. coli.*

Future Work: We will screen *E. coli* which are containing *leuteus* DNA for the ability to support bioconversion. Plasmids that convey the activity will be restriction mapped and subcloned into shorter fragments and rescreened. In this fashion the open reading frame will be identified that contains the anaerobic hydroxylase. The open reading frame will be further tailored for expression in the T7 expression system for the production of large amounts of protein. The protein will be purified to homogeneity, biochemically characterized. At the same time the gene will be inserted into a binary transformation vector suitable for *Agrobacterium* and introduced into *Arabidopsis thaliana* under the control of a strong seed specific promoter. The composition of seed fatty acids will be compared to that of controls containing a blank plasmid.

FOLLOW-ON FUNDING:

None, we are still developing data with which to apply for more funding.

LDRD FUNDING:

FY 1998	$ 99,646
FY 1999 (est.)	$ 104,000

Target Design for an AGS-based Spallation Neutron Source

J. Hastings *98-42*

PROJECT DESCRIPTION:

The AGS is a unique proton source as a driver for a spallation neutron source (SNS). It is not the accelerator one would build for a purpose built SNS but its high proton energy and low repetition rate are appealing features that can be used to advantage. The LDRD project addresses the initial design question of an appropriate target to take advantage of the AGS.

TECHNICAL PROGRESS AND RESULTS - Fiscal Year 1998:

Purpose: The project investigated the use of an iridium (Ir) rod target design for an AGS based SNS. The concept has been used very successfully at CERN as an anti-proton target and is well matched to the SNS needs using the AGS as a proton driver since the PS proton synchrotron at CERN has almost identical parameters to the AGS. The long-term objective is to build an SNS at BNL using the AGS as a proton driver and the critical issue is optimum target design.

Approach: The approach is to use accepted simulation codes (LAHET) to look at the neutronics performance of an Ir rod target and establish baseline power deposition information for use at a later stage in the thermal-mechanical design of such a target.

Technical Progress and Results: Preliminary results are encouraging. The overall performance appears competitive with other concepts but holds the promise because of the compact design for significant gains when a 'full system' including moderators and reflectors is evaluated. The advantages of compact design have already been demonstrated at existing SNS in the comparison between the Japanese facility KENS and the ISIS facility in the United Kingdom. In the preliminary design phase lead, lead fluoride, and beryllium are investigated as possible reflectors. Ambient temperature light water and 80K light water ice are proposed as initial moderators. Both moderators are decoupled by cadmium containing moderator chamber walls. The small size of the target has the advantage that the moderators can be placed close to the target. Finally, since a large fraction of the radioactive inventory is contained in the iridium rod, removal and disposition of this incentory should be relatively simple and inexpensive.

ACCOMPLISHMENTS:

Publication H. Ludewig, J. Hastings, P. Montanez, and M. Todosow, Preliminary Design Studies for an Iridium Rod Target at the BNL-AGS, BNL 65767 (1998).

LDRD FUNDING:

FY 1998	$ 100,787

Sensitive Detection and Rapid Identification of Biological Agents by Single Molecule Detection

Ming Wu *98-58*
Mark Ray

PROJECT DESCRIPTION:

The objective of this LDRD is to integrate the techniques of fluorescence immuno-assays, capillary electrophoresis (CE), and single-molecule detection (SMD) in to a single compact instrument for the rapid and reliable identification of biological agents. An integrated instrument based on these techniques is expected to be capable of analyzing as few as 100 tagged biological agents in *micro*-liter samples within minutes. The proposed analytical system has uses in the areas of BW-related agent detection, environmental monitoring, and medical testing.

TECHNICAL PROGRESS AND RESULTS – Fiscal Year 1998:

Purpose: The *rapid detection and reliable identification* of biological agents is of utmost importance to those concerned with national security, public health and environmental protection. Our goal is to develop a sensor, which can identify biological agents with high selectivity and sensitivity, and have negligible false positives and false negatives.

Approach: Experimental procedures for identification include: (1) incubation of a sample containing suspect antigens with the fluorescence-labeled antibodies; (2) injection of the sample into a capillary tube and its separation by the capillary electrophoresis; (3) discrimination of the individual fluorescence labeled antibody-antigen complexes in a micro-Flow Cytometer by single-molecule detection using laser-induced fluorescence. The selective nature of antibody binding provides a highly accurate means of identification of target biological agents. The highly selective bindings of antibodies will be exploited to attach fluorescent tags. Capillary electrophoresis will then be used to rapidly separate fluorescence labeled antibody-antigen complexes from the unbound antibodies and other components of the complex mixtures. This separation is critical in reducing or even eliminating false-positive identifications in the detection of the biological agents. The capillary will be coupled into a micro-Flow Cytometer. Laser-based techniques capable of single molecule detection will be used to detect the fluorescent tags.

Technical Progress and Results: During FY 1998, research was focused on construction of the detection apparatus and development data acquisition and analysis software. A frequency-doubled Nd:YAG laser, producing 50 mW cw light at 532 nm was used as the excitation source. The laser beam passed through a half wave plate and a Glan laser linear polarizer. The intensity of the laser beam on the sample was controlled by adjusting the wave plate. The laser beam was expanded and collimated before it is focused into the center of a quartz flow cell with a 250 μm square channel. A capillary electrophoresis device was coupled to the flow cell. The fluorescence signal was collected by a 40X, (N.A. 0.85) objective lens and passed through a slit before being focused on a compact solid-state avalanche photodiode detector (APD). A Multi-Channel Scaler (MCS) mediates the data collection in a PC computer. Software is under development for the basic data

acquisition and spectral analyses. A schematic drawing of the apparatus is shown in Figure 1.

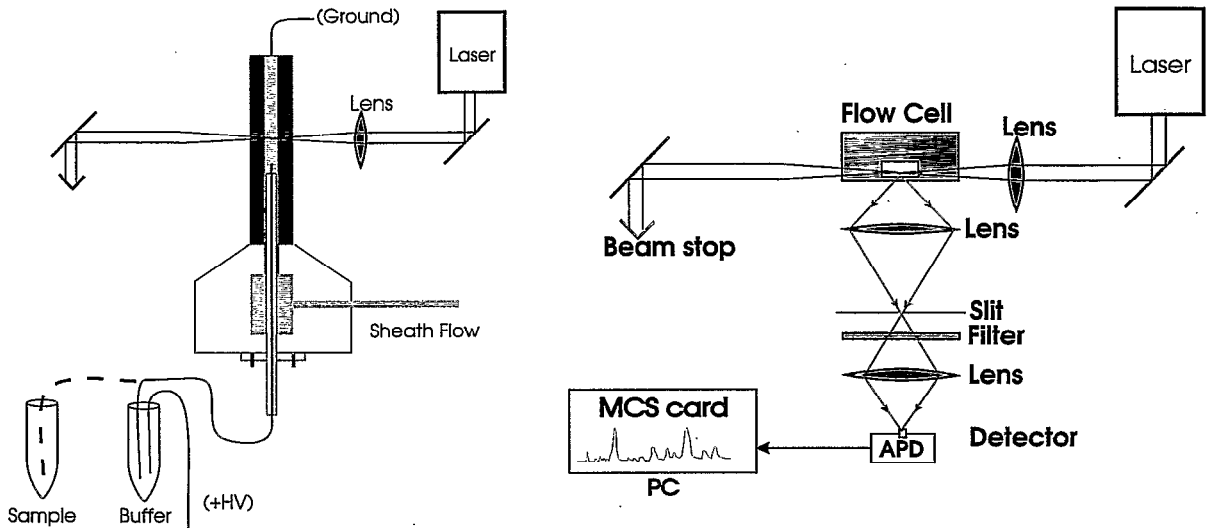

Figure 1: Schematic drawings of the apparatus constructed during FY 98. (left): side view of the apparatus; (right): top view of the apparatus.

The apparatus aims to detect B-Phycoerythrin (B-PE) and B-PE labeled antibody-antigen conjugates. It can also be used for DNA fragment sizing. B-PE is a highly fluorescent compound belonging to a class of proteins (phycobiliproteins) found in the light harvesting structures (phycobilisomes) of red algae and cyanobacteria. B-PE comprises three polypeptide subunits forming a $(\alpha\beta)_6\gamma$ aggregate containing a total of 34 bilin chromophores. In aqueous solution, isolated B-PE has intense absorption between 500 and 565 nm. The absorption cross section, σ, at 532 nm is 8.3×10^{-15} cm^2. As a point of reference, the cross-section of a single B-PE molecule is nominally equivalent to that of ~ 20 rhodamine-6G molecules. Furthermore, the fluorescence quantum yield of B-PE, Φ_f, is 0.98. Preliminary results show that the current apparatus can detect single B-PE molecules in 1X D-PBS buffer, as shown in Figure 2.

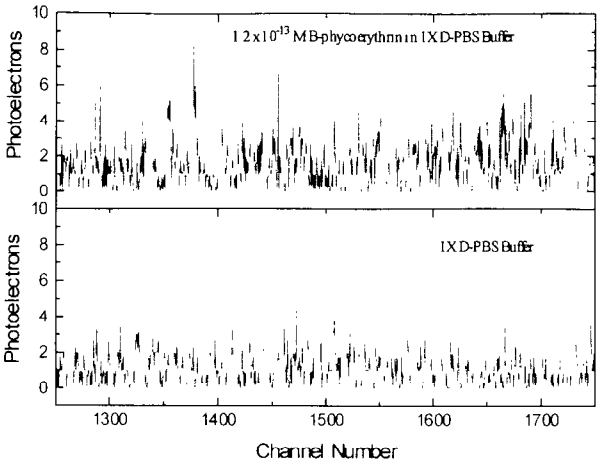

Figure 2: Detecting B-PE in Flow.

FOLLOW-ON FUNDING:

A proposal was submitted in response to US Army Edgewood Research, Development and Engineering Center (ERDEC), Board Agency Announcement (BAA) 98-1. The proposal was forwarded to the Joint Program Office for Biological Defense for consideration for funding.

LDRD FUNDING:

FY 1998	$ 99,223
FY 1999 (est.)	$ 100,000

LABORATORY DIRECTED RESEARCH AND DEVELOPMENT

1999 PROPOSED PROGRAM*

*New projects authorized for funding as of October 1, 1998.

Project Number 99-01

Ultra-fast Detector based on Optical Techniques
Y. Semertzidis

"Particle detectors currently offer either good time or spatial resolution but not both. Detectors with good intrinsic time resolution, i.e., less than 1 ns, usually cover relatively small useful areas and cost usually limits arranging them in very large arrays. There is a pressing need for large area detectors with intrinsic time resolution less than 100 ps which would enable many experiments to substantially reduce accidental rates and sensitivity to background."

FY 1999 Funding $125,000

Project Number 99-03

Development of a State-of-the Art Object Oriented Analysis Framework
T. Wenaus

"We propose to initiate a project focused on an innovative approach to a technical challenge on the cutting edge of modern computing. Specifically, we intend to develop an object-oriented analysis framework capable of:

- processing, and mining heretofore unprecedented amounts of data
- coordinating software development, use, and maintenance between many individuals separated by time and or distance
- utilizing object-oriented concepts to enhance software robustness and reusability
- leveraging commodity hardware to provide the most cost-effective compute power possible
- integrating commercial software with application-specific software."

FY 1999 Funding $100,000

Project Number 99-05

Aerosol Module for Climate Models Using Advanced Computer Techniques
C. Benkovitz

"We and others have presented a body of work over the past decade that indicates that anthropogenic aerosols are exerting an influence on climate change that is comparable (but of opposite sign) to the anthropogenic greenhouse effect. It is now generally agreed that it is necessary to include this aerosol forcing in climate models to provide an accurate representation of climate forcing over the industrial period. Given the necessity of including aerosols in climate models, methods must be developed that would allow aerosol chemical and microphysical processes to be represented in the next generation of climate models. Therefore, the overall main objective of this proposal is to develop computations techniques to include aerosol transport and evolution processes in climate models."

FY 1999 Funding $100,000

Project Number 99-06

ECO-1 Development of Preliminary Plans for Science, Facilities, Site Selection, Modeling and Roadmapping for the Environmental Carbon Observatory (ECO)
G. Hendrey

"Planning for ECO by this LDRD project is *innovative*. No innovative "new frontier" is in development of the roadmap for integration of FACE and Ameriflux with

many science disciplines through explicit modeling activities, across spatial and temporal scales, to allow a synthesis of process-level information into global-scale analyses and prediction."

FY 1999 Funding $350,000

Project Number 99-10

Brookhaven Center for Dataintensive Computing
J. Davenport

The Center will work collaboratively with research groups at BNL, Stony Brook, and elsewhere to build a Center of Excellence and become a national resource in the area of high performance computing, especially computational problems where data storage, retrieval and data mining are critically important."

FY 1999 Funding $359,000

Project Number 99-26

Electron Diffraction Studies of Charge Ordering in Transition-Metal Oxides
Y. Zhu

"This proposal represents an effort to combine the analytical power of the new DAS Transmission Electron Microscope (TEM) with existing sample preparation expertise at DAS and with the investigation of charge ordering in perovskite-related oxides, now primarily done in Solid State Physics. The goal is to directly observe the charge order in the charge stripe phases using an electron diffraction method developed recently in the Materials Science Division of DAS."

FY 1999 Funding $95,000

Project Number 99-28

Evaluation of a Millimeter Quasi-Optical Source for Non-Destructive Detection & Analysis
M. Ruckman

"This LDRD program will evaluate the use of a millimeter quasi-optical source for non-destructive materials analysis. Russian Backwave Oscillator (BWO) technology, obtained through the Initiatives for Proliferation Prevention (IPP) program, will be used to detect unknown liquid or solid materials in packages. The proposed work will provide data concerning the use of BWO technology for non-intrusive inspection and improve the chances of securing support for future research and development in several areas of interest to the Department of Defense, Department of Energy, and several independent agencies."

FY 1999 Funding $85,000

Project Number 99-40

Microdistribution Studies of Boron 10 for Boron Neutron Capture Therapy Using Transmission Electron Microscopy
R. Ma

"We propose to conduct a feasibility study on the ppm intracellular boron detection using the two high-performance Transmission Electron Microscope (TEM) at BNL. The goal is to measure the ^{10}B concentration in single cells and contiguous zones of extracellular matrix (blood boron analysis will be performed separately). These techniques will provide much-needed information for BNCT clinical trials as well as for boron drug development at BNL."

FY 1999 Funding $125,000

Project Number 99-41

Efficasy of Unidirectional Microbeam Radiation Therapy in Treating Malignant Tumors: Preclinical Studies in Rats and Mice

A. Dilmanian

"In conventional radiation therapy, damage to normal tissues surrounding the tumor is thought to stem largely from injury to endothelial cells, leading to necrosis. Unidirectional Microbeam Irradiation (UMBI) of animals at the NSLS showed two remarkable effects: a) exceptional sparing of normal tissues and b) tumor ablation or palliation in rats with intracranial or subcutaneous 9L gliosarcoma (9LGS) tumors, while retaining the tissue-sparing effects to the surrounding normal tissue. Several hypotheses regarding the biology behind UMBI's two effects will be examined, using normal rats and mice, and rodents bearing intracranial or subcutaneous tumors."

FY 1999 Funding $100,000

Project Number 99-45

Toxin Bio-Information Resource

S. Swaminathan

"We propose to develop a robust bio-informational resource that will collect, assimilate, synthesize, analyze and disseminate the basic molecular and structural information about potential Biological Warfare (BW) agents."

FY 1999 Funding $75,000

Project Number 99-46

Experimental and Theoretical Investigation of Transition Metal Oxides

J. Hill

"The goal of this project is to push forward the development of new techniques in the study of transition metal oxides; materials that are currently at the forefront of materials science research, because of their technological applications and because of the fundamental issues involved in the study of strongly correlated electron systems. The program will be based around recent advances made at BNL in resonant x-ray scattering techniques that provide new opportunities to study these materials."

FY 1999 Funding $85,000

Project Number 99-48

Pulsed Laser Deposition Facility

P. Johnson

"In this proposal, we seek funding to initiate the development of a Pulsed Laser Deposition (PLD) Facility for the growth of oxides at BNL in collaboration with Dr. Barry Wells of the Physics Department and University of Connecticut. It is envisioned that eventually this facility would add to a more general Lab-wide materials preparation capability and provide in-situ growth capabilities for research programs in the Physics Department and in the NSLS."

FY 1999 Funding $120,000

Project Number 99-50

Ultrashort Bunch Length Monitor

W. Graves

"Simulations indicate that the electron bunch compressor at the Source Development Lab can produce electron bunches as short as 100 fs FWHM. Bunch lengths on this scale cannot be measured by either traditional accelerator methods or the fastest streak cameras. However, optical methods developed by laser scientists to measure ultrashort light pulses are

applicable. The idea is to produce a short pulse of radiation from the electron bunch that accurately reproduces its temporal profile."

FY 1999 Funding $110,000

Project Number 99-51
DUV-FEL Amplifier Development
E. Johnson

"A critical element of the Deep Ultra-Violet Free Electron Laser (DUV-FEL) project is the optical amplifier. As a starting point, we have secured the loan of the NISUS undulator from the U.S. Army. Initial experiments will be conducted in the visible due to the ready availability and high quality of optical diagnostics. We will then commence with seeded beam studies using the laser system available at the Source Development Lab to provide a high quality output beam. We intend to conduct experiments to prove the viability of the subharmonically seeded beam FEL as the basis for a DUV FEL facility."

FY 1999 Funding $500,000

Project Number 99-53
Development of High Brightness Electron Sources
I. Ben Zvi

"The BNL Accelerator Test Facility is a world-class leader in the development of laser photocathode RF guns to produce such beams and advanced diagnostics to measure them. RF guns are, as of now, far from any fundamental limits on the achievable emittance. We propose an LDRD project that will use the ATF's advanced diagnostics and leadership in photocathode RF guns to increase the brightness of the electron beams produced by these guns by more than an order of magnitude."

FY 1999 Funding $200,000

Project Number 99-56
Attosecond Pulse Generation in High Harmonics
L. DiMauro

"The diagnostic techniques required to accurately determine the coherence properties of the harmonics and the predicted nonlinearities in the temporal phase are not feasible at shorter wavelengths. Brookhahven is in a unique position to tackle this problem, having the only existing short pulse high intensity mid-infrared laser capable of doing this job in the Chemistry Department."

FY 1999 Funding $110,000

Project Number 99-57
Development of a 2-D Ion Imaging Detector for VUV-FEL Applications
M. White

"In this project, we propose to develop a two-dimensional (2-D) ion-imaging spectrometer for the study of surface reaction dynamics, which takes full advantage of the intensity and tunability of the proposed BNL DUV-FEL."

FY 1999 Funding $100,000

Project Number 99-59
Application of Quantitative MRI: Water Content and Blood-Brain-Barrier Permeability in Multiple Sclerosis
W. Rooney

"This application seeks pilot funding to apply quantitative techniques developed at BNL's High-Feld MRI Laboratory to study fundamental disease processes in multiple sclerosis. This application proposes

quantitative magnetic resonance imaging studies of MS patients and healthy controls to determine a) if brain water content is increase in MS, b) if BBB permeability is increased in MS, and c) if increased water content and BBB permeability are predictive of disease progression. We will also test whether these changes represent a primary underlying (perhaps causative or predisposing) condition, or a secondary response to active disease."

FY 1999 Funding $75,000

Project Number 99-62

***In Situ* Time Resolved Studies of Catalysts for NO_X and SO_x Decomposition using Synchrotron Radiation**

J. Rodriguez

"Our project has two main objectives. One focuses on the development of new and unique instrumentation for the characterization of catalytic materials under realistic industrial conditions at the NSLS. The second phase of the project uses this instrumentation to investigate and optimize $DeNO_x$ and $DeSO_x$ materials that are of great technological importance. If successful, this project will produce useful $DeNO_x$ and $DeSO_x$ materials leading to commercial patents and significant amounts of external funding from the chemical industry."

FY 1999 Funding $125,000

Project Number 99-63

Support of RHIC Computing Effort

T. Daniels

"The RHIC Computing Facility (RCF) will consist of a large reconstruction machine that will be made up of several hundred commodity computers integrated into one system, a terrabyte storage system, a high bandwidth network, and other systems. This LDRD will provide funds for research in the design, testing and implementation of state-of-the-art systems that may assist the RCF in the development of their systems."

FY 1999 Funding $525,000